

World Journal of *Cardiology*

World J Cardiol 2018 October 26; 10(10): 123-190



**EDITORIAL**

- 123 T-cells in myocardial infarction: Culprit instigators or mere effectors?

Liberale L, Bonaventura A, Montecucco F

REVIEW

- 127 Overview of coronary artery variants, aberrations and anomalies

Kastellanos S, Aznaouridis K, Vlachopoulos C, Tsiamis E, Oikonomou E, Tousoulis D

MINIREVIEWS

- 141 Chronic ischemic mitral valve regurgitation and surgical perspectives

Altarabsheh SE, Deo SV, Rababa'h A, Obeidat YM, Haddad O

ORIGINAL ARTICLE**Observational Study**

- 145 Successful endovascular treatment in patients with acute thromboembolic ischemia of the lower limb including the crural arteries

Giusca S, Raupp D, Dreyer D, Eisenbach C, Korosoglou G

- 153 Incidental congenital coronary artery vascular fistulas in adults: Evaluation with adenosine-¹³N-ammonia PET-CT

Said SAM, Agool A, Moons AHM, Basalus MWZ, Wagenaar NRL, Nijhuis RLG, Schroeder-Tanka JM, Slart RHJA

SYSTEMATIC REVIEW

- 165 Undiscovered pathology of transient scaffolding remains a driver of failures in clinical trials

Kharlamov AN

CASE REPORT

- 187 Takotsubo syndrome - different presentations for a single disease: A case report and review of literature

Fuensalida A, Cortés M, Gabrielli L, Méndez M, Martínez A, Martínez G

ABOUT COVER

Editorial Board Member of *World Journal of Cardiology*, Mahesh Anantha-Narayanan, MD, Academic Fellow, Doctor, Division of Cardiovascular Sciences, University of Minnesota, Minneapolis, MN 55455, United States

AIM AND SCOPE

World Journal of Cardiology (*World J Cardiol*, *WJC*, online ISSN 1949-8462, DOI: 10.4330) is a peer-reviewed open access journal that aims to guide clinical practice and improve diagnostic and therapeutic skills of clinicians.

WJC covers topics concerning arrhythmia, heart failure, vascular disease, stroke, hypertension, prevention and epidemiology, dyslipidemia and metabolic disorders, cardiac imaging, pediatrics, nursing, and health promotion. Priority publication will be given to articles concerning diagnosis and treatment of cardiology diseases. The following aspects are covered: Clinical diagnosis, laboratory diagnosis, differential diagnosis, imaging tests, pathological diagnosis, molecular biological diagnosis, immunological diagnosis, genetic diagnosis, functional diagnostics, and physical diagnosis; and comprehensive therapy, drug therapy, surgical therapy, interventional treatment, minimally invasive therapy, and robot-assisted therapy.

We encourage authors to submit their manuscripts to *WJC*. We will give priority to manuscripts that are supported by major national and international foundations and those that are of great basic and clinical significance.

INDEXING/ABSTRACTING

World Journal of Cardiology (*WJC*) is now abstracted and indexed in Emerging Sources Citation Index (Web of Science), PubMed, PubMed Central, Scopus, China National Knowledge Infrastructure (CNKI), and Superstar Journals Database.

EDITORS FOR THIS ISSUE

Responsible Assistant Editor: *Xiang Li*
Responsible Electronic Editor: *Yun-Xiao Jian Wu*
Proofing Editor-in-Chief: *Lian-Sheng Ma*

Responsible Science Editor: *Ying Dou*
Proofing Editorial Office Director: *Jin-Lei Wang*

NAME OF JOURNAL

World Journal of Cardiology

ISSN

ISSN 1949-8462 (online)

LAUNCH DATE

December 31, 2009

FREQUENCY

Monthly

EDITORIAL BOARD MEMBERS

All editorial board members resources online at <http://www.wjgnet.com/1949-8462/editorialboard.htm>

EDITORIAL OFFICE

Jin-Lei Wang, Director
World Journal of Cardiology
Baishideng Publishing Group Inc

7901 Stoneridge Drive, Suite 501, Pleasanton, CA 94588, USA

Telephone: +1-925-2238242

Fax: +1-925-2238243

E-mail: editorialoffice@wjgnet.com

Help Desk: <http://www.f6publishing.com/helpdesk>

<http://www.wjgnet.com>

PUBLISHER

Baishideng Publishing Group Inc

7901 Stoneridge Drive, Suite 501,

Pleasanton, CA 94588, USA

Telephone: +1-925-2238242

Fax: +1-925-2238243

E-mail: bpoffice@wjgnet.com

Help Desk: <http://www.f6publishing.com/helpdesk>

<http://www.wjgnet.com>

PUBLICATION DATE

October 26, 2018

COPYRIGHT

© 2018 Baishideng Publishing Group Inc. Articles published by this Open-Access journal are distributed under the terms of the Creative Commons Attribution Non-commercial License, which permits use, distribution, and reproduction in any medium, provided the original work is properly cited, the use is non commercial and is otherwise in compliance with the license.

SPECIAL STATEMENT

All articles published in journals owned by the Baishideng Publishing Group (BPG) represent the views and opinions of their authors, and not the views, opinions or policies of the BPG, except where otherwise explicitly indicated.

INSTRUCTIONS TO AUTHORS

<http://www.wjgnet.com/bpg/gerinfo/204>

ONLINE SUBMISSION

<http://www.f6publishing.com>

T-cells in myocardial infarction: Culprit instigators or mere effectors?

Luca Liberale, Aldo Bonaventura, Fabrizio Montecucco

Luca Liberale, Center for Molecular Cardiology, University of Zürich, Schlieren 8952, Switzerland

Luca Liberale, Aldo Bonaventura, Fabrizio Montecucco, First Clinic of Internal Medicine, Department of Internal Medicine, University of Genoa, Genoa 16132, Italy

Fabrizio Montecucco, IRCCS Ospedale Policlinico San Martino Genoa - Italian Cardiovascular Network, 16132 Genoa, Italy

ORCID number: Luca Liberale (0000-0003-1472-7975); Aldo Bonaventura (0000-0002-4747-5535); Fabrizio Montecucco (0000-0003-0823-8729).

Author contributions: Liberale L wrote the manuscript; Bonaventura A and Montecucco F revised the draft and gave suggestions for its improvement.

Conflict-of-interest statement: Liberale L, Bonaventura A and Montecucco F declare no conflict of interest related to this publication.

Open-Access: This article is an open-access article which was selected by an in-house editor and fully peer-reviewed by external reviewers. It is distributed in accordance with the Creative Commons Attribution Non Commercial (CC BY-NC 4.0) license, which permits others to distribute, remix, adapt, build upon this work non-commercially, and license their derivative works on different terms, provided the original work is properly cited and the use is non-commercial. See: <http://creativecommons.org/licenses/by-nc/4.0/>

Manuscript source: Invited manuscript

Correspondence to: Luca Liberale, MD, Postdoctoral Fellow, Doctor, First Clinic of Internal Medicine, Department of Internal Medicine, University of Genoa, 6 viale Benedetto XV, Genoa 16132, Italy. luca.liberale@uzh.ch
Telephone: +39-10-3537940
Fax: +39-10-3538686

Received: May 29, 2018

Peer-review started: May 29, 2018

First decision: June 14, 2018

Revised: June 20, 2018

Accepted: June 28, 2018

Article in press: June 28, 2018

Published online: October 26, 2018

Abstract

Immune system activation and dysfunction characterize the early phase of reperfusion after a myocardial infarction (MI). Despite initially neglected, adaptive immunity has been recently showed to play an important role in this setting. In fact, the immune system can recognize sequestered antigens released by the necrotic tissue, initiating a deleterious autoimmune vicious circle leading to worse outcome. In their recent work, Angelini *et al* shed the light on a new feature of post-MI which involves two "old players" of post-ischemic myocardial injury: CD31 and matrix metalloproteinase (MMP)-9. Specifically, the authors showed that an enhancement of MMP-9 release could determine the cleavage of inhibitory CD31 from CD4+ T-cells surface in patients with Acute Coronary Syndromes (ACS). These findings open the room for new studies investigating the role of MMP9 in other pathological processes associated with a reduction of CD31 functionality, such as plaque instability and rupture. Of interest, in the case of a causative role for CD31 shedding in ACS would be confirmed, there might be a potential role for the administration of CD31 protein or analogue compounds to blunt post-ischemic cardiac inflammation and improve ACS outcome.

Key words: Matrix metalloproteinase; Lymphocytes; Autoimmunity; Inflammation; Myocardial infarction; Adaptive immunity

© The Author(s) 2018. Published by Baishideng Publishing Group Inc. All rights reserved.

Core tip: CD31 and matrix metalloproteinases (MMP)-9 are known mediators that are upregulated during reperfusion after cardiac ischemia. By inhibiting T-cell

receptor-dependent lymphocyte activation, the functional CD31 could reduce post-ischemic inflammatory response; while MMP-9 is deeply involved in inflammatory cell recruitment and myocardial remodeling. A recent paper published in European Heart Journal linked these mediators by showing CD31 cleavage to be MMP-9 dependent in patients with acute coronary syndromes (ACS). Whether this process is causative of ACS or rather its effect still needs to be clarified.

Liberale L, Bonaventura A, Montecucco F. T-cells in myocardial infarction: Culprit instigators or mere effectors? *World J Cardiol* 2018; 10(10): 123-126 Available from: URL: <http://www.wjgnet.com/1949-8462/full/v10/i10/123.htm> DOI: <http://dx.doi.org/10.4330/wjc.v10.i10.123>

INTRODUCTION

Acute Coronary Syndromes (ACS)-including unstable angina and myocardial infarction (MI) are the most detrimental atherosclerosis-related complications being the leading causes of mortality worldwide and a considerable source of morbidity^[1]. Although outstanding leap forwards of primary and secondary prevention measures, the issue of the residual risk for ischemic complication is still unsolved^[2]. Also, it is now well-recognized that after a prompt reperfusion, as it is the case of vast majority of patients suffering from MI, the ischemic hearts need to face an additional damage directly induced by the re-establishment of blood flow itself^[3]. The role of innate immunity in the determination of both residual risk and ischemia/reperfusion injury has been studied from decades and is now better established^[4-6]. The adaptive immune system (*i.e.*, T-cells and B-cells) have only recently come into focus. Indeed, lymphocytes' ability to react only against specific non-self-antigens, as opposed to the reactivity against non-specific danger signal showed by innate immunity, excluded these mediators from the list of "guilty" parties for a long time. Only recently, the recognition of a role for the release of sequestered antigens from the necrotic tissue in the progressive diversification of autoreactive lymphocytes (*i.e.*, epitope spreading) shed the light on the potential involvement of adaptive auto-reactivity in the determination of post-MI outcome^[7]. After an ACS, the necrotic heart tissue releases several danger-associated molecular patterns (DAMPs) together with cardiac intracellular proteins^[8,9]. In this highly inflamed micro-environment, cardiac antigens can be recognized by autoreactive lymphocyte clones and trigger autoimmunity processes. Afterward, the same immune-mediated tissue injury supplies the amount of autoantigens necessary to maintain the auto-reactivity thus sustaining the dysfunctional immune cardiac process^[9]. This editorial refers to the outstanding research article entitled "matrix metalloproteinases-9 might affect adaptive immunity in non-ST segment elevation ACS by increasing CD31 cleavage on CD4+ cells", recently

published by Angelini *et al.*^[10] in European Heart Journal.

T-CELLS AND ACS

Although several studies have implicated T-cells in the pathophysiology of ACS, the knowledge about their specific role is still elusive. Considering the heterogeneity of T-cell subsets and the quickly evolving local and systemic environment after ACS, a tight regulation of rapidly changing T-cell phenotypes with regulator or effector functions is likely^[11]. Experimental evidence highlights infiltrating T-cells as effector lymphocytes which have been antigen-restricted and primed in the heart-draining lymph nodes. Of interest, after ACS, particular subsets of pro-inflammatory CD28- CD4+ and Th17 lymphocytes are released in the blood stream and produce large amounts of interferon- γ and IL-17: Detrimental cytokines with known ability to increase cardiomyocyte death, fibroblast proliferation and pro-fibrotic gene expression^[12-14]. Not only detrimental T-cells with effector functions are increased after ACS but they also display dysfunctional features. Indeed, they overexpress CD40 ligand in this way being more easily activated by antigen presenting cells^[15]. Furthermore, a direct cytotoxic effect of infiltrating autoreactive CD8+ T-lymphocytes with specificity towards cardiac myosin has been described^[16]. To further potentiate the detrimental role of T lymphocytes in the setting of MI, the raise of pro-inflammatory lymphocyte subsets is accompanied by a reciprocal reduction in CD4+CD25+Foxp3+ regulatory T-lymphocytes with a beneficial cardiac protective role^[17].

MMP-9 AND CD31: A DANGEROUS ASSOCIATION

Post-transcriptional CD31 modifications showed capacity to affect normal T-lymphocyte function. Indeed, CD31 (also known as platelet endothelial cell adhesion molecule-1) was shown to regulate T lymphocyte activity through the inhibition of T cell receptor (TCR) signalling^[18]. Of interest, CD31 extracellular domain is shed from the lymphocyte surface during ACS and this contributes to the over activation of adaptive immunity^[19]. In their recent article, Angelini *et al.*^[10] added one more piece to this puzzle by showing matrix metalloproteinase (MMP)-9 to be involved in CD31 cleavage in lymphocytes from ACS patients. Firstly, they confirm CD31 shedding to be a specific feature of lymphocytes in ACS, as compared to samples from healthy subjects but also patients with stable angina (SA). Then, the authors demonstrated *in vitro* that down-regulation of the functional CD31 domain in ACS is associated with TCR activation and is led by post-transcriptional mechanisms since post-stimulation levels of CD31 mRNA were similar in ACS and SA cells. Finally, after observing CD31 to be a possible substrate for MMP-9 by using an dedicated software predicting novel substrates and their cleavage sites, the auth-

ors show lymphocytes from ACS patients to produce higher enzyme levels after stimulation and CD31 active domain to be preserved by MMP-9 inhibition. Based on these results, the authors propose a new sequence of events that might characterize ACS onset in which the increased release of MMP-9 causes CD31 cleavage, thus affecting TCR-dependent T-cell activation and causing T-cell hyperactivity^[10].

PERSPECTIVES

Angelini *et al.*^[10] added knowledge to the field of dysfunctional adaptive immunity in ACS. At the same time, they raise new appealing questions. In particular, CD31 is known to mediate also endothelial-endothelial interactions, thus allowing the constitution of the continuous and protective intimal cell monolayer^[20]. Now, further investigations are advisable to assess whether the inflammation-induced overproduction of MMP-9^[21] could reduce these interactions and potentially contribute to endothelial erosion and plaque instability. Under this point of view, CD31 was previously described to target macrophage activation, as well as cytokine and chemokine release within atherosclerotic plaques and aneurysmal peri-aorta^[22]. Also, it would be of interest to show CD31 modifications in lymphocytes to take act before ACS onset. In general, this is a very common weakness of studies focused on cellular phenotype during ACS due to the requirement of intact cells for fluorescent-activated sorting which does not allow sample storage before the dosage. Animal studies could help in assessing this causal connection.

Given the fact that CD31 protein or analog molecules are already available^[23], answering these questions could point out CD31 replacement as a potential therapeutic approach to blunt inflammation and modulate tissue damage in acute cardiovascular diseases (such as MI and stroke) that are characterized by an impaired adaptive immunity.

REFERENCES

- 1 Benjamin EJ, Virani SS, Callaway CW, Chamberlain AM, Chang AR, Cheng S, Chiuve SE, Cushman M, Delling FN, Deo R, de Ferranti SD, Ferguson JF, Formage M, Gillespie C, Isasi CR, Jiménez MC, Jordan LC, Judd SE, Lackland D, Lichtman JH, Lisabeth L, Liu S, Longenecker CT, Lutsey PL, Mackey JS, Matchar DB, Matsushita K, Mussolino ME, Nasir K, O'Flaherty M, Palaniappan LP, Pandey A, Pandey DK, Reeves MJ, Ritchey MD, Rodriguez CJ, Roth GA, Rosamond WD, Sampson UKA, Satou GM, Shah SH, Spartano NL, Tirschwell DL, Tsao CW, Voeks JH, Willey JZ, Wilkins JT, Wu JH, Alger HM, Wong SS, Muntner P; American Heart Association Council on Epidemiology and Prevention Statistics Committee and Stroke Statistics Subcommittee. Heart Disease and Stroke Statistics-2018 Update: A Report From the American Heart Association. *Circulation* 2018; **137**: e67-e492 [PMID: 29386200 DOI: 10.1161/CIR.0000000000000558]
- 2 Piepoli MF, Hoes AW, Agewall S, Albus C, Brotons C, Catapano AL, Cooney MT, Corrà U, Cosyns B, Deaton C, Graham I, Hall MS, Hobbs FDR, Løchen ML, Löllgen H, Marques-Vidal P, Perk J, Prescott E, Redon J, Richter DJ, Sattar N, Smulders Y, Tiberi M, van der Worp HB, van Dis I, Verschuren WMM, Binno S; ESC Scientific Document Group. 2016 European Guidelines on cardiovascular disease prevention in clinical practice: The Sixth Joint Task Force of the European Society of Cardiology and Other Societies on Cardiovascular Disease Prevention in Clinical Practice (constituted by representatives of 10 societies and by invited experts) Developed with the special contribution of the European Association for Cardiovascular Prevention & Rehabilitation (EACPR). *Eur Heart J* 2016; **37**: 2315-2381 [PMID: 27222591 DOI: 10.1093/eurheartj/ehw106]
- 3 Yellon DM, Hausenloy DJ. Myocardial reperfusion injury. *N Engl J Med* 2007; **357**: 1121-1135 [PMID: 17855673 DOI: 10.1056/NEJMr071667]
- 4 Carbone F, Liberale L, Bonaventura A, Cea M, Montecucco F. Targeting Inflammation in Primary Cardiovascular Prevention. *Curr Pharm Des* 2016; **22**: 5662-5675 [PMID: 27549380 DOI: 10.2174/1381612822666160822124546]
- 5 Montecucco F, Liberale L, Bonaventura A, Vecchiè A, Dallegri F, Carbone F. The Role of Inflammation in Cardiovascular Outcome. *Curr Atheroscler Rep* 2017; **19**: 11 [PMID: 28194569 DOI: 10.1007/s11883-017-0646-1]
- 6 Bonaventura A, Liberale L, Vecchiè A, Casula M, Carbone F, Dallegri F, Montecucco F. Update on Inflammatory Biomarkers and Treatments in Ischemic Stroke. *Int J Mol Sci* 2016; **17**: pii: E1967 [PMID: 27898011 DOI: 10.3390/ijms17121967]
- 7 Vanderlugt CL, Miller SD. Epitope spreading in immune-mediated diseases: implications for immunotherapy. *Nat Rev Immunol* 2002; **2**: 85-95 [PMID: 11910899 DOI: 10.1038/nri724]
- 8 Lv H, Lipes MA. Role of impaired central tolerance to α -myosin in inflammatory heart disease. *Trends Cardiovasc Med* 2012; **22**: 113-117 [PMID: 22902177 DOI: 10.1016/j.tcm.2012.07.005]
- 9 Liao YH, Cheng X. Autoimmunity in myocardial infarction. *Int J Cardiol* 2006; **112**: 21-26 [PMID: 16837084 DOI: 10.1016/j.ijcard.2006.05.009]
- 10 Angelini G, Flego D, Vinci R, Pedicino D, Trotta F, Ruggio A, Piemontese GP, Galante D, Ponzo M, Biasucci LM, Liuzzo G, Crea F. Matrix metalloproteinase-9 might affect adaptive immunity in non-ST segment elevation acute coronary syndromes by increasing CD31 cleavage on CD4+ T-cells. *Eur Heart J* 2018; **39**: 1089-1097 [PMID: 29211854 DOI: 10.1093/eurheartj/ehx684]
- 11 Bluestone JA, Mackay CR, O'Shea JJ, Stockinger B. The functional plasticity of T cell subsets. *Nat Rev Immunol* 2009; **9**: 811-816 [PMID: 19809471 DOI: 10.1038/nri2654]
- 12 Yan X, Shichita T, Katsumata Y, Matsuhashi T, Ito H, Ito K, Anzai A, Endo J, Tamura Y, Kimura K, Fujita J, Shimura K, Shen W, Yoshimura A, Fukuda K, Sano M. Deleterious effect of the IL-23/IL-17A axis and $\gamma\delta$ T cells on left ventricular remodeling after myocardial infarction. *J Am Heart Assoc* 2012; **1**: e004408 [PMID: 23316306 DOI: 10.1161/JAHA.112.004408]
- 13 Liuzzo G, Biasucci LM, Trotta F, Brugaletta S, Pinnelli M, Digianuario G, Rizzello V, Rebuzzi AG, Rumi C, Maseri A, Crea F. Unusual CD4+CD28null T lymphocytes and recurrence of acute coronary events. *J Am Coll Cardiol* 2007; **50**: 1450-1458 [PMID: 17919564 DOI: 10.1016/j.jacc.2007.06.040]
- 14 Liuzzo G, Kopecky SL, Frye RL, O'Fallon WM, Maseri A, Goronzy JJ, Weyand CM. Perturbation of the T-cell repertoire in patients with unstable angina. *Circulation* 1999; **100**: 2135-2139 [PMID: 10571971 DOI: 10.1161/01.CIR.100.21.2135]
- 15 Aukrust P, Müller F, Ueland T, Berget T, Aaser E, Brunsvig A, Solum NO, Forfang K, Frøland SS, Gullestad L. Enhanced levels of soluble and membrane-bound CD40 ligand in patients with unstable angina. Possible reflection of T lymphocyte and platelet involvement in the pathogenesis of acute coronary syndromes. *Circulation* 1999; **100**: 614-620 [PMID: 10441098 DOI: 10.1161/01.CIR.100.6.614]
- 16 Huber SA, Graveline D, Born WK, O'Brien RL. Cytokine production by Vgamma(+) T-cell subsets is an important factor determining CD4(+) Th-cell phenotype and susceptibility of BALB/c mice to coxsackievirus B3-induced myocarditis. *J Virol* 2001; **75**: 5860-5869 [PMID: 11390587 DOI: 10.1128/JVI.75.13.5860-5869.2001]
- 17 Han SF, Liu P, Zhang W, Bu L, Shen M, Li H, Fan YH, Cheng

- K, Cheng HX, Li CX, Jia GL. The opposite-direction modulation of CD4+CD25+ Tregs and T helper 1 cells in acute coronary syndromes. *Clin Immunol* 2007; **124**: 90-97 [PMID: 17512253 DOI: 10.1016/j.clim.2007.03.546]
- 18 **Clement M**, Fornasa G, Guedj K, Ben Mkaddem S, Gaston AT, Khallou-Laschet J, Morvan M, Nicoletti A, Caligiuri G. CD31 is a key coinhibitory receptor in the development of immunogenic dendritic cells. *Proc Natl Acad Sci USA* 2014; **111**: E1101-E1110 [PMID: 24616502 DOI: 10.1073/pnas.1314505111]
- 19 **Flego D**, Severino A, Trotta F, Previtero M, Ucci S, Zara C, Pedicino D, Massaro G, Biasucci LM, Liuzzo G, Crea F. Altered CD31 expression and activity in helper T cells of acute coronary syndrome patients. *Basic Res Cardiol* 2014; **109**: 448 [PMID: 25344833 DOI: 10.1007/s00395-014-0448-3]
- 20 **Lertkiatmongkol P**, Liao D, Mei H, Hu Y, Newman PJ. Endothelial functions of platelet/endothelial cell adhesion molecule-1 (CD31). *Curr Opin Hematol* 2016; **23**: 253-259 [PMID: 27055047 DOI: 10.1097/MOH.0000000000000239]
- 21 **Papazafiropoulou A**, Tentolouris N. Matrix metalloproteinases and cardiovascular diseases. *Hippokratia* 2009; **13**: 76-82 [PMID: 19561775]
- 22 **Fornasa G**, Clement M, Groyer E, Gaston AT, Khallou-Laschet J, Morvan M, Guedj K, Kaveri SV, Tedgui A, Michel JB, Nicoletti A, Caligiuri G. A CD31-derived peptide prevents angiotensin II-induced atherosclerosis progression and aneurysm formation. *Cardiovasc Res* 2012; **94**: 30-37 [PMID: 22293851 DOI: 10.1093/cvr/cvs076]
- 23 **Groyer E**, Nicoletti A, Ait-Oufella H, Khallou-Laschet J, Varthaman A, Gaston AT, Thaumat O, Kaveri SV, Blatny R, Stockinger H, Mallat Z, Caligiuri G. Atheroprotective effect of CD31 receptor globulin through enrichment of circulating regulatory T-cells. *J Am Coll Cardiol* 2007; **50**: 344-350 [PMID: 17659202 DOI: 10.1016/j.jacc.2007.04.040]

P- Reviewer: Aksu T, Altarabsheh SE, Dai X, Iacoviello M

S- Editor: Ji FF **L- Editor:** A **E- Editor:** Wu YXJ



Overview of coronary artery variants, aberrations and anomalies

Stylianos Kastellanos, Konstantinos Aznaouridis, Charalambos Vlachopoulos, Eleftherios Tsiamis, Evangelos Oikonomou, Dimitris Tousoulis

Stylianos Kastellanos, Konstantinos Aznaouridis, Cardiology Department, Castle Hill Hospital, Hull and East Yorkshire NHS Trust, Cottingham HU16 5JQ, United Kingdom

Stylianos Kastellanos, Konstantinos Aznaouridis, Charalambos Vlachopoulos, Eleftherios Tsiamis, Evangelos Oikonomou, Dimitris Tousoulis, Peripheral Vessels Unit and EKKAN (Unit for the athletes and for hereditary cardiovascular diseases), 1st Department of Cardiology, Hippokration Hospital, Medical School of National and Kapodistrian University of Athens, Athens 11527, Greece

ORCID number: Stylianos Kastellanos (0000-0002-3274-3074); Konstantinos Aznaouridis (0000-0002-0706-4424); Charalambos Vlachopoulos (0000-0002-9904-3558); Eleftherios Tsiamis (0000-0002-2725-6319); Evangelos Oikonomou (0000-0001-8079-0599); Dimitris Tousoulis (0000-0001-7492-4984).

Author contributions: Kastellanos S collected the clinical data, designed and drafted the manuscript and approved the final version; Aznaouridis K conceived the idea for this review, designed and critically revised the manuscript and approved the final version; Vlachopoulos C, Tsiamis E, Oikonomou E and Tousoulis D critically revised the manuscript and approved the final version.

Conflict-of-interest statement: No potential conflicts of interest. No financial support.

Open-Access: This article is an open-access article which was selected by an in-house editor and fully peer-reviewed by external reviewers. It is distributed in accordance with the Creative Commons Attribution Non Commercial (CC BY-NC 4.0) license, which permits others to distribute, remix, adapt, build upon this work non-commercially, and license their derivative works on different terms, provided the original work is properly cited and the use is non-commercial. See: <http://creativecommons.org/licenses/by-nc/4.0/>

Manuscript source: Invited manuscript

Correspondence to: Konstantinos Aznaouridis, MD, PhD, Doctor, Consultant Interventional Cardiologist, Peripheral Vessels Unit and EKKAN (Unit for the athletes and for hereditary

cardiovascular diseases), 1st Department of Cardiology, Hippokration Hospital, Medical School of National and Kapodistrian University of Athens, 114 Vas. Sofias Avenue, Athens 11527, Greece. conazna@yahoo.com
Telephone: +30-697-2024534

Received: April 16, 2018

Peer-review started: April 16, 2018

First decision: June 6, 2018

Revised: August 12, 2018

Accepted: August 31, 2018

Article in press: August 31, 2018

Published online: October 26, 2018

Abstract

Coronary artery anomalies and variants are relatively uncommon congenital disorders of the coronary artery anatomy and constitute the second most common cause of sudden cardiac death in young competitive athletes. The rapid advancement of imaging techniques, including computed tomography, magnetic resonance imaging, intravascular ultrasound and optical coherence tomography, have provided us with a wealth of new information on the subject. Anomalous origin of a coronary artery from the contralateral sinus is the anomaly most frequently associated with sudden cardiac death, in particular if the anomalous coronary artery has a course between the aorta and the pulmonary artery. However, other coronary anomalies, like anomalous origin of the left coronary artery from the pulmonary artery, atresia of the left main stem and coronary fistulae, have also been implicated in cases of sudden cardiac death. Patients are usually asymptomatic, and in most of the cases, coronary anomalies are discovered incidentally during coronary angiography or on autopsy following sudden cardiac death. However, in some cases, symptoms like angina, syncope, heart failure and myocardial infarction may occur. The aims of this article are to present a

brief overview of the diverse coronary variants and anomalies, focusing especially on anatomical features, clinical manifestations, risk of sudden cardiac death and pathophysiologic mechanism of symptoms, as well as to provide valuable information regarding diagnostic workup, follow-up, therapeutic choices and timing of surgical treatment.

Key words: Ectopic coronary arteries; Coronary artery anomalies; Coronary fistulae; Coronary artery variants; Myocardial bridging; Coronary artery anatomy; Sudden cardiac death

© **The Author(s) 2018.** Published by Baishideng Publishing Group Inc. All rights reserved.

Core tip: Coronary artery anomalies and variants are a diverse group of congenital disorders of the coronary artery anatomy with a wide variety of clinical manifestations. Though relatively uncommon and usually discovered incidentally during coronary angiography, they have garnered interest because they are the second most common cause of sudden cardiac death in young competitive athletes. Though by no means entirely exhaustive, this overview aims to act as a guide for the practicing cardiologist along the complex web of these disorders and may facilitate the assessment, investigation, follow-up and treatment of patients diagnosed with or suspected of having a coronary artery anomaly.

Kastellanos S, Aznaouridis K, Vlachopoulos C, Tsiamis E, Oikonomou E, Tousoulis D. Overview of coronary artery variants, aberrations and anomalies. *World J Cardiol* 2018; 10(10): 127-140 Available from: URL: <http://www.wjgnet.com/1949-8462/full/v10/i10/127.htm> DOI: <http://dx.doi.org/10.4330/wjc.v10.i10.127>

INTRODUCTION

Coronary artery anomalies and variants are a diverse group of congenital disorders of the coronary artery anatomy with a wide variety of clinical manifestations. Though relatively uncommon and usually discovered incidentally during coronary angiography, they have attracted interest as they constitute the second most frequent cause of sudden death in young adults participating in competitive sports^[1,2]. Though by no means entirely exhaustive, this overview aims to act as a guide for the practicing cardiologist along the complex web of these disorders and may facilitate the assessment, investigation, follow-up and treatment of patients diagnosed with or suspected of having a coronary artery anomaly. The majority of the figures presented are from our personal dataset.

It is important to have definite morphological criteria to describe normal coronary arteries. Angelini^[3] has suggested criteria of normality of coronary anatomy, using several morphological features of the coronary

arteries, such as number of ostia, location, course and branches. We also need to distinguish between normal variants of coronary anatomy and proper coronary anomalies. Anatomical features of the coronary arteries should be considered variants rather than congenital anomalies when they are prevalent in more than 1% of general population^[4,5].

NORMAL CORONARY ANATOMY

Before venturing to explore the various coronary anatomy variations and anomalies, it is worth going through a brief overview of normal coronary anatomy. Normally there are two main coronary arteries, which stem from the sinuses of Valsalva and descend towards the cardiac apex. The left main stem (LMS) originates from the left sinus of Valsalva and crosses between the main pulmonary artery and the left atrial appendage. LMS has an average length of 2-4 cm and normally bifurcates into the left anterior descending artery (LAD) and the left circumflex artery (LCX). The right coronary artery (RCA) stems from the right sinus of Valsalva. The LAD descends towards the apex of the heart in the epicardial fat across the anterior interventricular sulcus. Its length varies between 10 and 13 cm and gives rise to diagonal and septal branches. It supplies the anterior wall, the apex and a significant portion of the interventricular septum. The LCX has a length of 5-8 cm and crosses the coronary sulcus on the diaphragmatic cardiac surface. It gives rise to the obtuse marginal branches and supplies mostly the lateral wall of the left ventricle. The RCA passes to the right between the pulmonary artery and the right auricle, descends across the right atrioventricular sulcus and continues posteriorly after the acute margin of the heart. Normal length is 12-14 cm. During its course, it may give rise to several branches, like the conus branch, sinoatrial branch, right ventricular branch, atrioventricular nodal branch, posterior descending branch (PDA) and posterolateral branch. It can broadly be considered as the artery that supplies the right side of the heart^[1,6]. According to Angelini^[3], the coronary anatomy falls within the spectrum of normality when: (1) there are two to four coronary ostia located at the upper midsection of the anterior aspect of the right and left sinuses of Valsalva. This is because sometimes the LAD and LCX may have separate origins from the left sinus, whereas the RCA and the conus branch may have separate origins from the right sinus; (2) a proximal stem bifurcating into major arteries is present only in the left coronary system (LMS bifurcating into LAD and LCX); (3) coronary arteries originate from the aortic wall with an angle of 45°-90°, follow an extramural (subepicardial) course, provide adequate branches for the perfusion of myocardium and terminate at the capillary bed distally; and (4) RCA perfuses the right ventricular free wall, LAD perfuses the anteroapical wall and the obtuse marginal branch of LCX perfuses the free wall of the left ventricle (essential perfusion territories).

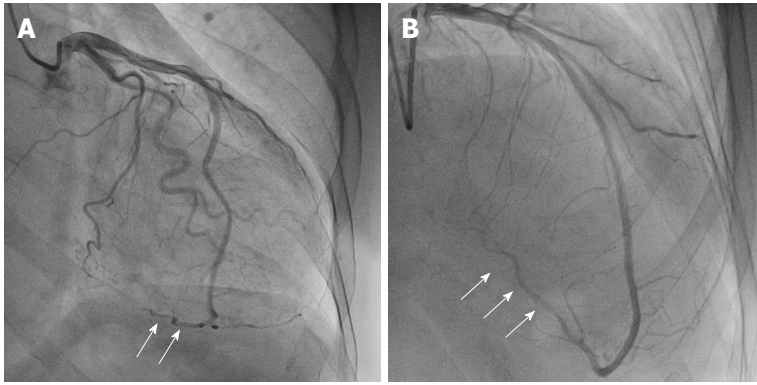


Figure 1 Wrap-around left anterior descending artery. A, B: Angiographic views of a large left anterior descending artery that wraps around the apex of the heart and supplies blood to part of the inferior wall (arrows) in anteroposterior caudal (A) and cranial view (B). From the authors' personal dataset.

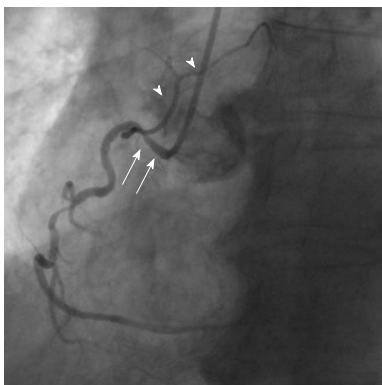


Figure 2 Shepherd's crook right coronary artery. Arrows show the prominent ascending course of proximal right coronary artery segment and an equally prominent, almost 180° switchback turn (left anterior oblique view). Arrowheads show the sinoatrial branch. From the authors' personal dataset.

CORONARY ARTERY VARIANTS

Based on the 1% rule mentioned above, frequent variations of the coronary arteries like those involving coronary dominance, take-off and course, supply of the inferior wall, the sinoatrial and atrioventricular nodes as well as the presence of a separate conus branch, a ramus intermedius branch and myocardial bridging fall within the limits of normality. The PDA usually arises from the RCA, in which case we have right coronary dominance (in 70% of the population); however, it may also arise from the LCX (left dominance - 10% of cases) or both (co-dominance - 20%)^[7].

Supply of the inferior wall may also present several variations. The PDA may be very small or have an early take-off. In the case of a small PDA, perfusion of the inferior wall is usually provided by RCA, LCX and obtuse marginal branches. Occasionally LAD may be a very long vessel that goes beyond the apex of the heart and reaches the inferior interventricular groove, thus perfusing the apical inferior wall of the heart (wraparound LAD) (Figure 1)^[8].

The sinoatrial branch supplies the sinoatrial node and usually arises from the proximal RCA in 60% of cases (Figure 2). However, it may also arise from the proximal

LCX or more rarely from the distal segment of either of these vessels^[9]. The atrioventricular nodal branch that provides blood to the atrioventricular node usually arises from the distal segment of whichever artery is dominant, RCA (more frequently) or LCX^[7].

Another frequent normal variant is the presence of a ramus intermedius branch. In this case, the LMS trifurcates into three branches instead of two as usual, the LAD, the LCX and the ramus intermedius branch. This branch usually takes the route of a diagonal or obtuse marginal branch and supplies the lateral and inferior walls of the heart^[10].

Other normal variants include an acute take-off of the LCX, in which case there is an angle $< 45^\circ$ between the LMS and the LCX, probably caused by a distal point of origin of the LCX^[11]. A "shepherd's crook" RCA, in which the RCA follows a tortuous and high course with a prominent ascending course of its proximal segment and an equally prominent, almost 180° switchback turn (Figure 2), may comprise a technical challenge in interventional cardiology due to the poor support provided by the guiding catheters^[7]. Other variants include separate origin of the conus branch directly from the right sinus of Valsalva^[12], presence of a descending septal branch originating from the RCA that supplies part of the basal interventricular septum (Figure 3) and high take-off of a coronary ostium (5 mm or more above the aortic sinotubular junction), in which case the affected coronary artery (usually the RCA) takes an intramural course within the wall of the ascending aorta and is then externalized at its normal origin site^[7,13-15].

All aforementioned variants are clinically benign and pose no threat to patients. Usually they are incidental findings during coronary angiography performed for other reasons and do not require any diagnostic work-up, further investigation or treatment. At most, some of them, like the shepherd's crook RCA, may present technical challenges during coronary intervention for other issues, due to difficulty in engaging angiographic catheters and guides. In addition, a descending septal branch, which originates from the RCA and supplies part of the interventricular septum, may be used as a target

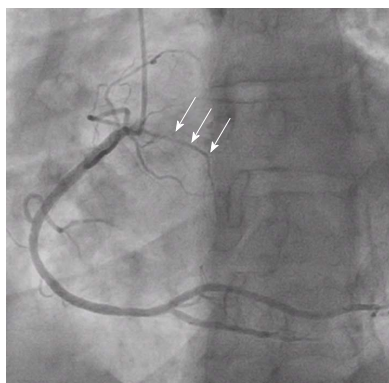


Figure 3 Descending septal branch. A branch of proximal right coronary artery (arrows) providing blood to part of the basal interventricular septum (left anterior oblique view with shallow cranial angulation). This branch may occasionally have a separate origin from the right sinus of Valsalva. From the authors' personal dataset.

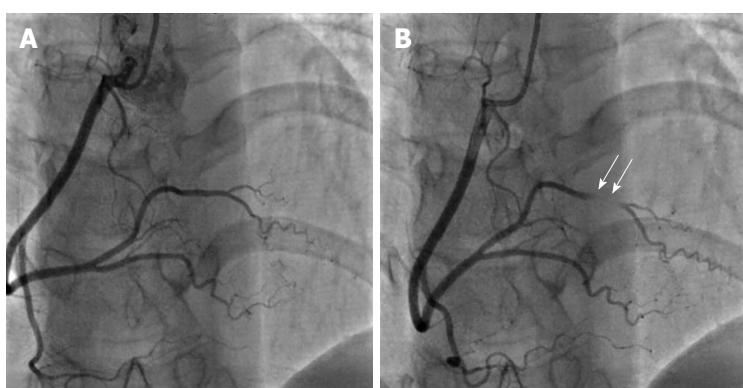


Figure 4 Myocardial bridging. A: Anteroposterior view with cranial angulation shows normal appearance of right coronary artery in diastole; B: Complete obliteration of a short segment of the posterolateral branch in systole (arrows) due to myocardial bridging. From the authors' personal dataset.

for alcohol septal ablation in symptomatic patients with hypertrophic obstructive cardiomyopathy whose basal septum is supplied by this branch of the RCA. In addition, a descending septal branch from the RCA may be an important source of collateral retrograde filling of a proximally occluded LAD.

MYOCARDIAL BRIDGING: ANOMALY OR VARIANT?

There is some confusion whether myocardial bridges constitute an anomaly or a normal variation. The prevalence of myocardial bridging varies between 0.15%-25% angiographically and 5%-86% at autopsy, and therefore its frequency in the general population suggests that it should be considered a normal variant^[1,3,5,16]. A myocardial bridge is defined as an atypical course of a coronary artery intramyocardially, which may result in compression of the vessel during systole (Figure 4). It must be pointed out that myocardial bridging is a fixed defect that is entirely different to the dynamic phenomenon of coronary artery spasm. Coronary spasm entails intense vasoconstriction of an epicardial coronary artery due to hyper-reactivity of vascular smooth muscle cells and occasionally some degree of endothelial

dysfunction in the presence of vasoconstrictor stimuli, leading to occlusion or near occlusion of the vessel and symptoms of Prinzmetal angina or acute coronary syndrome. Myocardial bridging usually involves the proximal and mid segment of the LAD and the length of the intramyocardial segment ranges between 10 and 50 mm. Patients with myocardial bridging are usually asymptomatic and the condition is considered benign^[17]. However, there have been reports of rare cases of myocardial bridging related to ischemia and atypical angina. Possible causes are endothelial dysfunction, a delay in the diastolic reopening of the intramyocardial segment of the artery that was compressed during systole and a deeper intramyocardial course of the bridge, as opposed to the more benign superficial myocardial bridges^[18-20]. Endothelial dysfunction is frequent in cases of myocardial bridging and may be revealed by functional studies, like intracoronary acetylcholine challenge. Any kind of percutaneous intervention on myocardial bridges is not supported at present due to the risks involved (restenosis, crushing and fracture of the stent)^[4,21].

The presence of myocardial bridging in patients with hypertrophic cardiomyopathy (HCM) is a point of contention both in terms of clinical significance and

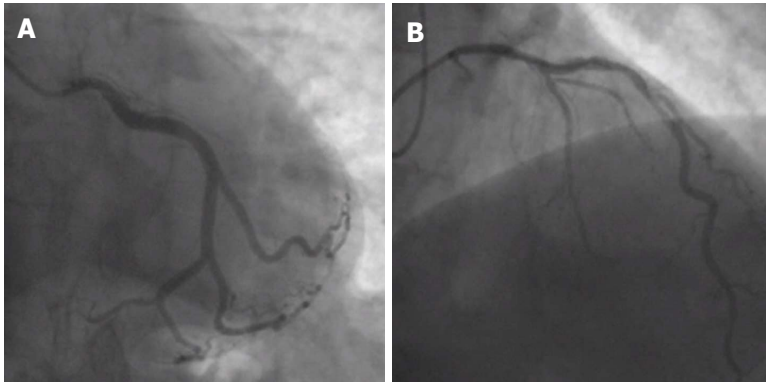


Figure 5 Absence of left main stem. A, B: Separate ostia of left circumflex artery (A, anteroposterior caudal view) and left anterior descending artery (B, shallow right anterior oblique view with cranial angulation) indicating a congenital absence of left main stem. From the authors' personal dataset.

therapeutic management. Myocardial bridging is much more frequent in patients with HCM compared to the general population, with a prevalence of up to 30%^[22]. In HCM patients, myocardial bridging tends to be of the deep intramyocardial course of the LAD variety, but it does not seem to affect the prognosis and risk of sudden death in adults^[22-24]. Therefore, in adult asymptomatic patients with HCM, myocardial bridging appears to be a benign condition that does not warrant any treatment. However, the issue remains open regarding younger and/or symptomatic patients with HCM. Myocardial bridging has not been ruled out as a possible cause of ischemia and sudden death in younger individuals with HCM and may be associated with angina symptoms in adult patients. Provided there is a positive test for functional ischemia in the LAD territory, treatment with stent implantation, coronary artery bypass surgery or surgical unroofing *via* supra-arterial myotomy may improve quality of life in adult symptomatic patients with HCM and documented myocardial bridging, as well as reduce risk of sudden cardiac death and alleviate symptoms in younger patients^[23].

CLASSIFICATION OF CORONARY ARTERY ANOMALIES

Several classification schemes have been proposed for coronary artery anomalies. Based on clinical significance some authors categorize them as major and minor. Based on functional relevance they can be classified as: (1) anomalies that are associated with definite ischemia (for example, anomalous origin of the LMS from the pulmonary artery or atresia of a coronary artery); (2) anomalies that are not associated with ischemia (for example, separate ostia of LAD and LCX with absence of LMS, split LAD or split RCA); and (3) anomalies with exceptional ischemia (like anomalous origin of coronary artery from the contralateral sinus and coronary fistulae). However, the most detailed and accurate classification has been proposed by Angelini^[3] and is based on anatomical features. According to this classification, coronary anomalies can be characterized

as: (1) anomalies of origination and course of coronaries (separate ostia of LAD and LCX, anomalous location of coronary ostia within the aortic root, outside the sinuses of Valsalva or at the contralateral sinus, single coronary artery); (2) anomalies of intrinsic coronary anatomy (split RCA/LAD, ostial stenosis/atresia, ectasia, hypoplasia, intramural course/bridging, absent coronary artery, ectopic origin of first septal branch, ectopic origin of PDA from the LAD or a septal branch); (3) anomalies of coronary termination (mainly fistulas); and (4) anomalous collateral vessels.

Table 1 summarizes the most common variations, aberrations and anomalies for coronary anatomy, based on anomalies of origin, course, intrinsic coronary anatomy and termination.

ANOMALIES OF ORIGATION AND COURSE

Absence of LMS

Absence of the LMS (separate ostia of LAD and LCX) is the most common coronary anomaly, with an incidence ranging between 0.41%-0.67% (Figure 5). It is a benign anomaly that causes no hemodynamic impairment or ischemic consequences^[15,25].

Anomalous location of coronary ostia

A coronary ostium may have an anomalous origin but may be still located within the proper coronary sinus; in those cases, the coronary ostium may originate from a higher position or a lower position compared to the normal site of origin, or may stem from the commissural level. On the other hand, when the anomalous coronary ostium is located outside the proper coronary sinuses, it can present in a wide variety of locations, like the non-coronary sinus of Valsalva, the ventricles and ectopic sites in the aorta or the large arteries (ascending or descending aorta, anonymous artery, carotid arteries), or even smaller arteries (bronchial arteries, internal thoracic artery, etc). Anomalous origin of a coronary artery from the contralateral sinus of Valsalva is particularly interesting from a clinical point of view,

Table 1 Classification of coronary artery variants, aberrations and anomalies

| |
|--|
| Variations/anomalies of origin and course |
| 1 Separate ostia of LAD and LCX (absent left main stem) |
| 2 Separate ostium of conus branch |
| 3 Anomalous location of coronary ostium |
| Within sinuses of Valsalva |
| High, low or commissural |
| From posterior ("non-coronary") sinus |
| Outside sinuses of Valsalva |
| Ascending aorta, aortic arch, innominate artery |
| Descending aorta |
| Bronchial arteries |
| Pulmonary arteries |
| Anomalous origin from contralateral sinus |
| 4 Single coronary artery |
| Variations/anomalies of intrinsic coronary anatomy |
| 1 Trifurcation of left main (presence of ramus branch) |
| 2 Wrap-around LAD (supplying apical inferior wall) |
| 3 Descending septal branch from RCA (supplying basal septum) |
| 4 Split RCA |
| 5 Split LAD |
| 6 Hypoplasia of coronary artery |
| 7 Atresia of coronary artery |
| 8 Ectasia of coronary arteries |
| 9 Myocardial bridging |
| Anomalies of coronary termination |
| 1 Fistulas |
| 2 Small number of arteriolar/capillary ramifications |

LAD: Left anterior descending artery; LCX: Left circumflex artery; RCA: Right coronary artery.

because these anomalies can be associated with sudden cardiac death, especially when the anomalous coronary artery crosses interarterially between the aorta and the pulmonary artery^[26-30].

Anomalous origin of coronary ostium from contralateral sinus

A coronary artery that originates from the contralateral sinus of Valsalva can follow five potential paths towards its perfusion territory: (1) pre-pulmonic, anterior to the right ventricular outflow tract (usually benign, though rarely associated with angina); (2) retro-aortic, posterior to the aortic root (no hemodynamic consequences); (3) trans-septal, with a subpulmonic intramyocardial course; (4) retro-cardiac, behind the mitral and tricuspid valves, in the posterior atrioventricular groove; and (5) inter-arterial, between the aorta and the pulmonary artery^[1-3].

The inter-arterial path has clinical significance, as it has been associated with an increased risk of sudden cardiac death, especially in young athletes^[1-4,31,32]. The causes are not clear and several explanations have been proposed. In some cases, autopsy findings have shown an acute angle in the take-off of the anomalous coronary artery with a slit-like lumen and a proximal course between the aorta and the pulmonary trunk^[2]. In other cases, histological examination has also shown an intramural course of the anomalous coronary within the aortic wall. It has been proposed that the

acute angulation and slit-like ostium of the anomalous coronary vessel predispose to myocardial ischemia. Exercise-induced expansion of the aortic root and the pulmonary trunk compresses and exacerbates the slit-like ostium, resulting in further ischemia^[4,6,33,34]. A scissors-like mechanism that compresses the anomalous coronary between the aorta and the pulmonary artery has also been suggested^[3,35]. Intravascular ultrasound studies have demonstrated an intramural proximal intussusception of the ectopic artery at the aortic wall for a variable distance^[36,37]. The intussuscepted segment of the vessel is smaller in circumference compared to its more distal segment (circumferential hypoplasia), and its cross-section is ovoid instead of circular. These parameters lead to a lateral luminal compression that is present throughout the whole of the cardiac cycle but even more pronounced during systole^[3,37]. Furthermore, the intramural segment has thin inner and outer aortic wall layers. Therefore, the section of the aorta that is penetrated by the ectopic artery is a localized weak spot, prone to more extensive distensibility, which can further exacerbate stenosis and ischemia^[37].

Ectopic RCA originating from the left sinus of Valsalva has a frequency of 0.03%-0.92% (Figure 6), and ectopic LAD arising from the RSV has a frequency of 0.03% (Figure 7)^[1]. Both of these anomalies may be associated with an intramural inter-arterial course, in which case there is an increased risk of sudden cardiac death. Ectopic origin of the LCX from the right sinus of Valsalva (Figure 8) or from the proximal RCA is the second most common coronary artery anomaly, with a frequency of 0.37%^[1,14,38,39], but it is considered benign and the course of the ectopic LCX is usually retroaortic or retrocardiac^[4,15].

It must be noted that anomalous origin of a coronary artery from an opposite sinus of Valsalva is related with sudden death mostly in young athletes < 35 years old but less frequently in older patients. Symptoms like angina, syncope, heart failure and myocardial infarction may appear in both age groups but are seen more frequently in older patients. It has been proposed that stiffening of the aortic wall in older adults is the reason why sudden death is less frequent in this age group^[3,40]. Diagnosis of anomalous origin of a coronary artery from the contralateral sinus is often difficult, since most of the times patients are asymptomatic prior to sudden cardiac death. However, there have been some reports of premonitory symptoms like syncope or chest pain prior to sudden death^[2,41,42]. Diagnostic workup in patients with the above symptoms (especially young athletes) must include electrocardiography, Holter monitoring and focused expert echocardiography. If at least two normally located coronary ostia can be identified with echocardiography, no further investigations are needed^[3]. However, if echocardiographic findings are inconclusive, further imaging with computed tomography or magnetic resonance imaging is recommended^[3,43-45]. Treadmill evaluation is unfortunately hampered by a high incidence of false positive and false negative

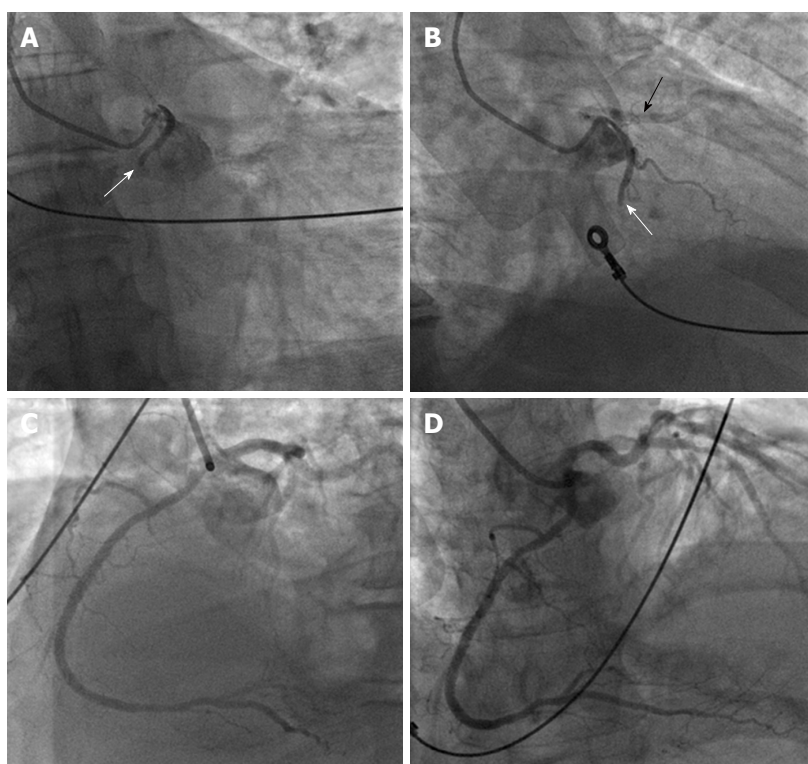


Figure 6 Ectopic right coronary artery originating from the left sinus of Valsalva. A, B: Proximal occlusion of anomalous right coronary artery (RCA) (white arrows) with origin from the left sinus of Valsalva in a patient with inferior wall ST elevation myocardial infarction (A: anteroposterior caudal view; B: right anterior oblique view). The black arrow in panel B shows a patent proximal left anterior descending artery in non-selective angiography of the left coronary artery (LCA); C, D: Left anterior oblique view with cranial angulation (C) and anteroposterior cranial view (D) show the LCA and an excellent final angiographic of the anomalous RCA after successful primary percutaneous coronary intervention. From the authors' personal data and from Ref.[73] (modified with permission).

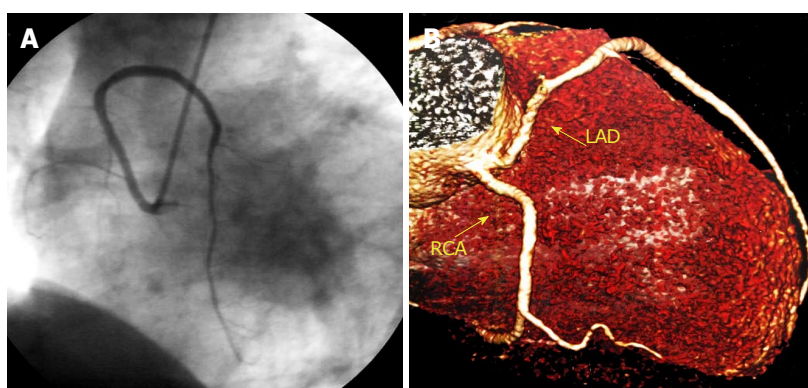


Figure 7 Ectopic left anterior descending artery originating from the right sinus of Valsalva. A: Left anterior oblique view with cranial angulation of the left anterior descending artery (LAD) originating from the right Valsalva sinus in coronary angiogram; B: Reconstructed image from computed tomography coronary angiogram showing both LAD and right coronary artery arising from the right sinus of Valsalva. From the authors' personal dataset. LAD: Left anterior descending; RCA: Right coronary artery.

results^[2,37,46]. If the anomaly is confirmed, patients should undergo nuclear stress testing to evaluate exercise-induced ischemia and to establish a baseline for follow-up. Coronary angiography may reveal additional obstructive coronary disease, and intracoronary imaging establishes the severity of the condition^[3,4]. Intravascular ultrasound and/or optical coherence tomography findings that determine the severity of an anomalous origin of a coronary artery from an opposite sinus include the length of the intramural segment, the hypoplasia index that quantifies the severity of the circumferential hypoplasia

(ratio of the circumference of the intramural segment vs the circumference of the more distal epicardial segment of the vessel), the vessel asymmetry score (ratio of transverse to longitudinal diameter in a cross-sectional image from intravascular ultrasound) and the systolic vs diastolic cross-sectional area of stenosis during a cardiac cycle at rest and during simulated exercise with infusion of saline, atropine and dobutamine (SAD test)^[4,47]. When an anomalous left coronary artery (LCA) with origin from the right sinus of Valsalva is diagnosed incidentally during coronary angiography, specific

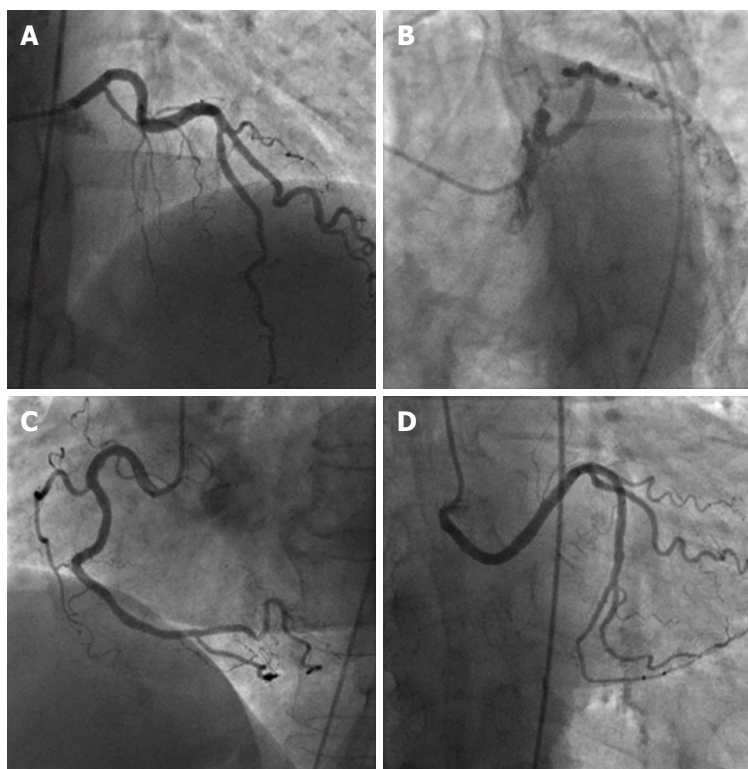


Figure 8 Ectopic left circumflex artery originating from the right sinus of Valsalva. A, B: Left coronary artery providing left anterior descending artery, with absence of left circumflex artery (LCX) (A: anteroposterior cranial view; B: left anterior oblique view with caudal angulation); C, D: Separate origin of right coronary artery (C, left anterior oblique view) and aberrant LCX from the right sinus of Valsalva (D, anteroposterior caudal view). From the authors' personal dataset.

angiographic anatomical findings help differentiate between the inter-arterial and the more benign trans-septal varieties of this anomaly, since in the trans-septal origin the LMS gives rise to the first septal branch, presents a mild concentric myocardial bridge effect at the distal segment and connects with mid-LAD^[4]. However, computed tomography remains the most accurate method to characterize the course of ectopic coronary arteries.

Asymptomatic patients with anomalous RCA arising from the left sinus of Valsalva with a negative nuclear stress test need regular follow-up only. Symptomatic patients and asymptomatic patients with a positive nuclear stress test must be further assessed with intra-coronary imaging with intravascular ultrasound or optical coherence tomography, and if a significant stenosis or high risk features are found, percutaneous coronary intervention with stent^[3,36,48] or surgical repair should be offered. Patients with anomalous LMS arising from the right sinus of Valsalva should undergo surgical repair regardless of symptoms, if younger than 35 years old. Older patients should undergo surgery if they develop symptoms or if they have a positive nuclear stress test^[4]. Surgical options include osteoplasty (creation of a new ostium at the end of the ectopic artery's intramural segment), direct reimplantation of the ectopic artery at the aortic root (a challenging procedure) and unroofing of the intramural segment (excising of the common wall located between the aorta and the anomalous coronary)^[4,33,49-51]. Currently, unroofing is the most

favorable of these procedures. Bypass surgery with an internal mammary artery is not preferred, because of the high risk of regression of the graft lumen due to competitive flow^[4,52,53].

Anomalous origin of coronary arteries outside the aortic root

The most dramatic clinical appearance in this group of congenital coronary anomalies occurs when the ectopic coronary arises from the pulmonary artery. The RCA originates from the pulmonary artery in 0.002% of the general population. In this anomaly, blood flows from the LCA to the RCA *via* collaterals and further back into the pulmonary artery. Most patients with this anomaly are asymptomatic; however, sudden cardiac death, heart failure and syncope have been occasionally reported^[1,15,25].

Anomalous origin of the LCA from the pulmonary artery (ALCAPA) is called Bland-White-Garland syndrome and has a low prevalence of 0.008%. The RCA is dilated and provides extensive collaterals to LCA. This condition may coexist with aortic coarctation and a patent ductus arteriosus. Most patients (about 85%) develop symptoms of myocardial ischemia and heart failure in infancy (Figure 9) and die within the first year of life. However, a minority of patients may remain asymptomatic and survive into adulthood, probably because of adequate blood flow to the LCA territory from the RCA collaterals (Figure 10). Treatment is surgical and reimplantation of the LMS onto the aorta is

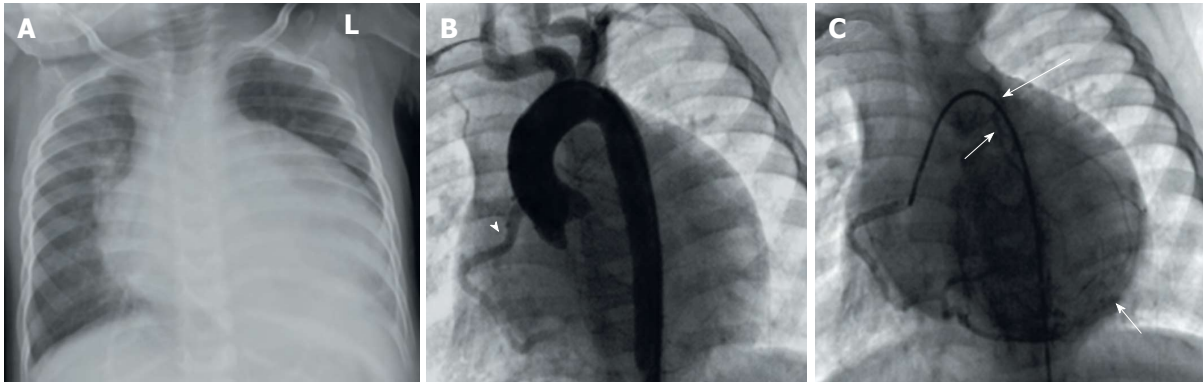


Figure 9 Anomalous origin of the left coronary artery from the pulmonary artery in infant. A: Cardiomegaly in chest X-ray; B: Aortogram showing only right coronary artery (RCA) originating from the aortic sinuses (arrowhead) but no left coronary artery; C: Selective angiography of RCA shows extensive collaterals from the RCA backfilling the left system and the pulmonary artery (arrows). Reproduced from ref. [74].

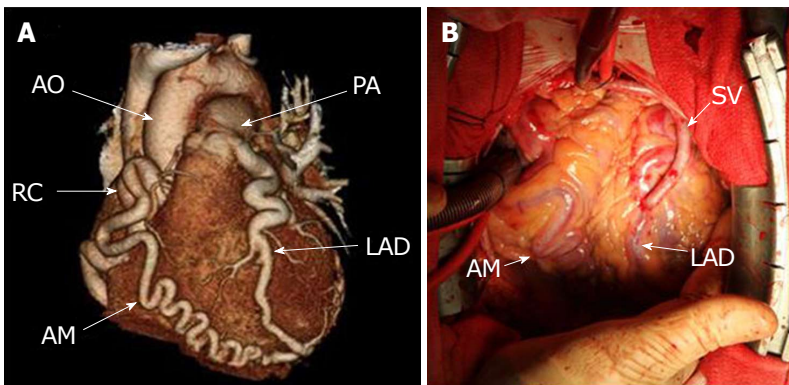


Figure 10 Anomalous origin of the left coronary artery from the pulmonary artery in adult. A: Three-dimensional reconstruction of computed tomography images showing prominent collaterals from right coronary artery to the left anterior descending artery (LAD), while LAD originates from the pulmonary artery; B: Coronary bypass grafting with a saphenous vein graft to the LAD. Reproduced from ref. [75]. SV: Saphenous vein; RC: Right coronary; LAD: Left anterior descending.

the preferred method. However, the procedure is more technically challenging in adults due to the frailty of the coronary artery. Ligation of the LCA ostium and coronary artery bypass grafting with venous or arterial grafts is a viable alternative in these cases (Figure 10)^[14,15,25,54,55]. The LAD arises from the pulmonary artery extremely rarely in 0.0008% of the general population and is associated with myocardial ischemia and sudden cardiac death^[1,15,38]. There have also been reports of all coronary arteries originating from the pulmonary artery. Patients die within the first month of life, and the condition frequently coexists with patent ductus arteriosus and other major congenital cardiac anomalies^[25,56]. Finally, cases of accessory coronary arteries arising from the pulmonary artery have been documented. The most frequent artery involved is the conus branch, and this anomaly has no clinical significance^[1,25].

Single coronary artery

There have been several reports of presence of a single coronary artery with a variety of anatomies. A single coronary artery may originate either from the left or the right Valsalva sinus and may sometimes coexist with other congenital anomalies^[1]. Lipton *et al.*^[57] proposed an anatomical classification of single coronary arteries

based on location of the ostium (R: right Valsalva sinus, L: left Valsalva sinus), anatomical distribution (I: single coronary artery following course of normal left or RCA, II: a coronary artery with abnormal origin from the proximal segment of the other coronary artery, III: single coronary artery with a origin from the right Valsalva sinus, with the LAD and LCX originating separately from the common trunk) and course of the transverse trunk (A: anterior course to the great vessels, B: between the aorta and the pulmonary artery, P: posterior course, S: septal course, C: combined type).

When the single coronary artery has an origin from the left sinus, the RCA may originate from the proximal or mid segment of the LAD and follows a course anterior to the pulmonary artery or between the aorta and the pulmonary artery towards the right atrioventricular groove (Figure 11). The prevalence of this anomaly is around 0.024%-0.066% in the general population^[1,58,59]. This anomaly is usually benign, provided that the course of the anomalous RCA is not inter-arterial. If, however, the anomalous RCA crosses between the aorta and the pulmonary artery, myocardial ischemia and sudden cardiac death may occur^[29,58,60,61]. Rarely, the RCA may be supplied by the distal LCX (Figure 12).

When the single coronary artery originates from

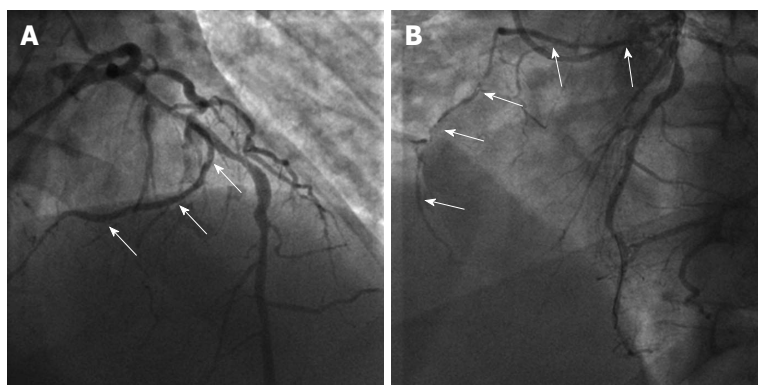


Figure 11 Single coronary artery from the left sinus. A, B: Angiographic images showing the origin (arrows in A, anteroposterior cranial view) and course (arrows in B, left anterior oblique view) of the right coronary artery from the mid segment of left anterior descending artery. From the authors' personal dataset and from Ref. [76] (modified with permission).

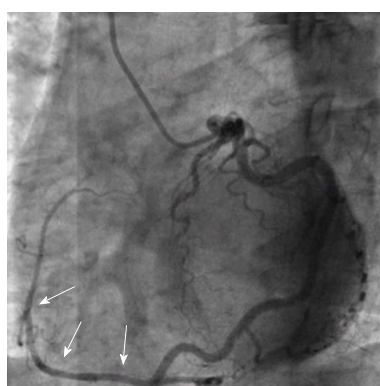


Figure 12 Single coronary artery from the left sinus. Angiographic images showing the origin and course (arrows) of the aberrant right coronary artery from the distal segment of left circumflex artery (left anterior oblique view). From the authors' personal dataset.

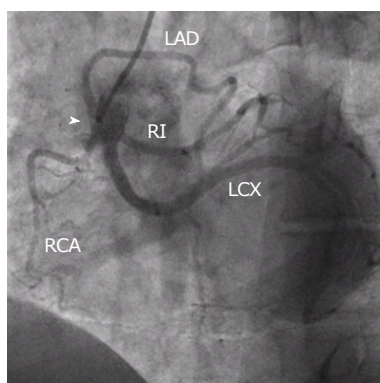


Figure 13 Single coronary artery originating from the right sinus. Common trunk from the right sinus (arrowhead) providing right coronary artery, left anterior descending artery, left circumflex artery and ramus intermedius. From the authors' personal dataset. RCA: Right coronary artery; LAD: Left anterior descending; LCX: Left circumflex artery; RI: Ramus intermedius.

the right sinus (Figure 13), the LCA follows an anterior or inter-arterial path towards its perfusion territory. Prevalence is around 0.02%-0.05%, and this condition is associated with sudden cardiac death more frequently than an anomalous single coronary artery originating from the left sinus. The anterior variant is usually - but

not always - benign, whereas the inter-arterial variant is the potentially most threatening one^[1,15,62].

ANOMALIES OF INTRINSIC CORONARY ANATOMY

Split RCA

A split RCA is the most common type of coronary artery anomaly, with a frequency around 1% in the general population. It is a benign anomaly in which the RCA has a split PDA (Figure 14). The split RCA is divided early into an anterior and posterior branch. The anterior branch runs through the free wall of the right ventricle and supplies a PDA that follows the distal posterior interventricular groove, whereas the posterior branch follows the right atrioventricular groove and leads to a PDA that runs through the proximal segment of the posterior interventricular groove^[1,63-65].

Split LAD

There have been reported four types of split LAD. In types 1-3, the LAD branches into two subdivisions, a short one that terminates high in the anterior interventricular groove and a longer one that branches off the proper LAD, descends on the left (type 1) or the right (type 2) ventricular side of the anterior interventricular groove or intramyocardially (type 3) and finally reenters the anterior interventricular groove distally. Sometimes in type 3 the intramyocardial LAD never emerges but instead provides septal branches to the apical septum. Type 4 is an entirely different entity, in which a short LAD originates from the LMS and terminates high in the anterior interventricular groove, while a duplicated LAD arises from the RCA and follows a pre-pulmonic, septal or inter-arterial course towards the distal anterior interventricular groove. This anomaly is relatively benign; however, it may complicate significantly surgical intervention^[7,66,67].

Atresia of LMS

True atresia of the LMS is an extremely rare congenital

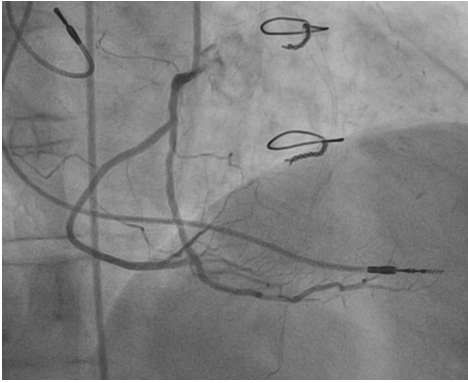


Figure 14 Split right coronary artery. Right coronary artery is divided early into two branches, both of which supply posterior descending arteries. From the authors' personal dataset.

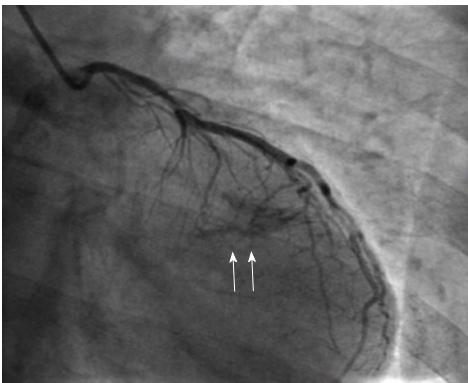


Figure 15 Coronary fistula. Opacification of the left ventricle during injection of the left coronary artery (arrows) indicate the presence of a fistula. From the authors' personal dataset.

disorder in which there is neither left coronary ostium nor LMS. The LAD and the LCX connect but end blindly proximally. The left system receives blood retrogradely *via* collaterals from the RCA, but in most cases blood flow is inadequate for the needs of the perfusion territory, resulting in symptoms of myocardial ischemia and an increased risk of sudden cardiac death. This condition often coexists with supraaortic stenosis and other congenital cardiac defects. Patients usually become symptomatic during infancy or early childhood, but there have been reports of patients who remained asymptomatic during childhood and young adulthood and developed symptoms later in life. Due to poor prognosis, atresia of the LMS requires surgical intervention with coronary artery bypass grafting and an internal mammary artery graft to the LAD in adults, whereas in children surgical reconstruction of the LMS with a baffle of ascending aorta may be preferable^[1,68].

Hypoplasia of coronary arteries

Congenital hypoplasia of coronary arteries presents as a narrowed luminal diameter (less than 1.5 mm) in one or two of the three main coronary arteries with no compensatory branches. Limitations to blood flow caused by the narrow lumen lead to symptoms of myocardial

ischemia and sudden cardiac death. Most frequent variants in reported cases are hypoplasia of both LCX and RCA and hypoplasia of the LAD. Treatment options are extremely limited. Transmyocardial revascularization and implantable cardioverter-defibrillator have been suggested in the literature^[13,69-71].

ANOMALIES OF CORONARY TERMINATION

Coronary fistulae are defined as abnormal connections between the termination of a coronary artery or its branches and a low-pressure vascular space, like a cardiac chamber or a great vessel (Figure 15). They may present as small discrete fistulae or more complex arteriovenous malformations. Reported prevalence is 0.3%-0.87% in the general population. Most patients are asymptomatic; however, there have been reports of symptoms of myocardial ischemia, heart failure, arrhythmia and sudden cardiac death, pulmonary hypertension, rupture and endocarditis, usually after the age of 50.

Several mechanisms for the causes of these symptoms have been proposed. Fistulae draining into the right heart chambers (60% of cases) function as left to right shunts and may cause right ventricular volume overload. Termination in a low pressure space causes enlargement and tortuosity of the fistulous coronary artery that leads to vascular wall degeneration, aneurysmatic dilatation and predisposition to rupture. Furthermore, the dilatation of the involved coronary artery may cause distortion of the aortic root and aortic valve disruption and regurgitation. Myocardial ischemia may result from two separate mechanisms: (1) a persistent or episodic steal of blood flow from the normal coronary branches to the competing fistulous low-pressure tract; and (2) stenosis and obstruction of side branches secondary to thrombus formation related to ulceration and atherosclerosis in the aneurysmal coronary artery. Indications for closing a coronary fistula are not well established. Symptomatic patients should definitely be treated as well as patients with a pulmonary to systemic flow ratio that exceeds 1.5 and patients with severe aneurysmal degeneration. Available options are surgical closure at the drainage site or catheter-based repair with catheter occlusion devices. It is generally recommended to intervene before adulthood, since negative postoperative remodeling of the fistulous artery is much more common in children compared to adults^[4,15,17,37,38].

Furthermore, we have recently described a fistulous tract from the left ventricle to the Thebesian venous network of the myocardium^[72]. Thebesian veins are small valveless veins in the walls of all four heart chambers that act as an alternative channel of nutrition to the myocardium or as venous drainage conduits. They are more prevalent in the right heart chambers, but they can also appear in the left ventricle. We described the case of inadvertent angiography of a large



Figure 16 Inadvertent cardiac phlebography through the Thebesian network. A, B: Right anterior oblique views in systole (A) and diastole (B) during left ventriculography show a minor subendocardial staining (arrowhead) and opacification of a posterior interventricular vein (arrows), due to opening of a 'functional' fistula between the left ventricle and the cardiac vein through the Thebesian network. From the authors' personal dataset and from Ref. [72] (with permission).

posterior interventricular cardiac vein during a left ventriculogram. This happened because the end-hole of the angiographic catheter inadvertently engaged the endocardial opening of a small Thebesian vein, leading to retrograde opacification of the cardiac vein through the Thebesian network (Figure 16)^[72].

CONCLUSION

It becomes apparent that the term "coronary artery anomalies" covers a very wide spectrum of anatomical entities with diverse clinical manifestations and varying degrees of severity. Coronary artery variants have a prevalence of at least 1% in the general population and are mostly clinically benign. On the other hand, coronary artery anomalies are much more uncommon, and their clinical significance varies from benign without ischemic consequences to ischemia-related symptoms and arrhythmias leading to an increased risk of sudden cardiac death. Anomalous origin of a coronary ostium from the contralateral sinus is the anomaly most frequently associated with sudden cardiac death, in particular in the case of anomalous LCA from the right sinus or if the anomalous coronary artery has a course between the aorta and the pulmonary artery or other high-risk features. Other coronary anomalies, like anomalous origin of the LCA from the pulmonary artery or atresia of the LMS, have also been associated with extensive ischemia and high risk of sudden cardiac death early in infancy or in early adulthood. Accurate diagnosis, risk-assessment and appropriate choice of treatment are of utmost importance, since coronary artery anomalies constitute the second most common cause of sudden cardiac death in young competitive athletes. The rapid advancement of imaging techniques, including intravascular ultrasound, optical coherence, computed tomography and magnetic resonance imaging, have provided us with a wealth of new information on the subject as well as more accurate diagnostic criteria regarding the severity of these conditions that allow risk-stratification for sudden cardiac death and provide guidelines for optimal treatment. Consultation of focused experts by individual cardiologists

in cases of suspected or diagnosed coronary artery anomalies and systematic referral of diagnosed patients to specialized centers play a significant role in timely diagnosis, appropriate management and successful prevention of sudden cardiac death.

REFERENCES

- 1 **Villa AD**, Sammut E, Nair A, Rajani R, Bonamini R, Chiribiri A. Coronary artery anomalies overview: The normal and the abnormal. *World J Radiol* 2016; **8**: 537-555 [PMID: 27358682 DOI: 10.4329/wjr.v8.i6.537]
- 2 **Basso C**, Maron BJ, Corrado D, Thiene G. Clinical profile of congenital coronary artery anomalies with origin from the wrong aortic sinus leading to sudden death in young competitive athletes. *J Am Coll Cardiol* 2000; **35**: 1493-1501 [PMID: 10807452 DOI: 10.1016/S0735-1097(00)00566-0]
- 3 **Angelini P**. Coronary artery anomalies: an entity in search of an identity. *Circulation* 2007; **115**: 1296-1305 [PMID: 17353457 DOI: 10.1161/CIRCULATIONAHA.106.618082]
- 4 **Moscucci M**. Grossman and Baim's Cardiac Catheterization, Angiography, and Intervention. 8th Edition. Lippincott Williams Wilkins (LWW), 2005: 335-353
- 5 **Angelini P**, Villason S, Chan AV, Diez JG. Normal and anomalous coronary arteries in humans. In: Angelini P, ed. *Coronary Artery Anomalies: A Comprehensive Approach*. Philadelphia: Lippincott Williams Wilkins, 1999: 27-150
- 6 **Ali M**, Hanley A, McFadden EP, Vaughan CJ. Coronary artery anomalies: a practical approach to diagnosis and management. *Heart Asia* 2011; **3**: 8-12 [PMID: 27325972 DOI: 10.1136/ha.2010.003244]
- 7 **Shriki JE**, Shinbane JS, Rashid MA, Hindoyan A, Withey JG, DeFrance A, Cunningham M, Oliveira GR, Warren BH, Wilcox A. Identifying, characterizing, and classifying congenital anomalies of the coronary arteries. *Radiographics* 2012; **32**: 453-468 [PMID: 22411942 DOI: 10.1148/rg.322115097]
- 8 **Apitzsch J**, Kühl HP, Mühlenbruch G, Mahnken AH. Unusual malignant coronary artery anomaly: results of coronary angiography, MR imaging, and multislice CT. *Cardiovasc Intervent Radiol* 2010; **33**: 389-393 [PMID: 19657692 DOI: 10.1007/s00270-009-9663-y]
- 9 **Karadag B**, Ayan F, Ismailoglu Z, Goksedef D, Ataev Y, Vural VA. Extraordinary cause of ischemic chest pain in a young man: congenital ostial atresia of the right coronary artery. *J Cardiol* 2009; **54**: 335-338 [PMID: 19782277 DOI: 10.1016/j.jjcc.2009.01.008]
- 10 **Chiribiri A**, Ishida M, Nagel E, Botnar RM. Coronary imaging with cardiovascular magnetic resonance: current state of the art. *Prog Cardiovasc Dis* 2011; **54**: 240-252 [PMID: 22014491 DOI: 10.1016/j.pcad.2011.09.002]
- 11 **Angelini P**, Trujillo A, Sawaya F, Lee VV. "Acute takeoff" of the

- circumflex artery: a newly recognized coronary anatomic variant with potential clinical consequences. *Tex Heart Inst J* 2008; **35**: 28-31 [PMID: 18427647]
- 12 **Boffano C**, Chiribiri A, Cesarani F. Native whole-heart coronary imaging for the identification of anomalous origin of the coronary arteries. *Int J Cardiol* 2009; **137**: e27-e28 [PMID: 18687486 DOI: 10.1016/j.ijcard.2008.05.075]
 - 13 **Menke DM**, Waller BF, Pless JE. Hypoplastic coronary arteries and high takeoff position of the right coronary ostium. A fatal combination of congenital coronary artery anomalies in an amateur athlete. *Chest* 1985; **88**: 299-301 [PMID: 4017686 DOI: 10.1378/chest.88.2.299]
 - 14 **Frescura C**, Basso C, Thiene G, Corrado D, Pennelli T, Angelini A, Daliento L. Anomalous origin of coronary arteries and risk of sudden death: a study based on an autopsy population of congenital heart disease. *Hum Pathol* 1998; **29**: 689-695 [PMID: 9670825 DOI: 10.1016/S0046-8177(98)90277-5]
 - 15 **Yamanaka O**, Hobbs RE. Coronary artery anomalies in 126,595 patients undergoing coronary arteriography. *Cathet Cardiovasc Diagn* 1990; **21**: 28-40 [PMID: 2208265 DOI: 10.1002/ccd.1810210110]
 - 16 **Angelini P**, Trivellato M, Donis J, Leachman RD. Myocardial bridges: a review. *Prog Cardiovasc Dis* 1983; **26**: 75-88 [PMID: 6346395 DOI: 10.1016/0033-0620(83)90019-1]
 - 17 **Young PM**, Gerber TC, Williamson EE, Julsrud PR, Herfkens RJ. Cardiac imaging: Part 2, normal, variant, and anomalous configurations of the coronary vasculature. *AJR Am J Roentgenol* 2011; **197**: 816-826 [PMID: 21940568 DOI: 10.2214/AJR.10.7249]
 - 18 **Morales AR**, Romanelli R, Tate LG, Boucek RJ, de Marchena E. Intramural left anterior descending coronary artery: significance of the depth of the muscular tunnel. *Hum Pathol* 1993; **24**: 693-701 [PMID: 8319950 DOI: 10.1016/0046-8177(93)90004-Z]
 - 19 **Ferreira AG Jr**, Trotter SE, König B Jr, Décourt LV, Fox K, Olsen EG. Myocardial bridges: morphological and functional aspects. *Br Heart J* 1991; **66**: 364-367 [PMID: 1747296 DOI: 10.1136/hrt.66.5.364]
 - 20 **Kumari M**, Rha SW, Poddar KL, Park JY, Choi BG, Kim YK, Na JO, Choi CU, Lim HE, Kim JW, Park CG, Seo HS, Oh DG. Clinical and angiographic characteristics of coronary endothelial dysfunction severity in patients with myocardial bridge as assessed by acetylcholine provocation test. *J Am Coll Cardiol* 2011; **57**: E1513 [DOI: 10.1016/S0735-1097(11)61513-1]
 - 21 **Haager PK**, Schwarz ER, vom Dahl J, Klues HG, Reffellmann T, Hanrath P. Long term angiographic and clinical follow up in patients with stent implantation for symptomatic myocardial bridging. *Heart* 2000; **84**: 403-408 [PMID: 10995410 DOI: 10.1136/heart.84.4.403]
 - 22 **Sorajja P**, Ommen SR, Nishimura RA, Gersh BJ, Tajik AJ, Holmes DR. Myocardial bridging in adult patients with hypertrophic cardiomyopathy. *J Am Coll Cardiol* 2003; **42**: 889-894 [PMID: 12957438 DOI: 10.1016/S0735-1097(03)00854-4]
 - 23 **Basso C**, Thiene G, Mackey-Bojack S, Frigo AC, Corrado D, Maron BJ. Myocardial bridging, a frequent component of the hypertrophic cardiomyopathy phenotype, lacks systematic association with sudden cardiac death. *Eur Heart J* 2009; **30**: 1627-1634 [PMID: 19406869 DOI: 10.1093/eurheartj/ehp121]
 - 24 **Olivetto I**, Cecchi F, Yacoub MH. Myocardial bridging and sudden death in hypertrophic cardiomyopathy: Salome drops another veil. *Eur Heart J* 2009; **30**: 1549-1550 [PMID: 19491131 DOI: 10.1093/eurheartj/ehp216]
 - 25 **Roberts WC**. Major anomalies of coronary arterial origin seen in adulthood. *Am Heart J* 1986; **111**: 941-963 [PMID: 3518378 DOI: 10.1016/0002-8703(86)90646-0]
 - 26 **Corrado D**, Thiene G, Nava A, Rossi L, Pennelli N. Sudden death in young competitive athletes: clinicopathologic correlations in 22 cases. *Am J Med* 1990; **89**: 588-596 [PMID: 2239978 DOI: 10.1016/0002-9343(90)90176-E]
 - 27 **Thiene G**, Nava A, Corrado D, Rossi L, Pennelli N. Right ventricular cardiomyopathy and sudden death in young people. *N Engl J Med* 1988; **318**: 129-133 [PMID: 3336399 DOI: 10.1056/NEJM198801213180301]
 - 28 **Burke AP**, Farb A, Virmani R, Goodin J, Smialek JE. Sports-related and non-sports-related sudden cardiac death in young adults. *Am Heart J* 1991; **121**: 568-575 [PMID: 1825009 DOI: 10.1016/0002-8703(91)90727-Y]
 - 29 **Liberthson RR**. Sudden death from cardiac causes in children and young adults. *N Engl J Med* 1996; **334**: 1039-1044 [PMID: 8598843 DOI: 10.1056/NEJM199604183341607]
 - 30 **Corrado D**, Basso C, Schiavon M, Thiene G. Screening for hypertrophic cardiomyopathy in young athletes. *N Engl J Med* 1998; **339**: 364-369 [PMID: 9691102 DOI: 10.1056/NEJM199808063390602]
 - 31 **Van Camp SP**, Bloor CM, Mueller FO, Cantu RC, Olson HG. Nontraumatic sports death in high school and college athletes. *Med Sci Sports Exerc* 1995; **27**: 641-647 [PMID: 7674867 DOI: 10.1249/0005768-199505000-00005]
 - 32 **Taylor AJ**, Rogan KM, Virmani R. Sudden cardiac death associated with isolated congenital coronary artery anomalies. *J Am Coll Cardiol* 1992; **20**: 640-647 [PMID: 1512344 DOI: 10.1016/0735-1097(92)90019-J]
 - 33 **Mustafa I**, Gula G, Radley-Smith R, Durrer S, Yacoub M. Anomalous origin of the left coronary artery from the anterior aortic sinus: a potential cause of sudden death. Anatomic characterization and surgical treatment. *J Thorac Cardiovasc Surg* 1981; **82**: 297-300 [PMID: 7253693]
 - 34 **Barriales-Villa R**, Moris de la Tassa C. Congenital coronary artery anomalies with origin in the contralateral sinus of Valsalva: which approach should we take?. *Rev Esp Cardiol* 2006; **59**: 360-370 [PMID: 16709389 DOI: 10.1157/13087058]
 - 35 **Grollman JH Jr**, Mao SS, Weinstein SR. Arteriographic demonstration of both kinking at the origin and compression between the great vessels of an anomalous right coronary artery arising in common with a left coronary artery from above the left sinus of Valsalva. *Cathet Cardiovasc Diagn* 1992; **25**: 46-51 [PMID: 1555225 DOI: 10.1002/ccd.1810250110]
 - 36 **Angelini P**, Velasco JA, Ott D, Khoshnevis GR. Anomalous coronary artery arising from the opposite sinus: descriptive features and pathophysiologic mechanisms, as documented by intravascular ultrasonography. *J Invasive Cardiol* 2003; **15**: 507-514 [PMID: 12947211]
 - 37 **Angelini P**. Coronary artery anomalies--current clinical issues: definitions, classification, incidence, clinical relevance, and treatment guidelines. *Tex Heart Inst J* 2002; **29**: 271-278 [PMID: 12484611]
 - 38 **Baltaxe HA**, Wixson D. The incidence of congenital anomalies of the coronary arteries in the adult population. *Radiology* 1977; **122**: 47-52 [PMID: 830353 DOI: 10.1148/122.1.47]
 - 39 **Bunce NH**, Lorenz CH, Keegan J, Lesser J, Reyes EM, Firmin DN, Pennell DJ. Coronary artery anomalies: assessment with free-breathing three-dimensional coronary MR angiography. *Radiology* 2003; **227**: 201-208 [PMID: 12601193 DOI: 10.1148/radiol.2271020316]
 - 40 **Cheitlin MD**. Coronary anomalies as a cause of sudden death in the athlete. In: Estes NAM, Salem DN, Wang JJP, eds. Sudden Cardiac Death in the Athlete. Armonk NY: Futura Publishing Co, 1998, 379-391
 - 41 **Roberts WC**, Siegel RJ, Zipes DP. Origin of the right coronary artery from the left sinus of valsalva and its functional consequences: analysis of 10 necropsy patients. *Am J Cardiol* 1982; **49**: 863-868 [PMID: 7064835 DOI: 10.1016/0002-9149(82)91970-1]
 - 42 **Ghosh PK**, Agarwal SK, Kumar R, Chandra N, Puri VK. Anomalous origin of right coronary artery from left aortic sinus. *J Cardiovasc Surg (Torino)* 1994; **35**: 65-70 [PMID: 8120081]
 - 43 **Angelini P**, Velasco JA, Flamm S. Coronary anomalies: incidence, pathophysiology, and clinical relevance. *Circulation* 2002; **105**: 2449-2454 [PMID: 12021235 DOI: 10.1161/01.CIR.0000016175.49835.57]
 - 44 **Hejmadi A**, Sahn DJ. What is the most effective method of detecting anomalous coronary origin in symptomatic patients? *J Am Coll Cardiol* 2003; **42**: 155-157 [PMID: 12849676 DOI: 10.1016/S0735-1097(03)00510-2]
 - 45 **Post JC**, van Rossum AC, Bronzwaer JG, de Cock CC, Hofman MB, Valk J, Visser CA. Magnetic resonance angiography of anomalous coronary arteries. A new gold standard for delineating the proximal

- course? *Circulation* 1995; **92**: 3163-3171 [PMID: 7586299 DOI: 10.1161/01.CIR.92.11.3163]
- 46 **Waller BF**. Exercise-related sudden death in young (age less than or equal to 30 years) and old (age greater than 30 years) conditioned subjects. *Cardiovasc Clin* 1985; **15**: 9-73 [PMID: 4092221]
 - 47 **Angelini P**, Flamm SD. Newer concepts for imaging anomalous aortic origin of the coronary arteries in adults. *Catheter Cardiovasc Interv* 2007; **69**: 942-954 [PMID: 17486584 DOI: 10.1002/ccd.21140]
 - 48 **Hariharan R**, Kacere RD, Angelini P. Can stent-angioplasty be a valid alternative to surgery when revascularization is indicated for anomalous origination of a coronary artery from the opposite sinus? *Tex Heart Inst J* 2002; **29**: 308-313 [PMID: 12484615]
 - 49 **Van Son JA**, Haas GS. Anomalous origin of left main coronary artery from right sinus of Valsalva: modified surgical treatment to avoid neo-coronary ostial stenosis. *Eur J Cardiothorac Surg* 1996; **10**: 467-469 [PMID: 8817146 DOI: 10.1016/S1010-7940(96)80118-7]
 - 50 **Angelini P**, Walmsley RP, Liberos A, Ott DA. Symptomatic anomalous origination of the left coronary artery from the opposite sinus of valsalva. Clinical presentations, diagnosis, and surgical repair. *Tex Heart Inst J* 2006; **33**: 171-179 [PMID: 16878619]
 - 51 **García-Rinaldi R**, Sosa J, Olmeda S, Cruz H, Carballido J, Quintana C. Surgical treatment of right coronary arteries with anomalous origin and slit ostium. *Ann Thorac Surg* 2004; **77**: 1525-1529 [PMID: 15111136 DOI: 10.1016/j.athoracsur.2003.08.084]
 - 52 **Angelini P**. Letter by Angelini regarding article, "long-term outcome and impact of surgery on adults with coronary arteries originating from the opposite coronary cusp". *Circulation* 2011; **124**: e383 [PMID: 21969323 DOI: 10.1161/CIRCULATIONAHA.111.023614]
 - 53 **Krasuski RA**, Magyar D, Hart S, Kalahasti V, Lorber R, Hobbs R, Pettersson G, Blackstone E. Long-term outcome and impact of surgery on adults with coronary arteries originating from the opposite coronary cusp. *Circulation* 2011; **123**: 154-162 [PMID: 21200009 DOI: 10.1161/CIRCULATIONAHA.109.921106]
 - 54 **Alexi-Meskishvili V**, Nasser BA, Nordmeyer S, Schmitt B, Weng YG, Böttcher W, Hübner M, Berger F, Hetzer R. Repair of anomalous origin of the left coronary artery from the pulmonary artery in infants and children. *J Thorac Cardiovasc Surg* 2011; **142**: 868-874 [PMID: 21665229 DOI: 10.1016/j.jtcvs.2011.04.006]
 - 55 **Barbetakis N**, Efsthathiou A, Efsthathiou N, Papagiannopoulou P, Soulountsi V, Fessatidis I. A long-term survivor of Bland-White-Garland syndrome with systemic collateral supply: a case report and review of the literature. *BMC Surg* 2005; **5**: 23 [PMID: 16356181 DOI: 10.1186/1471-2482-5-23]
 - 56 **Alexander RW**, Griffith GC. Anomalies of the coronary arteries and their clinical significance. *Circulation* 1956; **14**: 800-805 [PMID: 13374855 DOI: 10.1161/01.CIR.14.5.800]
 - 57 **Lipton MJ**, Barry WH, Obrez I, Silverman JF, Wexler L. Isolated single coronary artery: diagnosis, angiographic classification, and clinical significance. *Radiology* 1979; **130**: 39-47 [PMID: 758666 DOI: 10.1148/130.1.39]
 - 58 **Yurtdaş M**, Gülen O. Anomalous origin of the right coronary artery from the left anterior descending artery: review of the literature. *Cardiol J* 2012; **19**: 122-129 [PMID: 22461044 DOI: 10.5603/CJ.2012.0023]
 - 59 **Sloan K**, Majdalany D, Connolly H, Schaff H. Inferior wall myocardial infarction caused by anomalous right coronary artery. *Can J Cardiol* 2008; **24**: e102-e103 [PMID: 19052676 DOI: 10.1016/S0828-282X(08)70704-9]
 - 60 **Isner JM**, Shen EM, Martin ET, Fortin RV. Sudden unexpected death as a result of anomalous origin of the right coronary artery from the left sinus of Valsalva. *Am J Med* 1984; **76**: 155-158 [PMID: 6691354 DOI: 10.1016/0002-9343(84)90765-4]
 - 61 **Wann S**, Schuchard G. Images in clinical medicine. Anomalous origin of the right coronary artery. *N Engl J Med* 2006; **355**: e8 [PMID: 16943395 DOI: 10.1056/NEJMim050051]
 - 62 **Flessas D**, Mamarelis I, Maniatis V, Souretis G, Laschos N, Kotoulas C, Lazaridis K. An unusual pattern of three major components of the cardiovascular system: multimodality imaging and review of the literature. *J Cardiothorac Surg* 2013; **8**: 61 [PMID: 23557147 DOI: 10.1186/1749-8090-8-61]
 - 63 **Sawaya FJ**, Sawaya JI, Angelini P. Split right coronary artery: its definition and its territory. *Tex Heart Inst J* 2008; **35**: 477-479 [PMID: 19156248]
 - 64 **Güel O**, Yazici M, Durna K, Demircan S. A rare coronary anomaly: double right coronary artery. *Clin Cardiol* 2007; **30**: 309 [PMID: 17551955 DOI: 10.1002/clc.20009]
 - 65 **Erbagci H**, Davutoglu V, Turkmen S, Kizilkan N, Gumusburun E. Double right coronary artery: review of literature. *Int J Cardiovasc Imaging* 2006; **22**: 9-11 [PMID: 16362174 DOI: 10.1007/s10554-005-5139-6]
 - 66 **Agarwal PP**, Kazerooni EA. Dual left anterior descending coronary artery: CT findings. *AJR Am J Roentgenol* 2008; **191**: 1698-1701 [PMID: 19020238 DOI: 10.2214/AJR.08.1193]
 - 67 **Spindola-Franco H**, Grose R, Solomon N. Dual left anterior descending coronary artery: angiographic description of important variants and surgical implications. *Am Heart J* 1983; **105**: 445-455 [PMID: 6829406 DOI: 10.1016/0002-8703(83)90363-0]
 - 68 **Musiani A**, Cernigliaro C, Sansa M, Maselli D, De Gasperi C. Left main coronary artery atresia: literature review and therapeutical considerations. *Eur J Cardiothorac Surg* 1997; **11**: 505-514 [PMID: 9105816 DOI: 10.1016/S1010-7940(96)01121-9]
 - 69 **Roberts WC**, Glick BN. Congenital hypoplasia of both right and left circumflex coronary arteries. *Am J Cardiol* 1992; **70**: 121-123 [PMID: 1615857 DOI: 10.1016/0002-9149(92)91407-U]
 - 70 **McFarland CA**, Svamy RSA. Hypoplastic coronary artery disease: a rare cause of sudden cardiac death and its treatment with an implantable defibrillator. *J Cardiol Cases* 2011; **4**: e148-e151 [DOI: 10.1016/j.jccase.2011.08.005]
 - 71 **Fraisse A**, Quilici J, Canavy I, Savin B, Aubert F, Bory M. Images in cardiovascular medicine. Myocardial infarction in children with hypoplastic coronary arteries. *Circulation* 2000; **101**: 1219-1222 [PMID: 10715271 DOI: 10.1161/01.CIR.101.10.1219]
 - 72 **Aznaouridis K**, Masoura C, Kastellanos S, Alahmar A. Inadvertent cardiac phlebography. *World J Cardiol* 2017; **9**: 558-561 [PMID: 28706592 DOI: 10.4330/wjc.v9.i6.558]
 - 73 **Aznaouridis K**, Alahmar A. Transradial primary angioplasty of anomalous right coronary artery from the left sinus of Valsalva. *Indian Heart J* 2017; **69**: 411-413 [PMID: 28648443 DOI: 10.1016/j.ihj.2017.05.001]
 - 74 **Farzanah I**. ALCAPA: The Al Capone of coronary artery anomalies. *SA Journal of Radiology* 2012; **16**: 100-101 [DOI: 10.4102/sajr.v16i3.290]
 - 75 **Dionne PO**, Poirier N, Forcillo J, Stevens LM, Chartrand-Lefebvre C, Mansour S, Noiseux N. A rare case of anomalous origin of the left main coronary artery in an adult patient. *J Cardiothorac Surg* 2013; **8**: 15 [PMID: 23336304 DOI: 10.1186/1749-8090-8-15]
 - 76 **Waleed M**, Aznaouridis K. Anomalous Origin of the "Nonculprit" Right Coronary Artery From the Left Anterior Descending Artery in a Patient With Anterolateral ST-Segment Elevation Myocardial Infarction. *JACC Cardiovasc Interv* 2015; **8**: e223-e225 [PMID: 26476604 DOI: 10.1016/j.jcin.2015.07.019]

P- Reviewer: Anan R, Barik R, Scicchitano P, Tomizawa N
S- Editor: Ji FF **L- Editor:** Filipodia **E- Editor:** Wu YXJ



Chronic ischemic mitral valve regurgitation and surgical perspectives

Salah Eldien Altarabsheh, Salil V Deo, Abeer Rababa'h, Yagthan M Obeidat, Osama Haddad

Salah Eldien Altarabsheh, Division of Cardiovascular Surgery, Queen Alia Heart Institute, Amman 11953, Jordan

Salil V Deo, Division of Cardiovascular Surgery, Harrington Heart and Vascular Institute, Case Western Reserve University, Cleveland, OH 44106, United States

Abeer Rababa'h, Department of Clinical Pharmacy, Jordan University of Science and Technology, Irbid 22110, Jordan

Yagthan M Obeidat, Department of Cardiac Surgery, AlMana General Hospital, AL Khobar 31952, Saudi Arabia

Osama Haddad, Department of Thoracic and Cardiovascular Surgery, Cleveland Clinic, Cleveland, OH 44195, United States

ORCID number: Salah Eldien Altarabsheh (0000-0002-1328-3340); Salil V Deo (0000-0002-4729-1461); Abeer Rababa'h (0000-0003-4619-2012); Yagthan M Obeidat (0000-0001-6551-9274); Osama Haddad (0000-0001-6308-6372).

Author contributions: Altarabsheh SE and Deo SV had almost equal contributions in writing the manuscript; Obeidat YM and Haddad O had equal contribution in editing the manuscript; Rababa'h A reviewed the manuscript.

Conflict-of-interest statement: We do not have any relevant disclosure pertaining to this study.

Open-Access: This article is an open-access article, which was selected by an in-house editor and fully peer-reviewed by external reviewers. It is distributed in accordance with the Creative Commons Attribution Non Commercial (CC BY-NC 4.0) license, which permits others to distribute, remix, adapt, build upon this work non-commercially, and license their derivative works on different terms, provided the original work is properly cited and the use is non-commercial. See: <http://creativecommons.org/licenses/by-nc/4.0/>

Manuscript source: Invited manuscript

Correspondence to: Salah Eldien Altarabsheh, MD, Consultant Cardiac Surgeon, Division of Cardiovascular Surgery, Queen Alia Heart Institute, Queen Rania St., Amman 11953, Jordan. salah936@yahoo.com

Telephone: +962-77-7181844
Fax: +962-2-7201075

Received: June 25, 2018
Peer-review started: June 26, 2018
First decision: July 9, 2018
Revised: August 4, 2018
Accepted: August 6, 2018
Article in press: August 7, 2018
Published online: October 26, 2018

Abstract

Chronic ischemic mitral valve regurgitation is a result of disturbed left ventricular geometry secondary to myocardial ischemia in the absence of intrinsic mitral valve pathology. It is a common complication after myocardial infarction, and patients who have ischemic mitral regurgitation (IMR) have a worse prognosis compared to patients who have ischemic heart disease alone, and this is directly related to the severity of IMR. Medical therapy has limited efficacy, and surgical options including various repair techniques and valve replacement had been tried with variable success. Still there is intense debate among surgeons whether to interfere with moderate degree IMR at the time of coronary artery revascularization.

Key words: Mitral regurgitation; Myocardial infarction; Ring annuloplasty; Valve replacement

© **The Author(s) 2018.** Published by Baishideng Publishing Group Inc. All rights reserved.

Core tip: Chronic ischemic mitral valve regurgitation is a valvular dysfunction secondary to myocardial infarction. Debates among surgeons surround the decision to intervene and the type of intervention in moderate degree ischemic regurgitation. A comprehensive approach addressing the whole pathology of myocardial ischemia and ventricular dysfunction may be of value.

Altarabsheh SE, Deo SV, Rababa'h A, Obeidat YM, Haddad O. Chronic ischemic mitral valve regurgitation, surgical perspectives. *World J Cardiol* 2018; 10(10): 141-144 Available from: URL: <http://www.wjgnet.com/1949-8462/full/v10/i10/141.htm> DOI: <http://dx.doi.org/10.4330/wjc.v10.i10.141>

INTRODUCTION

Chronic ischemic mitral regurgitation (IMR) is a complication that is determined by the extent and severity of myocardial infarction as well as ventricular dyssynchrony and afterload^[1]. In contrast to primary mitral valve regurgitation caused by structural valve abnormality in which there is an increasing agreement among surgeons for therapeutic options, IMR management options are still a matter of debate among clinicians^[2].

An increasing consensus among authors indicates that a severe form of IMR should be corrected, however surgical intervention with moderate forms of IMR at the time of coronary revascularization is still a matter of debate^[3]. There has been an evolution in surgical techniques of mitral valve repair over the years, however the continuous left ventricular remodeling process resulting in recurrence of the valve incompetence remained a major drawback of this approach^[4]. Mitral valve replacement preserving the subvalvular apparatus demonstrated a more durable valve competence and comparable left ventricular reverse remodeling and survival at a two year follow up period in comparison with mitral valve repair^[5].

DEFINITION AND BURDEN OF ISCHEMIC MITRAL VALVE REGURGITATION

IMR is defined classically as mitral valve regurgitation due to a previous myocardial infarction^[1]. Based on this definition, left ventricular remodeling consequences are considered integral parts leading to the development of IMR following myocardial infarction. Therefore, IMR is a complication of myocardial infarction due to structural left ventricular dysfunction in the presence of normal intrinsic mitral valve structure^[6]. This definition takes into consideration both the history of myocardial infarction as well as the resulting left ventricular abnormalities together. IMR is not a mitral valve disease per say, but a consequence of the disturbed closing and tethering forces related to the papillary muscle mechanics as a result of left ventricular remodeling following myocardial infarction^[6]. Other mitral valve pathologies may coexist with a previous history of myocardial infarction like rheumatic or myxomatous mitral valve disease. These do not indicate an ischemic mitral valve disease, therefore the description of the mitral valve regurgitation depends on the mitral valve structure and the left ventricular structural dysfunction. Carpentier classification in 1983 characterized the pathophysiology of IMR to either 1. Mitral leaflet motion restriction in systole, type IIIb or 2.

Isolated mitral annular dilatation, type I a^[7].

IMR is a significant clinical problem that affects 1.6-2.8 million people in the United States and it may happen in 10%-20% of patients with ischemic heart disease^[5,8]. With the new technologies implemented in the current era of coronary artery interventions and the aging population, one can expect that the incidence of IMR will increase, which had been demonstrated to have a significant negative impact on patient survival and the development of heart failure^[9].

Grigioni *et al*^[9] demonstrated in patients with Q wave after myocardial infarction that the prevalence of adverse events had been linked directly to the presence and degree of severity of IMR. When patients are matched in their base line characteristics those who had a severe degree of IMR (ERO > 20 mm) are six times more likely to have heart failure compared to patients without IMR regardless of the symptomatology status (RR 6.4, 95%CI: 2.9 to 14.3; $P < 0.0001$). Therefore, detecting and quantifying IMR is highly crucial in planning a treatment strategy following myocardial infarction.

CHOICE OF SURGICAL INTERVENTION IN SEVERE IMR, REPAIR VS REPLACEMENT

There is an agreement among clinicians that severe IMR should be surgically treated, however treatment of moderate IMR is still a matter of debate^[10]. Many changes have occurred in surgical approaches over the past years. Initially, mitral valve replacement with excision of the mitral valve apparatus was the primary choice because it restores the competency of the valve. The drawback of this approach is the impaired left ventricular function and geometry due to excision of the subvalvular apparatus^[8]. Mitral valve repair using ring annuloplasty was another solution because it preserves the subvalvular apparatus and theoretically preserves the mitral valve competency. Proponents of this therapeutic modality take in consideration the unique shape of the mitral annular configuration in determining the mitral competence by decreasing the leaflet stress during systole^[11]. This approach does work for type I IMR, however it incompletely corrects type IIIb dysfunction. The ideal solution is to adopt a comprehensive approach that will take all the aspects of the disease in consideration. Physiological changes are asymmetric in the left ventricle geometry as well as the annulus, so new advances had been designed even in the ring technology to reshape the annulus taking in consideration the saddle pattern of the mitral annular configuration^[12].

Whether to replace or repair severe chronic ischemic mitral valve regurgitation has been a subject of intense debate. The tradeoff between the durability of mitral valve repair is correcting a regurgitant valve vs an adverse consequence of prosthetic valve insertion. It was observed that patients, who had severe ischemic mitral valve regurgitation demonstrated a comparable

degree of left ventricular reverse remodeling between mitral valve repair and replacement at one year follow up^[5]. However, the rates of recurrent mitral valve regurgitation amongst the survivors of the repair cohort were 32.6% at one year and 46% at the two year follow up^[5]. Other forms of surgical options addressing the left ventricular geometrical changes had been tried with variable success rates. Fattouch *et al*^[13] reported a durable mitral valve repair with less than 3% recurrence rate of moderate mitral valve regurgitation by adopting papillary muscle relocation, non-restrictive mitral annuloplasty, and myocardial revascularization in patients with severe IMR.

Lorusso *et al*^[14] demonstrated that there was a comparable incidence of adverse outcomes between the repair and replacement matched groups in the short and long term follow up periods in patients with severe ischemic mitral valve regurgitation. However, mitral valve repair remained the strongest predictor for the need for mitral valve re-operation^[14].

MODERATE IMR AT THE TIME OF CORONARY ARTERY BYPASS GRAFT

There is general agreement among clinicians that significant IMR should be addressed at the time of coronary artery bypass graft (CABG). However, the drawback of this approach is that a combined procedure may increase the risk of surgery on a sick heart and doing coronary revascularization alone may improve ventricular status. Whether to treat moderate IMR at the time of CABG has been a real debate in the field of cardiology and cardiac surgery. This led to the conduction of four randomized controlled trials, which are the only ones published until now addressing this subject^[3,15-17].

Fattouch *et al*^[3] concluded that a mitral valve intervention for significant functional mitral valve regurgitation at the time of CABG might improve the degree of functional mitral regurgitation, the New York Heart association functional class, and left ventricular ejection fraction. Chan *et al*^[16] observed similar results as Fattouch *et al*. They demonstrated that there was an improvement in the degree of functional mitral regurgitation, reverse left ventricular remodeling, and functional capacity when mitral valve repair was added to coronary artery revascularization in the presence of moderate IMR.

A more recent conducted trial by Bouchard *et al*^[15] demonstrated that there was no obvious clinical benefits of adding mitral valve intervention at the time of CABG after one year follow up, despite the tempting value early in the post-operative period. However, the major drawback of this trial is that it included only 31 patients in both cohorts. Smith *et al*^[17] demonstrated that there was some degree of improvement of the mitral valve grade in association with mitral valve repair at the time of CABG. However, the incidence of adverse events was increased.

Evidence from observational studies also has been

a matter of debate. Aklog *et al*^[18] demonstrated that there was clear superiority in performing mitral valve repair for moderate IMR at the time of CABG compared to revascularization alone in correcting mitral valve incompetence. Kang *et al*^[19] demonstrated in their study that the addition of mitral valve intervention might increase operative mortality compared to patients who have CABG alone.

With these conflicting results in the randomized controlled trials addressing this issue, Altarabsheh *et al*^[20] published a systemic review and meta-analysis in 2017 that included the four randomized trials and seven relevant observational studies with a total of 1447 patients. They clearly demonstrated that the addition of mitral valve repair for moderate IMR at the time of CABG did not have survival or functional improvement at the five year follow up despite the fact that it may improve the degree of mitral valve competence.

CONCLUSION

IMR remains a significant complication of myocardial infarction and continued to have therapeutic challenges. Complex mechanisms involving mitral annulus and subvalvular apparatus play a role, and ideal surgical repair should take the whole pathology in consideration. Future repair techniques, which address disturbed left ventricular mechanics, may be of value, and currently mitral valve replacement preserving the subvalvular apparatus is a valid surgical option. Moderate IMR could be addressed by coronary revascularization alone at the time of CABG.

REFERENCES

- 1 Nappi F, Spadaccio C, Chello M, Mihos CG. Papillary muscle approximation in mitral valve repair for secondary MR. *J Thorac Dis* 2017; **9**: S635-S639 [PMID: 28740718 DOI: 10.21037/jtd.2017.06.98]
- 2 Tolis G Jr, Sundt TM 3rd. Surgical Strategies for Management of Mitral Regurgitation: Recent Evidence from Randomized Controlled Trials. *Curr Atheroscler Rep* 2015; **17**: 67 [PMID: 26486511 DOI: 10.1007/s11883-015-0549-y]
- 3 Fattouch K, Guccione F, Sampognaro R, Panzarella G, Corrado E, Navarra E, Calvaruso D, Ruvolo G. POINT: Efficacy of adding mitral valve restrictive annuloplasty to coronary artery bypass grafting in patients with moderate ischemic mitral valve regurgitation: a randomized trial. *J Thorac Cardiovasc Surg* 2009; **138**: 278-285 [PMID: 19619766 DOI: 10.1016/j.jtcvs.2008.11.010]
- 4 Hung J, Papakostas L, Tahta SA, Hardy BG, Bollen BA, Duran CM, Levine RA. Mechanism of recurrent ischemic mitral regurgitation after annuloplasty: continued LV remodeling as a moving target. *Circulation* 2004; **110**: II85-II90 [PMID: 15364844 DOI: 10.1161/01.CIR.0000138192.65015.45]
- 5 Acker MA, Parides MK, Perrault LP, Moskowitz AJ, Gelijns AC, Voisine P, Smith PK, Hung JW, Blackstone EH, Puskas JD, Argenziano M, Gammie JS, Mack M, Ascheim DD, Bagiella E, Moquete EG, Ferguson TB, Horvath KA, Geller NL, Miller MA, Woo YJ, D'Alessandro DA, Ailawadi G, Dagenais F, Gardner TJ, O'Gara PT, Michler RE, Kron IL; CTSN. Mitral-valve repair versus replacement for severe ischemic mitral regurgitation. *N Engl J Med* 2014; **370**: 23-32 [PMID: 24245543 DOI: 10.1056/NEJMoa1312808]

- 6 **Varma PK**, Krishna N, Jose RL, Madkaiker AN. Ischemic mitral regurgitation. *Ann Card Anaesth* 2017; **20**: 432-439 [PMID: 28994679 DOI: 10.4103/aca.ACA_58_17]
- 7 **Carpentier A**. Cardiac valve surgery--the "French correction". *J Thorac Cardiovasc Surg* 1983; **86**: 323-337 [PMID: 6887954]
- 8 **Boyd JH**. Ischemic mitral regurgitation. *Circ J* 2013; **77**: 1952-1956 [PMID: 23877709 DOI: 10.1253/circj.CJ-13-0743]
- 9 **Grigioni F**, Detaint D, Avierinos JF, Scott C, Tajik J, Enriquez-Sarano M. Contribution of ischemic mitral regurgitation to congestive heart failure after myocardial infarction. *J Am Coll Cardiol* 2005; **45**: 260-267 [PMID: 15653025 DOI: 10.1016/j.jacc.2004.10.030]
- 10 **Fattouch K**, Castrovinci S, Murana G, Moscarelli M, Speziale G. Surgical management of moderate ischemic mitral valve regurgitation: Where do we stand? *World J Cardiol* 2014; **6**: 1218-1222 [PMID: 25429333 DOI: 10.4330/wjc.v6.i11.1218]
- 11 **Grewal J**, Suri R, Mankad S, Tanaka A, Mahoney DW, Schaff HV, Miller FA, Enriquez-Sarano M. Mitral annular dynamics in myxomatous valve disease: new insights with real-time 3-dimensional echocardiography. *Circulation* 2010; **121**: 1423-1431 [PMID: 20231533 DOI: 10.1161/CIRCULATIONAHA.109.901181]
- 12 **Daimon M**, Fukuda S, Adams DH, McCarthy PM, Gillinov AM, Carpentier A, Filsoufi F, Abascal VM, Rigolin VH, Salzberg S, Huskin A, Langenfeld M, Shiota T. Mitral valve repair with Carpentier-McCarthy-Adams IMR ETlogix annuloplasty ring for ischemic mitral regurgitation: early echocardiographic results from a multi-center study. *Circulation* 2006; **114**: 1588-1593 [PMID: 16820643 DOI: 10.1161/CIRCULATIONAHA.105.001347]
- 13 **Fattouch K**, Castrovinci S, Murana G, Dioguardi P, Guccione F, Nasso G, Speziale G. Papillary muscle relocation and mitral annuloplasty in ischemic mitral valve regurgitation: midterm results. *J Thorac Cardiovasc Surg* 2014; **148**: 1947-1950 [PMID: 24656671 DOI: 10.1016/j.jtcvs.2014.02.047]
- 14 **Lorusso R**, Gelsomino S, Vizzardi E, D'Aloia A, De Cicco G, Lucà F, Parise O, Gensini GF, Stefano P, Livi U, Vendramin I, Pacini D, Di Bartolomeo R, Miceli A, Varone E, Glauber M, Parolari A, Giuseppe Arlati F, Alamanni F, Serraino F, Renzulli A, Messina A, Troise G, Mariscalco G, Cottini M, Beghi C, Nicolini F, Gherli T, Borghetti V, Pardini A, Caimmi PP, Micalizzi E, Fino C, Ferrazzi P, Di Mauro M, Calafiore AM; ISTIMIR Investigators. Mitral valve repair or replacement for ischemic mitral regurgitation? The Italian Study on the Treatment of Ischemic Mitral Regurgitation (ISTIMIR). *J Thorac Cardiovasc Surg* 2013; **145**: 128-139; discussion 137-138 [PMID: 23127376 DOI: 10.1016/j.jtcvs.2012.09.042]
- 15 **Bouchard D**, Jensen H, Carrier M, Demers P, Pellerin M, Perrault LP, Lambert J. Effect of systematic downsizing rigid ring annuloplasty in patients with moderate ischemic mitral regurgitation. *J Thorac Cardiovasc Surg* 2014; **147**: 1471-1477 [PMID: 23856201 DOI: 10.1016/j.jtcvs.2013.05.024]
- 16 **Chan KM**, Punjabi PP, Flather M, Wage R, Symmonds K, Roussin I, Rahman-Haley S, Pennell DJ, Kilner PJ, Dreyfus GD, Pepper JR; RIME Investigators. Coronary artery bypass surgery with or without mitral valve annuloplasty in moderate functional ischemic mitral regurgitation: final results of the Randomized Ischemic Mitral Evaluation (RIME) trial. *Circulation* 2012; **126**: 2502-2510 [PMID: 23136163 DOI: 10.1161/CIRCULATIONAHA.112.143818]
- 17 **Smith PK**, Puskas JD, Ascheim DD, Voisine P, Gelijns AC, Moskowitz AJ, Hung JW, Parides MK, Ailawadi G, Perrault LP, Acker MA, Argenziano M, Thourani V, Gammie JS, Miller MA, Pagé P, Overbey JR, Bagiella E, Dagenais F, Blackstone EH, Kron IL, Goldstein DJ, Rose EA, Moquete EG, Jeffries N, Gardner TJ, O' Gara PT, Alexander JH, Michler RE; Cardiothoracic Surgical Trials Network Investigators. Surgical treatment of moderate ischemic mitral regurgitation. *N Engl J Med* 2014; **371**: 2178-2188 [PMID: 25405390 DOI: 10.1056/NEJMoa1410490]
- 18 **Aklog L**, Filsoufi F, Flores KQ, Chen RH, Cohn LH, Nathan NS, Byrne JG, Adams DH. Does coronary artery bypass grafting alone correct moderate ischemic mitral regurgitation? *Circulation* 2001; **104**: 168-175 [PMID: 11568033 DOI: 10.1161/hc37t1.094706]
- 19 **Kang DH**, Kim MJ, Kang SJ, Song JM, Song H, Hong MK, Choi KJ, Song JK, Lee JW. Mitral valve repair versus revascularization alone in the treatment of ischemic mitral regurgitation. *Circulation* 2006; **114**: 1499-1503 [PMID: 16820626 DOI: 10.1161/CIRCULATIONAHA.105.000398]
- 20 **Altarabsheh SE**, Deo SV, Dunlay SM, Erwin PJ, Obeidat YM, Navale S, Markowitz AH, Park SJ. Meta-Analysis of Usefulness of Concomitant Mitral Valve Repair or Replacement for Moderate Ischemic Mitral Regurgitation With Coronary Artery Bypass Grafting. *Am J Cardiol* 2017; **119**: 734-741 [PMID: 28109559 DOI: 10.1016/j.amjcard.2016.11.024]

P- Reviewer: Li S, Ueda H, Said SAM **S- Editor:** Ji FF

L- Editor: Filipodia **E- Editor:** Wu YXJ



Observational Study

Successful endovascular treatment in patients with acute thromboembolic ischemia of the lower limb including the crural arteries

Sorin Giusca, Dorothea Raupp, Dirk Dreyer, Christoph Eisenbach, Grigorios Korosoglou

Sorin Giusca, Grigorios Korosoglou, Department of Cardiology and Vascular Medicine, GRN Hospital Weinheim, Weinheim 69469, Germany

Dorothea Raupp, Christoph Eisenbach, Department of Gastroenterology and Diabetology, GRN Hospital Weinheim, Weinheim 69469, Germany

Dirk Dreyer, Straub Medical AG, Wangs CH-7323, Switzerland

ORCID number: Sorin Giusca (0000-0001-6484-5553); Dorothea Raupp (0000-0002-4443-2126); Dirk Dreyer (0000-0003-0672-3704); Christoph Eisenbach (0000-0003-0948-4382); Grigorios Korosoglou (0000-0002-6038-2253).

Author contributions: Giusca S, Dreyer D and Korosoglou G designed the research; Giusca S, Raupp D, Eisenbach C and Korosoglou G performed the research; Giusca S, Dreyer D and Korosoglou G contributed analytic tools; Giusca S, Raupp D, Eisenbach C and Korosoglou G analyzed data; Giusca S, Raupp D, Dreyer D, Eisenbach C and Korosoglou G wrote the paper.

Institutional review board statement: This case report was exempt from the Institutional Review Board standards at University Hospital Heidelberg, Heidelberg, Germany.

Informed consent statement: The patients involved in this study gave their written informed consent authorizing use and disclosure of their protected health information.

Conflict-of-interest statement: Dirk Dreyer is an employee of the Straub Medical AG. All other authors have no conflicts of interests to declare.

Data sharing statement: No additional data are available.

STROBE statement: This report is presented as suggested by the STROBE statement, *i.e.*, according to the guidelines for reporting observational studies.

Open-Access: This article is an open-access article which was selected by an in-house editor and fully peer-reviewed by external reviewers. It is distributed in accordance with the Creative

Commons Attribution Non Commercial (CC BY-NC 4.0) license, which permits others to distribute, remix, adapt, build upon this work non-commercially, and license their derivative works on different terms, provided the original work is properly cited and the use is non-commercial. See: <http://creativecommons.org/licenses/by-nc/4.0/>

Manuscript source: Unsolicited manuscript

Correspondence to: Grigorios Korosoglou, MD, Professor, Department of Cardiology and Vascular Medicine, GRN Hospital Weinheim, Roentgenstrasse 1, Weinheim 69469, Germany. gkorosoglou@hotmail.com
Telephone: +49-6201-892142
Fax: +49-6201-892507

Received: May 13, 2018

Peer-review started: May 13, 2018

First decision: June 14, 2018

Revised: June 30, 2018

Accepted: August 11, 2018

Article in press: August 11, 2018

Published online: October 26, 2018

Abstract

AIM

To examine the efficacy and safety of the 6 French (6F) Rotarex®S catheter system in patients with acute limb ischemia (ALI) involving thromboembolic occlusion of the proximal and mid-crural vessels.

METHODS

The files of patients in our department with ALI between 2015 and 2017 were examined. In seven patients, the Rotarex®S catheter was used in the proximal segment of the crural arteries. Data related to the clinical examination, Doppler sonography, angiography and follow-up from these patients were further used for analysis.

RESULTS

Two patients (29%) had thrombotic occlusion of the common femoral artery, and the remaining five exhibited thrombosis of the superficial femoral artery and popliteal artery. Mechanical thrombectomy was performed in all cases using a 6F Rotarex®S catheter. Additional Rotarex®S catheter thrombectomy due to remaining thrombus formation with no reflow was performed in the anterior tibial artery in two of seven cases (29%), in the tibiofibular tract and posterior tibial artery in two of seven cases (29%) and in the tibiofibular tract and fibular artery in the remaining three of seven cases (43%). Ischemic symptoms resolved promptly in all, and none of the patients experienced a procedural complication, such as crural vessel dissection, perforation or thrombus embolization.

CONCLUSION

Mechanical debulking using the 6F Rotarex®S catheter system may be a safe and effective treatment option in case of thrombotic or thromboembolic occlusion of the proximal and mid-portion of crural arteries.

Key words: Thrombus aspiration; Rotarex®S mechanical debulking catheter; Crural arteries; Lower limb; Critical limb ischemia; Acute occlusion; Duplex sonography

© **The Author(s) 2018.** Published by Baishideng Publishing Group Inc. All rights reserved.

Core tip: Herein, we report on seven consecutive patients with acute limb ischemia, who were treated by an endovascular approach, using the 6 French (6F) Rotarex®S catheter system for local mechanical thrombectomy. The procedures were effective in all cases, restoring flow and abolishing ischemic symptoms without causing any complications. Thus, mechanical debulking using the 6F Rotarex®S catheter system may be a safe and effective treatment option in the case of thrombotic occlusion of the proximal and mid-portion of crural arteries, obviating the need for local thrombolysis, which is associated with an increased risk for major bleeding.

Giusca S, Raupp D, Dreyer D, Eisenbach C, Korosoglou G. Successful endovascular treatment in patients with acute thromboembolic ischemia of the lower limb including the crural arteries. *World J Cardiol* 2018; 10(10): 145-152 Available from: URL: <http://www.wjgnet.com/1949-8462/full/v10/i10/145.htm> DOI: <http://dx.doi.org/10.4330/wjc.v10.i10.145>

INTRODUCTION

Acute limb ischemia (ALI) constitutes a medical emergency defined as a severely reduced perfusion of the leg resulting from a total or subtotal arterial occlusion, with symptoms debuting < 14 d prior to presentation. It has an incidence of around 140/million/year and a prevalence of 1%-3%^[1,2]. Depending on the severity of

symptoms, patients can be grouped according to the Rutherford classification of lower extremity ischemia^[3]. Although significant advances have been made in the treatment of ALI, most of the studies still report an amputation rate of 10%-30% at 30 d^[4-6]. Patients with thromboembolic ALI are especially at high risk for major amputation and death due to sepsis and multi-organ dysfunction. Such patients are usually older than 75 years and show further co-morbidities, including atrial fibrillation and history of heart failure^[7].

Previous studies demonstrated the superiority of catheter-directed thrombolysis (CDT) compared to surgical treatment in regard to amputation-free survival in patients presenting with ALI^[6,8]. However, this technique has its clear limitations in patients with an increased bleeding risk. Therefore, percutaneous mechanical thrombectomy systems have emerged in the last years as a valid therapeutic option in patients with ALI^[9]. One such system, the Rotarex®S mechanical debulking catheter (Straub Medical, Wangs, Switzerland) is based on mechanical fragmentation and simultaneous aspiration of occlusion material, thus transporting the debris out of the patient. Several studies have shown a very high success rate of Rotarex®S alone or in combination with drug-coated balloons in terms of establishing vessel patency in patients with ALI^[5]. However, operators should be cautious when using the 6 French (6F) Rotarex®S catheter in arteries below-the-knee because this catheter system is limited to vessel diameters of ≥ 3 mm and might cause dissection or perforation when used in smaller diameter arteries. Herein, we present the clinical safety and effectiveness of the 6F Rotarex®S system in a miniseries of seven patients with acute lower limb ischemia affecting their crural arteries.

MATERIALS AND METHODS

The files of 102 patients with thrombotic occlusions of the lower extremities between January 2015 and December 2017 at the Department of Cardiology and Vascular Medicine, Academic Teaching Hospital Weinheim were examined. In seven patients, the Rotarex®S catheter was used in the proximal segment of the crural arteries, and the data from these patients were further used for the analysis. In the remaining 95 patients, the Rotarex®S catheter was used for mechanical thrombectomy in iliac and femoropopliteal arteries. The study was approved by the local ethics committee of the University Hospital Heidelberg (S-100/2017). Retrospective data were collected in accordance with the Declaration of Helsinki.

Interventional treatment

All patients received a bolus of 2500 U of heparin after placement of a 6F sheath introducer in the femoral artery. During interventional treatment, all patients also received heparin to reach an activated clotting time of > 300 s. If necessary, patients also received 500 mg

Table 1 Baseline characteristics of our seven patients

| | Patient A | Patient B | Patient C | Patient D | Patient E | Patient F | Patient G | All patients |
|-----------------------------|---|--|--|--|--|---|---|---|
| Sex | Male | Male | Male | Male | Male | Male | Male | All male (100%) |
| Age (yr) | 89 | 72 | 55 | 67 | 85 | 67 | 80 | 74 ± 11 |
| Cardiovascular risk factors | Hypertension Hyperlipidemia Type 2 DM | Hypertension Hyperlipidemia Type 2 DM | Hypertension Hyperlipidemia Type 2 DM Smoking | Hypertension Hyperlipidemia Smoking | Hypertension Hyperlipidemia Type 2 DM | Hypertension Hyperlipidemia Smoking | Hypertension Hyperlipidemia | Hypertension (100%) Hyperlipidemia (100%) Type 2 DM (57%) Smoking (43%) |
| PAD history | No | Surgical endarterectomy of the left common femoral artery 2012 | No | Prior Angioplasty and stent placement in the left popliteal artery 2015 | No | Prior Angioplasty and stent placement in the left popliteal artery 2016 | No | 3/7 (43%) |
| LV function | Moderately reduced | Normal | Normal | Normal | Severely reduced | Mildly reduced | Normal | Reduced in 3/7 (43%) |
| Symptoms onset | For 12 h | For 16 h | For 2 h | For 12 h | For 36 h | For 6 h | For 36 h | 17 ± 13 |
| CAD history | 3 vessel CAD | 3 vessel CAD | No | 3 vessel CAD | 3 vessel CAD | 3 vessel CAD | 3 vessel CAD | 6/7 (86%) |
| Baseline medication | Aspirin β-blocker ACE inhibitor Statin Diuretics | Aspirin β-blocker ACE inhibitor Statin | Aspirin ACE inhibitor Statin | Aspirin β-blocker ACE inhibitor Statin Diuretics | Aspirin β-blocker ACE inhibitor Statin Diuretics | Aspirin β-blocker ACE inhibitor Statin Diuretics | Aspirin β-blocker ACE inhibitor Statin | Aspirin (100%) β-blocker (86%) ACE inhibitor (100%) Statin (100%) Diuretics (57%) |
| Other comorbidities | Reduced renal function with estimated GFR of -40 mL/min/1.73 m ² Atrial fibrillation Heart failure NYHA III | Reduced renal function with estimated GFR of -50 mL/min/1.73 m ² Atrial fibrillation | None | Reduced renal function with estimated GFR of -45 mL/min/1.73 m ² Atrial fibrillation | Reduced renal function with estimated GFR of -55 mL/min/1.73 m ² Atrial fibrillation Heart failure NYHA III | Reduced renal function with estimated GFR of -50 mL/min/1.73 m ² | Reduced renal function with estimated GFR of -40 mL/min/1.73 m ² Atrial fibrillation Heart failure NYHA II | Reduced renal function (86%) Atrial fibrillation (71%) Heart failure (43%) |

ACE: Angiotensin converting enzyme; LV: Left ventricular; CAD: Coronary artery disease; PAD: Peripheral artery disease; NYHA: New York Heart Association; GFR: Glomerular filtration rate.

aspirin during and 300 mg clopidogrel during or after the interventional procedure. If additional thrombolysis was deemed necessary, a bolus of 10 mg recombinant tissue plasminogen activator (rtPA) was administered after placement of the dedicated thrombolysis catheter (Unifuse catheter, AngioDynamics, Netherlands). Postprocedural rtPA was continuously administered at an infusion rate of 1 mg/h for 6-18 h, adding heparin to achieve partial thromboplastin time of 50-60 s.

Statistical analysis

Continuous variables are presented as numbers, providing the corresponding range of each variable. Categorical variables are represented as percentages. Measures of the vessel diameters were conducted using ImageJ software (version 1.50, NIH, Bethesda, MD, United States).

RESULTS

Demographic characteristics and procedural data

We present a mini-series of seven patients (Patient A-G). Baseline characteristics of our patients are provided in Table 1. Patients were referred to our department with symptoms of ALI with new onset of pain, paleness and pulselessness during the last 17 ± 13 h. Duplex sonography revealed thrombotic occlusion of the common femoral

Table 2 Duplex sonography and digital subtraction angiography findings of our patients

| | Patient A | Patient B | Patient C | Patient D | Patient E | Patient F | Patient G |
|----------------------------|---|---|--|--|--|--|--|
| Duplex sonography findings | Thrombotic CFA occlusion | Thrombotic CFA occlusion | Thrombotic occlusion of the distal SFA | Thrombotic occlusion of the popliteal artery | Thrombotic occlusion of the distal SFA | Thrombotic occlusion of the distal SFA | Thrombotic occlusion of the popliteal artery |
| DSA findings | Thrombotic CFA occlusion | Thrombotic CFA occlusion | Thrombotic occlusion of the distal SFA and of the popliteal artery | Thrombotic occlusion of the popliteal artery | Thrombotic occlusion of the distal SFA and of the popliteal artery | Thrombotic occlusion of the distal SFA and of the popliteal artery | Thrombotic occlusion of the popliteal artery |
| Treated crural vessels | Proximal and mid tibial anterior artery | Proximal and mid tibial anterior artery | Proximal and mid posterior tibial artery | Tibiofibular tract and posterior tibial artery | Tibiofibular tract and fibular artery | Tibiofibular tract | Tibiofibular tract and fibular artery |
| Rotarex catheter | 6F | 6F | 6F | 6F | 6F | 6F | 6F |
| Local lysis | Yes | No | No | Yes | Yes | Yes | Yes |
| Second look DSA | Yes | No | No | Yes | Yes | Yes | Yes |

CFA: Common femoral artery; SFA: Superficial femoral artery; DSA: Digital subtraction angiography; 6F: 6 French.

Table 3 Overview of the diameters of the crural vessels, where 6 French Rotarex®S catheter thrombectomy was performed

| | Proximal anterior tibial artery | Mid anterior tibial artery |
|-----------|--|--|
| Patient A | 3.2 mm* | 2.8 mm |
| Patient B | 3.4 mm | 2.7 mm |
| Patient C | Proximal posterior tibial artery 3.5 mm | Mid posterior tibial artery 3.0 mm |
| Patient D | Tibiofibular tract 3.5 mm | Proximal posterior tibial artery 3.0 mm |
| Patient E | Tibiofibular tract 4.0 mm | Proximal fibular artery 2.5 mm |
| Patient F | Tibiofibular tract 3.5 mm | |
| Patient G | Tibiofibular tract 4 mm | Proximal fibular artery 3.5 mm |

* Proximal anterior tibial artery within moderate stenosis = 2.1 mm

artery (CFA) in two of seven cases (29%), and of the distal superficial femoral artery (SFA) and of the popliteal artery in the remaining five of seven cases (71%). The localization of arterial occlusion was confirmed in all cases by digital subtraction angiography. Mechanical thrombectomy was performed in all cases using a 6F Rotarex®S catheter and was combined by local lysis in five of seven cases (71%). Rotarex®S catheter thrombectomy was performed in the CFA and in the SFA in two of seven cases (29%), and in the SFA and in the popliteal artery in the remaining five of seven cases (71%). Additional Rotarex®S catheter thrombectomy due to remaining thrombus formation with no reflow in the crural arteries was performed in the anterior tibial artery in two of seven cases (29%), in the tibiofibular tract and posterior tibial artery in two of seven cases (29%) and in the tibiofibular tract and fibular artery in the remaining three of seven cases (43%)(Table 2).

Efficacy and safety data

In all seven cases, 6F Rotarex®S catheter thrombectomy resulted in vessel patency, whereas no vessel dissections or perforations were observed. Compared to the re-

maining 95 patients who received Rotarex®S catheter thrombectomy in iliac and femoropopliteal vessels, it should be noted that Rotarex®S efficacy was present in 93 of 95 cases (98%), whereas vessel dissection or perforation was observed in two of 95 cases (2%), which in both cases was treated using an endovascular approach by prolonged balloon inflation and by placement of a stent, respectively.

Size of the treated crural arteries

The size of the proximal crural arteries varied between 3.2 and 4.0 mm, whereas the size of the mid-portion of the crural arteries varied between 2.5 and 3.5 mm. An overview of the diameters of the proximal and mid-portions of the crural arteries of our patients, where mechanical thrombectomy was performed, can be appreciated in Table 3.

Post-procedural data

Ischemic symptoms promptly resolved in all patients after the index procedure. Duplex sonography on the following day exhibited patency of all of the treated crural arteries. In addition, further clinical course was

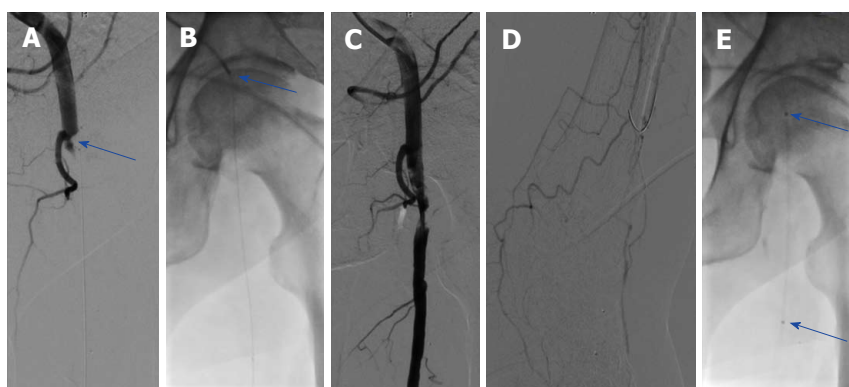


Figure 1 The angiography of patient A. A: Thrombotic occlusion of the common femoral artery (CFA) (blue arrow); B: Mechanical debulking using the Rotarex®S catheter (arrow); C,D: Anterograde flow was restored in the CFA after debulking with reduced flow in the foot arteries; E: Local thrombolysis was performed using a dedicated Unifuse catheter (arrow).



Figure 2 The angiography of patient A. The following day, a complete resolution of thrombus material was found in the common femoral artery. A-D: Superficial femoral artery and deep femoral artery (A-C) with new occlusion of the popliteal artery (D); E: Repeated Rotarex® debulking in the popliteal artery and continued to the proximal and median parts of the anterior tibial artery; F,G: Restoration of flow of the anterior tibial artery and of the foot.

uneventful in all seven patients, who were discharged within three days after mechanical thrombectomy. Five of seven (71%) patients were diagnosed with atrial fibrillation and were put on triple anticoagulation with 100 mg aspirin, 75 mg clopidogrel and oral anticoagulation for 4 wk, and were then continued with oral anticoagulation. The remaining two patients were treated with 100 mg aspirin and 75 mg clopidogrel for 3 mo and were then put on 100 mg aspirin daily. Representative images of our patients (Patient A-C) can be appreciated in Figures 1-4.

DISCUSSION

ALI is a serious medical condition that requires rapid diagnosis and prompt initiation of appropriate treatment. Depending on the clinical presentation and anatomy of the lesion, either an endovascular approach or a surgical therapy may be chosen. CDT is the classical method employed in the treatment of ALI. Mechanical thrombectomy techniques, on the other hand, represent a relatively new treatment in patients with ALI. Various devices using different mechanisms of action, (*i.e.*, fragmentation, aspiration or rheolytic

thrombectomy) were shown to be useful alone or associated with the use of additional thrombolytics or local thrombolysis (combined mechanical and pharmacologic thrombectomy) for the management of patients with ALI. The main advantage of mechanical thrombectomy consists of the reduction of thrombotic burden, which reduces or even avoids the need for local thrombolysis. This is of major importance, particularly in patients with contraindication to thrombolysis due to high bleeding risks.

Many mechanical thrombectomy devices are currently used for the endovascular treatment of ALI. The ThromCat XT catheter device consists of an atraumatic tip and a flexible steel helix and can provide an effective aspiration capacity of 0.63 mL/s even in vessels with relative large diameters^[10]. However, due to the small aspiration ports of this catheter system, it is limited to the treatment of fresh arterial occlusions, as it is difficult for the system to aspirate partially organized thrombotic material. The AngioJet (Possis Medical, Minneapolis, Minnesota, United States) on the other hand, is a combined pharmacologic and mechanical thrombectomy system, which is dedicated to peripheral interventions and uses active aspiration and Power Pulse™ lytic

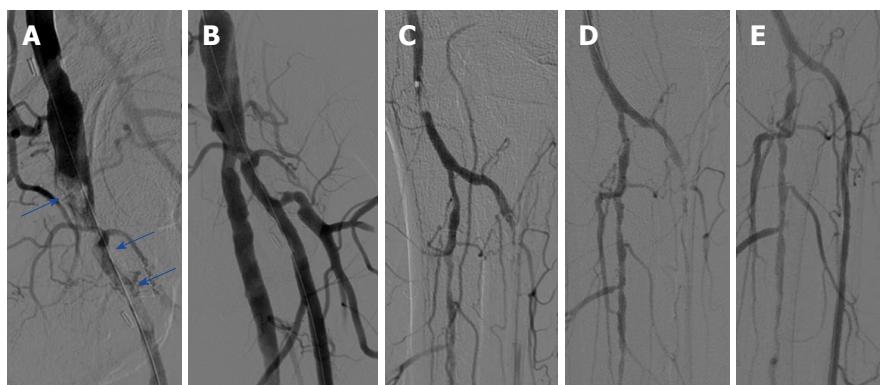


Figure 3 The angiography of patient B. A: Thrombotic occlusion of the common femoral artery and profunda femoral artery (blue arrows); B: Good angiographic reflux after repeated treatment with the 6F Rotarex®S mechanical debulking catheter; C: Thrombus formation in the popliteal and in the anterior tibial artery; D: No flow restoration in the anterior tibial artery after treatment with the 6F Rotarex®S in the popliteal artery; E: Flow restoration after deploying the Rotarex®S in the anterior tibial artery.

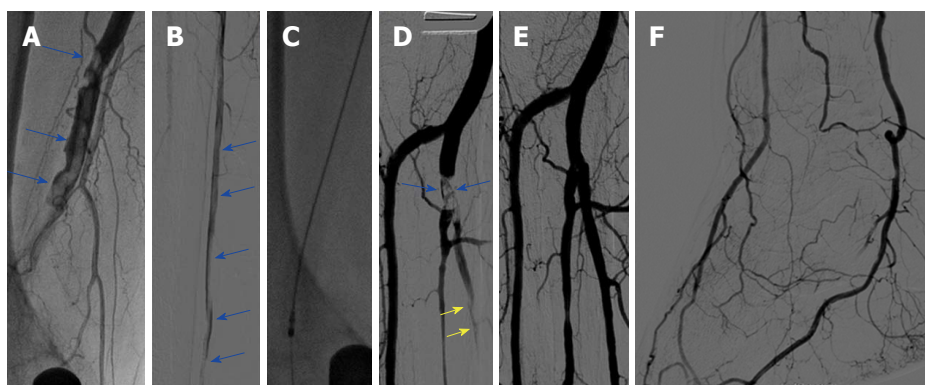


Figure 4 The angiography of patient C. A: Thrombotic occlusion of the right popliteal artery (blue arrows); B: Further thrombus formation in the right posterior tibial artery (blue arrows); C: Rotarex®S catheter in the popliteal artery; D: Remaining thrombus formation in the tibiofibular trunk and in the posterior tibial artery (arrows); E,F: Flow restoration in the foot after using the Rotarex®S in the proximal and median segments of the posterior tibial artery.

delivery to remove the thrombus and restore blood flow^[11]. It should be noted that only observational, non-randomized data are available for such devices, including the Rotarex®S system, whereas no direct comparisons for different thrombectomy devices have been reported so far.

The Rotarex®S system is a purely mechanical endovascular thrombectomy device (Straub Medical AG, Switzerland)^[12,13]. The system consists of an external drive system, which is connected to the Rotarex®S catheter *via* a magnetic clutch. Inside the catheter tube, a helix transmits the rotation from the drive system to the catheter head, which can rotate with up to 60000 rpm, thus creating a powerful vortex to debulk all detachable occlusion material from the vessel. The fragmented debris is subsequently aspirated through side slits in the catheter head. The inner helix simultaneously creates a strong suction force, following the Archimedes principle, and finally transports the fragmented material into an external collecting bag. The Rotarex®S catheter is currently available in three sizes, including 6F, 8F and 10F, and is inserted over a dedicated 0.018 guidewire. The aspiration efficacy is approximately 0.75 mL/s for

the 6F system, which can be safely used in vessels with a diameter of ≥ 3 mm to 5 mm.

Several studies have demonstrated the efficacy of this system in the treatment of patients with ALI^[14-18]. In this regard, a high success rate of $> 98\%$ was reported in a recent study, which elegantly demonstrated that purely mechanical thrombectomy by the Rotarex®S system was safer and more effective than thrombolysis, which was associated with higher rates of major bleedings, longer hospitalization durations and higher costs^[19]. Potential complications associated with the Rotarex®S endovascular system is peripheral embolization of thrombotic debris in peripheral foot arteries (in most of the cases after additional balloon angioplasty and not directly related to Rotarex®S thrombectomy) and vessel dissection or perforation in smaller vessels. Particularly in vessels smaller than 3 mm in diameter, perforation may occur due to complete filling of the vessel by the catheter, which may eventually suck the vessel wall into the side windows of the catheter head. Although such complications can in most cases be treated by prolonged balloon inflation or by stent placement without requiring surgical action^[16,20], the use of the 6F Rotarex®S system

is not currently generally recommended for crural arteries in the current literature^[21]. In this regard, the use of the Rotarex®S has been reported only in a relatively small number of patients with ALI involving below the knee vessels ($n = 4$ in the study of Stanek *et al.*^[18]).

To the best of our knowledge the present study is the first in the current literature, which in detail describes the efficacy and safety of the 6F Rotarex®S system in a miniseries of seven patients, who were all treated for ALI in the proximal or mid-part of relatively big crural arteries with good angiographic and clinical results. Although no vascular complications in terms of dissection or perforation occurred in the crural arteries, the use of the 6F Rotarex®S debulking system should be performed with caution in crural arteries.

In conclusion, mechanical debulking using the 6F Rotarex®S catheter system may be a safe and effective treatment option in case of thrombotic or thromboembolic occlusion of the proximal and mid portion of crural arteries in patients presenting with ALI, especially when local thrombolysis needs to be avoided due to increased bleeding risk.

ARTICLE HIGHLIGHTS

Research background

Endovascular treatment of acute limb ischemia (ALI) is increasingly gaining importance in older and multimorbid patients, compared to conventional surgical techniques. The Rotarex®S debulking system is one such endovascular device, which can be used for catheter-assisted thrombectomy in ALI. However, the use of the 6 French (6F) Rotarex®S system is not generally recommended for crural arteries in the current literature.

Research motivation

Limited data exist to date on the efficacy and safety of the 6F Rotarex®S system for thrombectomy in crural arteries.

Research objectives

Our study aimed to examine whether the 6F Rotarex®S system can be used effectively and safely for endovascular thrombectomy of crural arteries in patients with ALI.

Research methods

Retrospective analysis of all patients who were referred to our department for endovascular thrombectomy due to ALI between January 2015 and December 2017.

Research results

We identified seven patients who underwent endovascular Rotarex®S catheter thrombectomy in crural arteries due to remaining thrombus formation with no reflow. In two cases, thrombectomy was performed in the anterior tibial artery, in another two cases, in the posterior tibial artery and in the remaining three cases, in the fibular artery. In all seven cases, treatment resulted in restoration of the blood flow to the foot arteries, resolving ischemic symptoms. Vessel dissection or perforation did not occur in any of the seven cases.

Research conclusions

Endovascular thrombectomy using the 6F Rotarex®S catheter system may be safe and effective for the treatment of thrombotic occlusion of the proximal and mid portion of crural arteries. In particular, patients with high bleeding risk may profit from such a "mechanical only" treatment option without the need for additional thrombolysis.

Research perspectives

Larger prospective trials are necessary in the future to examine the efficacy and safety of the 6F Rotarex®S catheter system in smaller arteries of the lower limb.

REFERENCES

- 1 **Creager MA**, Kaufman JA, Conte MS. Clinical practice. Acute limb ischemia. *N Engl J Med* 2012; **366**: 2198-2206 [PMID: 22670905 DOI: 10.1056/NEJMcpl006054]
- 2 **Norgren L**, Hiatt WR, Dormandy JA, Nehler MR, Harris KA, Fowkes FG; TASC II Working Group. Inter-Society Consensus for the Management of Peripheral Arterial Disease (TASC II). *J Vasc Surg* 2007; **45 Suppl S**: S5-67 [PMID: 17223489 DOI: 10.1016/j.jvs.2006.12.037]
- 3 **Rutherford RB**, Baker JD, Ernst C, Johnston KW, Porter JM, Ahn S, Jones DN. Recommended standards for reports dealing with lower extremity ischemia: revised version. *J Vasc Surg* 1997; **26**: 517-538 [PMID: 9308598 DOI: 10.1016/S0741-5214(97)70045-4]
- 4 **Faglia E**, Clerici G, Clerissi J, Gabrielli L, Losa S, Mantero M, Caminiti M, Curci V, Lupattelli T, Morabito A. Early and five-year amputation and survival rate of diabetic patients with critical limb ischemia: data of a cohort study of 564 patients. *Eur J Vasc Endovasc Surg* 2006; **32**: 484-490 [PMID: 16730466 DOI: 10.1016/j.ejvs.2006.03.006]
- 5 **Lichtenberg MKW**, Stahlhoff WF. Endovascular-first strategy for acute and subacute limb ischaemia: Potential benefits of a pure mechanical thrombectomy approach Comment on Stanek et al, p. 49–56. *Vasa* 2016; **45**: 7-9 [PMID: 26986704 DOI: 10.1024/0301-1526/a000489]
- 6 **Ouriel K**, Veith FJ, Sasahara AA. A comparison of recombinant urokinase with vascular surgery as initial treatment for acute arterial occlusion of the legs. Thrombolysis or Peripheral Arterial Surgery (TOPAS) Investigators. *N Engl J Med* 1998; **338**: 1105-1111 [PMID: 9545358 DOI: 10.1056/NEJM199804163381603]
- 7 **Wasilewska M**, Gosk-Bierska I. Thromboembolism associated with atrial fibrillation as a cause of limb and organ ischemia. *Adv Clin Exp Med* 2013; **22**: 865-873 [PMID: 24431317]
- 8 **Ouriel K**, Shortell CK, DeWeese JA, Green RM, Francis CW, Azodo MV, Gutierrez OH, Manzione JV, Cox C, Marder VJ. A comparison of thrombolytic therapy with operative revascularization in the initial treatment of acute peripheral arterial ischemia. *J Vasc Surg* 1994; **19**: 1021-1030 [PMID: 8201703 DOI: 10.1016/S0741-5214(94)70214-4]
- 9 **Lukasiewicz A**. Treatment of acute lower limb ischaemia. *Vasa* 2016; **45**: 213-221 [PMID: 27129066 DOI: 10.1024/0301-1526/a000527]
- 10 **Deák Z**, Strube H, Sadeghi-Azandaryani M, Reiser MF, Treitl M. Rotational thrombectomy of acute peripheral vascular occlusions using the ThromCat XT device: techniques, indications and initial results. *Diagn Interv Radiol* 2011; **17**: 283-289 [PMID: 20976670 DOI: 10.4261/1305-3825.DIR.3687-10.2]
- 11 **Walker TG**. Acute limb ischemia. *Tech Vasc Interv Radiol* 2009; **12**: 117-129 [PMID: 19853229 DOI: 10.1053/j.tvir.2009.08.005]
- 12 **Stanek F**, Ouhrajkova R, Prochazka D. Mechanical thrombectomy using the Rotarex catheter—safe and effective method in the treatment of peripheral arterial thromboembolic occlusions. *Vasa* 2010; **39**: 334-340 [PMID: 21104623 DOI: 10.1024/0301-1526/a000058]
- 13 **Stanek F**, Ouhrajkova R, Prochazka D. Mechanical thrombectomy using the Rotarex catheter in the treatment of acute and subacute occlusions of peripheral arteries: immediate results, long-term follow-up. *Int Angiol* 2013; **32**: 52-60 [PMID: 23435392]
- 14 **Schmitt HE**, Jäger KA, Jacob AL, Mohr H, Labs KH, Steinbrich W. A new rotational thrombectomy catheter: system design and first clinical experiences. *Cardiovasc Intervent Radiol* 1999; **22**: 504-509 [PMID: 10556411 DOI: 10.1007/s002709900440]
- 15 **Bérczi V**, Deutschmann HA, Schedlbauer P, Tauss J, Hausegger KA. Early experience and midterm follow-up results with a new, rotational thrombectomy catheter. *Cardiovasc Intervent Radiol* 2002; **25**: 275-281 [PMID: 12042988 DOI: 10.1007/s00270-001-0095-6]
- 16 **Duc SR**, Schoch E, Pfyffer M, Jenelten R, Zollkofer CL.

- Recanalization of acute and subacute femoropopliteal artery occlusions with the rotarex catheter: one year follow-up, single center experience. *Cardiovasc Intervent Radiol* 2005; **28**: 603-610 [PMID: 16132388 DOI: 10.1007/s00270-004-0339-3]
- 17 **Zeller T**, Frank U, Bürgelin K, Schwarzwälder U, Horn B, Flügel PC, Neumann FJ. Long-term results after recanalization of acute and subacute thrombotic occlusions of the infra-aortic arteries and bypass-grafts using a rotational thrombectomy device. *Rofo* 2002; **174**: 1559-1565 [PMID: 12471529 DOI: 10.1055/s-2002-35942]
 - 18 **Stanek F**, Ouhrabkova R, Prochazka D. Percutaneous mechanical thrombectomy in the treatment of acute and subacute occlusions of the peripheral arteries and bypasses. *Vasa* 2016; **45**: 49-56 [PMID: 26986710 DOI: 10.1024/0301-1526/a000495]
 - 19 **Kronlage M**, Printz I, Vogel B, Blessing E, Müller OJ, Katus HA, Erbel C. A comparative study on endovascular treatment of (sub)acute critical limb ischemia: mechanical thrombectomy vs thrombolysis. *Drug Des Devel Ther* 2017; **11**: 1233-1241 [PMID: 28458517 DOI: 10.2147/DDDT.S131503]
 - 20 **Eisele T**, Muenz BM, Korosoglou G. Successful Endovascular Repair of an Iatrogenic Perforation of the Superficial Femoral Artery Using Self-Expanding Nitinol Supera Stents in a Patient with Acute Thromboembolic Limb Ischemia. *Case Rep Vasc Med* 2016; **2016**: 7376457 [PMID: 27213074 DOI: 10.1155/2016/7376457]
 - 21 **Wissgott C**, Kamusella P, Richter A, Klein-Wiegel P, Steinkamp HJ. [Mechanical rotational thrombectomy for treatment thrombolysis in acute and subacute occlusion of femoropopliteal arteries: retrospective analysis of the results from 1999 to 2005]. *Rofo* 2008; **180**: 325-331 [PMID: 18499908 DOI: 10.1055/s-2008-1027144]

P- Reviewer: Chang ST, Petix NR, Teragawa H, Said SA, Ueda H, Anan

R S- Editor: Dou Y

L- Editor: Filipodia **E- Editor:** Wu YXJ



Observational Study

Incidental congenital coronary artery vascular fistulas in adults: Evaluation with adenosine-¹³N-ammonia PET-CT

Salah AM Said, Aly Agool, Arno HM Moons, Mounir WZ Basalus, Nils RL Wagenaar, Rogier LG Nijhuis, Jutta M Schroeder-Tanka, Riemer HJA Slart

Salah AM Said, Mounir WZ Basalus, Rogier LG Nijhuis, Department of Cardiology, Hospital Group Twente, Almelo-Hengelo 7555 DL, Overijssel, The Netherlands

Aly Agool, Nils RL Wagenaar, Department of Nuclear Medicine, Hospital Group Twente, Almelo-Hengelo 7555 DL, Overijssel, The Netherlands

Arno HM Moons, Department of Cardiology, Slotervaart Hospital, Amsterdam 1066 EC, North Holland, The Netherlands

Jutta M Schroeder-Tanka, Department of Cardiology, Hospital Onze Lieve Vrouwe Gasthuis, Location West, Amsterdam 1061 AE, North Holland, The Netherlands

Riemer HJA Slart, Medical Imaging Center, Department of Nuclear Medicine and Molecular Imaging, University Medical Center Groningen, Groningen 9713 GZ, The Netherlands

Riemer HJA Slart, Faculty of Science and Technology, Biomedical Photonic Imaging, University of Twente, Enschede 7522 NB, The Netherlands

ORCID number: Salah AM Said (0000-0003-1221-9264); Aly Agool (0000-0003-1644-3597); Arno HM Moons (0000-0003-0647-9772); Mounir WZ Basalus (0000-0002-7008-5973); Nils RL Wagenaar (0000-0003-3966-1140); Rogier LG Nijhuis (0000-0001-6975-8053); Jutta M Schroeder-Tanka (0000-0001-5962-3286); Riemer HJA Slart (0000-0002-5565-1164).

Author contributions: All authors contributed to this paper; concept and design by Said SAM and Basalus MWZ; data acquisition by Moons AHM, Schroeder-Tanka JM and Nijhuis RLG; analysis of nuclear studies Agool A, Wagenaar NRL and Slart RHJA; Slart RHJA performed critical revision of manuscript; all authors have approved the final version of the paper.

Institutional review board statement: The study was reviewed and approved by the local medical ethical committee of the Eastern region, Enschede, The Netherlands (ID METC: K18-14, METC/18082.sai).

Informed consent statement: The study was reviewed and approved by the local medical ethical committee and the requirement to obtain informed consent was waived due to the retrospective nature of the report, the Eastern region, Enschede, The Netherlands (ID METC: K18-14, METC/18082.sai).

Conflict-of-interest statement: The authors declare that they have no competing interests.

STROBE statement: The authors have read the STROBE Statement-checklist of items, and the manuscript was prepared and revised according to the STROBE Statement-checklist of items.

Open-Access: This article is an open-access article which was selected by an in-house editor and fully peer-reviewed by external reviewers. It is distributed in accordance with the Creative Commons Attribution Non Commercial (CC BY-NC 4.0) license, which permits others to distribute, remix, adapt, build upon this work non-commercially, and license their derivative works on different terms, provided the original work is properly cited and the use is non-commercial. See: <http://creativecommons.org/licenses/by-nc/4.0/>

Manuscript source: Invited manuscript

Correspondence to: Salah AM Said, MD, PhD, Doctor, Staff Physician, Cardiologist, Department of Cardiology, Hospital Group Twente, Geerdinksweg 141, Almelo-Hengelo 7555 DL, Overijssel, The Netherlands. samsaid@home.nl

Telephone: +31-88-7085286

Fax: +31-88-7085289

Received: June 27, 2018

Peer-review started: June 30, 2018

First decision: July 19, 2018

Revised: August 21, 2018

Accepted: August 30, 2018

Article in press: August 30, 2018

Published online: October 26, 2018

Abstract

AIM

To assess the functionality of congenital coronary artery fistulas (CAFs) using adenosine stress ^{13}N -ammonia positron emission tomography computed tomography (PET-CT).

METHODS

Congenital CAFs were incidentally detected during coronary angiography (CAG) procedures in 11 adult patients (six males and five females) with a mean age of 64.3 years (range 41-81). Patients were collected from three institutes in the Netherlands. The characteristics of the fistulas (origin, pathway and termination), multiplicity of the origins and pathways of the fistulous vessels were assessed by CAG. Five patients underwent adenosine pharmacologic stress ^{13}N -ammonia PET-CT to assess myocardial perfusion and the functional behavior of the fistula.

RESULTS

Eleven patients with 12 CAFs, 10 unilateral and one bilateral, originating from the left anterior descending coronary artery ($n = 8$), right coronary artery ($n = 2$) and circumflex ($n = 2$). All fistulas were of the vascular type, terminating into either the pulmonary artery ($n = 11$) or coronary sinus ($n = 1$). The CAG delineated the characteristics of the fistula (origin, pathway and termination). Multiplicity of the origins and pathways of the fistulous vessels were common in most fistulas (8/12, 67% and 9/12, 75%, respectively). Multiplicity was common among the different fistula components (23/36, 64%). Adenosine pharmacologic stress ^{13}N -ammonia PET-CT revealed normal myocardial perfusion and ejection fraction in all but one patient, who showed a reduced ejection fraction.

CONCLUSION

PET-CT may be helpful for assessing the functional status of congenital CAFs in selected patients regarding clinical decision-making. Studies with a larger patient series are warranted.

Key words: Coronary angiography; Coronary-pulmonary artery fistulas; Adenosine ammonia positron emission tomography computed tomography; Coronary vascular fistulas; Congenital coronary artery fistulas

© The Author(s) 2018. Published by Baishideng Publishing Group Inc. All rights reserved.

Core tip: Congenital coronary artery fistulas are usually detected as a coincidental finding during non-invasive and invasive diagnostic modalities for the assessment of coronary artery disease. Positron emission tomography computed tomography (PET-CT) is not frequently applied for functional assessment. In the current study, five patients underwent adenosine ^{13}N -ammonia PET-CT to assess myocardial perfusion and the functional behavior of the fistula. PET-CT revealed normal myocardial per-

fusion and ejection fraction in all but one patient, who showed a reduced ejection fraction. Combined with semi-quantitative results, patients with normal flow, revealed by PET-CT, could be treated medically, thereby avoiding the need for transcatheter or surgical occlusion of the fistulas.

Said SAM, Agool A, Moons AHM, Basalus MWZ, Wagenaar NRL, Nijhuis RLG, Schroeder-Tanka JM, Slart RHJA. Incidental congenital coronary artery vascular fistulas in adults: Evaluation with adenosine- ^{13}N -ammonia PET-CT. *World J Cardiol* 2018; 10(10): 153-164 Available from: URL: <http://www.wjgnet.com/1949-8462/full/v10/i10/153.htm> DOI: <http://dx.doi.org/10.4330/wjc.v10.i10.153>

INTRODUCTION

Congenital coronary artery fistulas (CAFs) are most often incidentally found during coronary angiography (CAG)^[1], computed tomography coronary angiography (CTCA)^[2] and transthoracic echocardiography (TTE)^[3-5]. Coronary artery vascular and cameral fistulas are not only seen in humans, but are also occasionally observed in other mammals^[6]. CAFs are classified as anomalies of termination^[7]. Several diagnostic modalities are available for the morphological and functional detection of CAFs, including physical examination (presence of a continuous murmur), non-invasive methods such as echocardiography^[8,9], myocardial perfusion imaging (MPI)^[10,11], CTCA^[3,9,12] and cardiovascular magnetic resonance imaging (MRI)^[13], invasive techniques such as right heart catheterization, CAG and fractional flow reserve (FFR)^[1,14-18], and incidental detection during positron emission tomography computed tomography (PET-CT)^[19,20]. Exercise and pharmacological PET-CT is commonly applied for the assessment of myocardial perfusion and ischemia, and for the diagnosis and risk stratification of ischemic coronary artery disease (CAD)^[21,22]. Adenosine ^{13}N -ammonia PET-CT is useful for assessing coronary flow reserve and myocardial perfusion for risk stratification in patients with CAD^[23], the results of which influence patient management strategies^[24]. Myocardial ischemia can also be detected using single-photon emission computed tomography (SPECT) in patients with congenital CAFs^[15]. It is unclear whether congenital fistulas are associated with reduced myocardial perfusion, which is sometimes associated with impaired left ventricular function. Indications for surgical intervention or percutaneous therapeutic embolization are based on the patient's clinical presentation and on imaging findings. The aim of the present study was to evaluate the value of adenosine pharmacologic stress ^{13}N -ammonia PET-CT in a selected population of patients with incidentally identified congenital CAFs.

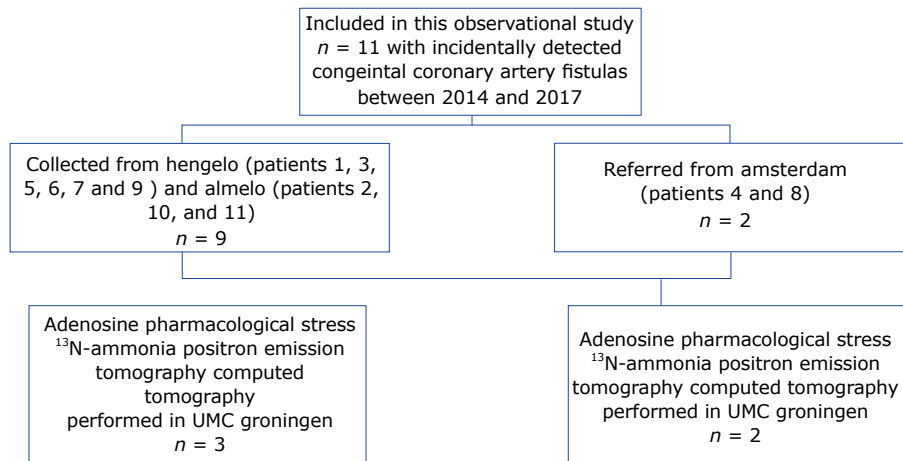


Figure 1 Flowchart of the study patients who were collected from 3 different non-academic Dutch institutes.

MATERIALS AND METHODS

Study subjects

We collected 11 patients (six males and five females; mean age of 64.3 years, range 41–81 years) with CAFs which were incidentally detected during routine CAG between 2014 and 2017. The FFR was not determined due to a lack of facilities. The patients were collected from three centers in the Netherlands as follows: Amsterdam, patients 4 and 8; Hengelo, patients 1, 3, 5, 6, 7 and 9; and Almelo, patients 2, 10 and 11 (Figure 1). Patient data was obtained from the databases of three Dutch cardiac catheterization laboratories (Slotervaart Hospital, Amsterdam; Onze Lieve Vrouwe Gasthuis, Amsterdam; and Hospital Group Twente, Almelo-Hengelo).

All patients underwent electrocardiography (ECG) and TTE. Five patients were further analyzed by adenosine stress/rest ^{13}N -ammonia PET-CT to quantify myocardial blood flow (MBF), myocardial perfusion and coronary flow reserve. Further studies to clarify the clinical presentation and fistula characteristics were performed at the clinician's discretion. Stress and rest MPI SPECT (Symbia S, Siemens Medical Solutions, Erlangen, Germany) were performed in one patient (patient 7), CTCA and MRI were performed in two patients (patients 2 and 4), and shunt calculation by the oximetric method was performed in four patients (patients 3, 4, 7 and 8).

The ECG-gated PET images were acquired using a whole-body 64-slice PET-CT scanner (Biograph True Point; Siemens Medical Solutions). The PET data were acquired in 3D list mode. Patients were studied after an overnight fast, and all refrained from caffeine-containing beverages or theophylline-containing medications for 24 h before the study. Myocardial perfusion was assessed at rest and during vasodilator stress induced by adenosine, using ^{13}N -ammonia as the perfusion radiotracer. Two CT-based transmission scans (120 kVp; 20–30 mA; helical scan mode with a pitch of 1.35) were obtained before and after the resting perfusion studies, performed with

normal breathing to correct for photon attenuation of PET. The procedure involved the intravenous administration of 400 MBq of ^{13}N -ammonia during rest and 400 MBq of ^{13}N -ammonia during adenosine-induced pharmacological stress.

The PET and SPECT images were interpreted semi-quantitatively using the standard American Heart Association 5-point scoring system^[25], and traditional metrics including summed difference score, summed stress score and summed rest score (SRS) were calculated. The SRS (in a fixed perfusion defect) was considered to be a measure of the extent and severity of a previous myocardial infarction (MI). Quantitative MBF values (mL/g per minute) at rest and under stress were computed for each sample on the polar map, as described previously^[21], using a three-tissue compartment pharmacokinetic model for ^{13}N -ammonia^[26]. Myocardial perfusion reserve (MPR) was calculated as the ratio between stress MBF and rest MBF (making it a unitless variable). The resting MBF was corrected for the rate-pressure product. The global MPR and stress MBF were calculated for the whole left ventricular region (defined by the left ventricle long-axis plane), representing the parameters of interest for our analysis.

The ECG-gated images were analyzed using the QGS software package (Cedars-Sinai, Los Angeles, CA, United States)^[27]. Short-axis images were processed, and ventricular edges and cavity volumes were calculated for each of the eight re-binned dynamic frames that were reconstructed for the average cardiac cycle. The algorithm for determining edges and calculating volume has been described previously.

Ethical considerations

The study was reviewed and approved by the local medical ethical committee of the eastern region, Enschede, the Netherlands (ID METC: K18-14, METC /18082.sai). As the patients' personal information was protected, and therefore could not be identified and anonymized, it was exempt from consent by the local medical ethical

Table 1 Symptoms, clinical presentation and physical findings of adult subjects with congenital coronary artery fistula

| Case | Fistula origin and termination | Symptoms and clinical presentation | Previous history and risk factors | Physical findings | BMI | Intervention |
|------|--------------------------------|---|--|--|------|---|
| 1 | RCA and LAD to PA | Chest pain NSTEMI/PMI (CK 390 U/L) | Tubular adenoma of sigmoid, celiac disease | Normal | 32.7 | None |
| 2 | LAD to PA | Chest pain NSTEMI (CK 573 U/L) | Old IMI Asthma | Normal | 25.9 | CABG and surgical closure of the fistula |
| 3 | LCx to PA | Chest pain | Blanco | Normal | 26.6 | Coiling of the fistula and PCI of LAD |
| 4 | RCA to CS | Dyspnea on exertion | Diaphragmatic hernia, asthma and hypertension | Systolic ejection murmur grade 2/6 2 d ICS | 28.2 | None |
| 5 | LAD to PA | Non-sustained VT | DM, COPD, hypertension, hypothyroidism | Systolic ejection murmur grade 2/6 2 d ICS | 33.4 | PCI of OM branch and FFR of LAD. Coiling of the fistula |
| 6 | LAD to PA | Dyspnea on exertion | COPD Severe mitral valve regurgitation | Apical mitral regurgitation murmur grade 2/6 | 25.5 | Mitral valve plasty |
| 7 | LAD to PA | Chest pain | Celiac disease | Normal | 24.2 | |
| 8 | LAD to PA | Angina pectoris | Hypercholesterolemia Positive family history for CAD | Systolic ejection murmur grade 2/6 2 d ICS | 21.1 | PCI of LAD |
| 9 | LCx to PA | Palpitation PAF and non-sustained VT Hypertension | Ischemic CVA | Normal | 24.8 | None |
| 10 | LAD to PA | Angina pectoris | NSTEMI 2010 (CK 328 U/L). PCI of RCA 2012 | Normal | 24.2 | Coiling of the fistula |
| 11 | LAD to PA | Chest pain | Hypertension, hypercholesterolemia Positive family history for CAD Smoker | Normal | 29.1 | None |

BMI: Body mass index; CABG: Coronary artery bypass grafting; CAD: Coronary artery disease; CK: Creatinine kinase; COPD: Chronic obstructive pulmonary disease; CS: Coronary sinus; CVA: Cerebral vascular disease; DM: Diabetes mellitus; FFR: Fractional flow reserve; ICS: Intercostal space; IMI: Inferior wall myocardial infarction; LAD: Left anterior descending coronary artery; LCx: Left circumflex coronary artery; NSTEMI: Non-ST elevation myocardial infarction; OM: Obtuse marginal branch; PA: Pulmonary artery; PAF: Paroxysmal atrial fibrillation; PCI: Percutaneous coronary intervention; PMI: Posterior myocardial infarction; RCA: Right coronary artery; VT: Ventricular tachycardia.

committee.

Statistical analysis

Categorical data are expressed as numbers with percentages, and continuous data are expressed as means with a range.

RESULTS

This retrospective case series included 11 (Figure 1) patients with 12 congenital coronary vascular fistulas (CVFs). Of those patients, five underwent adenosine pharmacologic stress ¹³N-ammonia PET-CT to assess myocardial perfusion and functionality of the fistula.

Clinical presentations and features (Table 1) included limited posterior MI (patient 1), angina pectoris and chest pain ($n = 6$), dyspnea on exertion ($n = 3$) and asymptomatic abnormal resting ECG ($n = 1$). One patient (patient 9) presented with palpitation, transient ischemic attack, paroxysmal atrial fibrillation and non-sustained ventricular tachycardia. Previous MI was reported in two patients (patients 2 and 10). Patient 5 had exercise-

induced non-sustained ventricular tachycardia. Physical examination was unremarkable in seven patients. Apical systolic murmur was heard in one patient, and systolic ejection murmur was heard in the second intercostal space in three patients.

In regard to the ECG, sinus rhythm was present in 10 patients and permanent atrial fibrillation was found in one patient. We also observed tall R-waves in precordial lead 2 ($n = 1$), signs of previous inferior MI ($n = 1$), non-specific repolarization abnormalities ($n = 4$), left bundle branch block ($n = 1$), left axis deviation ($n = 1$) and 1st degree atrioventricular delay ($n = 1$).

Echocardiography revealed normal findings in four patients, inferolateral hypokinesia in one patient, anteroseptal akinesia in one patient, mild aortic valvular stenosis with moderate aortic regurgitation (AR) in one patient, mild AR in one patient, mild mitral regurgitation (MR) in three patients, moderate to severe MR in one patient, and mild tricuspid regurgitation in three patients. Right ventricular systolic pressure was normal in all patients. Dilated coronary sinus (CS) was found in one patient (patient 4). One patient underwent

Table 2 Angiographic characteristics of fistula components

| Case | Fistula origin and termination | Yr of detection | Angiographic characteristics of fistula components | | | | | | | | |
|------|--------------------------------|-----------------|--|-----|---|---|-----|---|---|-----|---|
| | | | O | LCx | T | O | RCA | T | O | LAD | T |
| 1 | RCA and LAD to PA | 2014 | | P | | M | MT | M | S | MT | S |
| 2 | LAD to PA | 2015 | | | | | | | M | MT | M |
| 3 | LCx to PA | 2015 | S | ST | S | | | | | | |
| 4 | RCA to CS | 2015 | | | | S | ST | S | | | |
| 5 | LAD to PA | 2016 | | | | | | | S | ST | S |
| 6 | LAD to PA | 2016 | | | | | | | M | M | M |
| 7 | LAD to PA | 2016 | | | | | | | M | MT | M |
| 8 | LAD to PA | 2015 | | | | | | | M | MT | S |
| 9 | LCx to PA | 2016 | M | MT | M | | | | | | |
| 10 | LAD to PA | 2017 | | | | | | | M | M | M |
| 11 | LAD to PA | 2017 | | | | | | | M | MT | S |

CS: Coronary sinus; LAD: Left anterior descending coronary artery; LCx: Left circumflex coronary artery; RCA: Right coronary artery; PA: Pulmonary artery; M: Multiple; MT: Multiple and tortuous; S: Single; ST: Single and tortuous; T: Termination; O: Origin; P: Pathway.

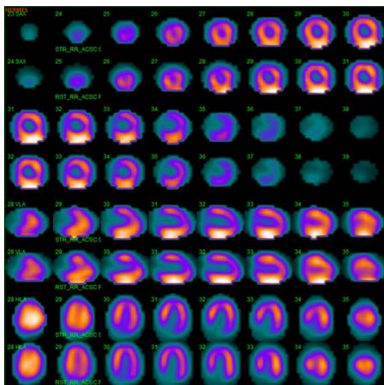


Figure 2 ^{99m}Tc -sestamibi single-photon emission computed tomography scintigraphy, demonstrating normal myocardial perfusion and a normal left ventricular ejection fraction.

^{99m}Tc -sestamibi SPECT scintigraphy (patient 7), which revealed normal myocardial perfusion (Figure 2) and a normal left ventricular ejection fraction (LVEF) of 0.67. Two patients underwent CTCA (patient 2, patient 4), which confirmed the diagnosis of coronary artery vascular fistulas.

Cardiovascular MRI was performed in two patients (patients 2 and 4), which revealed moderate left ventricular hypertrophy and signs of healed MI in three flow territories (patient 2). Shunt calculation by oximetry was performed in four patients (patients 3, 4, 7 and 8) who showed left-to-right shunt ratios of 1.75:1, 1.3:1, 1.1:1 and 2.0:1, respectively, with a mean of 1.53:1 (range 1.1-2.0).

CAG was used to delineate the characteristics of the fistula (origin, pathway and termination; Figures 3-10 and Table 2). The multiplicity of the origin of the fistulous vessels and the pathway were plural in most fistulas (8/12, 67% and 9/12, 75%, respectively). The termination was equally distributed between single (6/12, 50%) and multiple (6/12, 50%) fistulous vessels. Multiplicity was common among the different fistula components (23/36, 64%). Tortuosity of the

pathway was found in eight fistulas (8/12, 67%).

There were 10 unilateral (Figure 4) and one bilateral (Figure 3A and B) fistulas. All fistulas were of the coronary vascular type, terminating into the pulmonary artery (PA, $n = 11$; Figure 5) or the coronary sinus ($n = 1$; Figure 6), and originating from the left anterior descending coronary artery (LAD; $n = 8$; Figure 7), right coronary artery (RCA; $n = 2$; Figures 3B and 6) or left circumflex coronary artery (LCx; $n = 2$; Figures 5 and 10). The characteristics of the fistula (origin, pathway and termination) showed multiple origins of fistulous vessels and pathways in most fistulas (8/12, 67% and 9/12, 75%, respectively; Figure 9). Multiplicity was common among the different fistula components (22/36, 61%; Figures 3B, 4 and 10). In contrast, single (7/12, 58%) termination of the fistulous vessels was more common than multiple (5/12, 42%) termination of fistulous vessels.

Dilated RCA was found in one patient (patient 4; Figure 6A), while large and small aneurysmal formation was present in two patients (patients 2 and 6, respectively; Figures 4 and 8). The FFR was not measured. The ECG-gated imaging of adenosine stress/rest ^{13}N -ammonia PET-CT (Table 3) demonstrated homogenous distribution of perfusion in two patients, who showed no perfusion defects (patients 3 and 11). One patient showed diffuse, reversible reductions in perfusion in the apical and antero-septal regions, and partly in the basal anterior segment (patient 4) (Figure 11). In another patient, perfusion of the LAD area was slightly lower than the inferior segment, but it was equal to that of the lateral wall (patient 7). Normal perfusion with reduced LVEF (rest 33% and stress 39%) was probably underestimated in one patient (patient 8). In the five patients, the mean global stress/rest ratio for MPR was 2.9 (range 2.33-3.90). The mean regional stress/rest ratio was 3.0 for the LAD (range 2.35-4.50), 2.9 for the RCA (range 2.49-3.60) and 2.8 for the LCx (range 2.36-3.20). Blood flow through the LAD was slightly higher than flow through the RCA and LCx.

Table 3 Pharmacological adenosine stress/rest ¹³N-ammonia positron emission tomography computed tomography in 5 patients with unilateral coronary vascular fistulas

| Case | CAF | Stress/rest perfusion segments | | | | LVEF (%) | | Semi-quantitative findings | CAD | Prior procedure | Management of CAF |
|------|--------|--------------------------------|------|------|--------|----------|--------|--|------|-----------------|-------------------|
| | | LCx | RCA | LAD | Global | Rest | Stress | | | | |
| 3 | LCx-PA | 2.74 | 2.49 | 2.56 | 2.59 | 52 | 57 | No perfusion defects | 1-VD | PCI-LAD | PTE |
| 4 | RCA-CS | 2.65 | 2.7 | 2.71 | 2.69 | 65 | 65 | Diffuse reversible reduction of perfusion in the apical, antero-septal and partially in basal anterior segment | None | None | CMM |
| 7 | LAD-PA | 2.36 | 2.55 | 2.35 | 2.33 | 60 | 65 | Perfusion of LAD area is less than inferior segment | None | None | CMM |
| 8 | LAD-PA | 3.02 | 2.91 | 2.94 | 2.95 | 33 | 39 | Normal perfusion with reduced LVEF | 1-VD | PCI-LAD | CMM |
| 11 | LAD-PA | 3.2 | 3.6 | 4.5 | 3.9 | 65 | 65 | No perfusion defects | None | None | CMM |

CAD: Coronary artery disease; CAF: Coronary artery fistula; CMM: Conservative medical management; CS: Coronary sinus; LAD: Left anterior descending coronary artery; LCx: Left circumflex coronary artery; LVEF: Left ventricular ejection fraction; PA: Pulmonary artery; PCI: Percutaneous coronary intervention; PTE: Percutaneous transcatheter embolization; RCA: Right coronary artery; VD: Vessel disease.

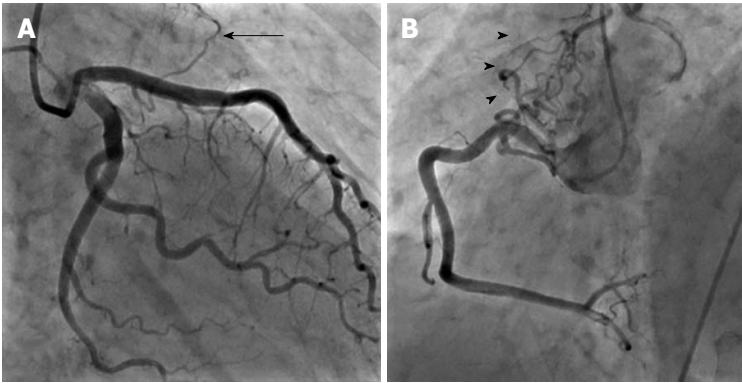


Figure 3 Bilateral fistulas. A: Bilateral fistulas from the left anterior descending coronary artery to the pulmonary artery with single origin, multiple pathway and single termination (arrow); B: Bilateral fistulas from the right coronary artery to the PA with multiple origin, pathway and termination (arrowheads).



Figure 4 Fistula from the proximal left anterior descending coronary artery to pulmonary artery with multiple origin, pathway and termination associated with large aneurysmal formation (arrow).

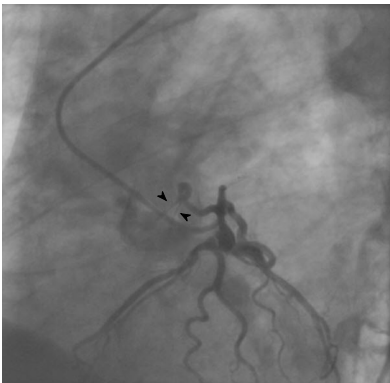


Figure 5 Fistula from the proximal left circumflex artery ending into the pulmonary artery characterized with single origin, pathway and termination emptying with double jets (arrowheads) ending into the pulmonary artery.

Absolute flow quantification in one patient (patient 3) yielded normal myocardial perfusion with high flow in the LCx, which was the fistula-related vessel, when compared to RCA and LAD flow, confirming successful percutaneous transcatheter embolization (PTE) closure of the fistulous vessel. On the other hand, semi-

quantitative analysis revealed normal perfusion in two patients and a diffuse reduction in perfusion in the other two patients. When combined with the semi-quantitative results, findings of normal flow by PET-CT indicate that conservative medical management (CMM) can be used as a management option for fistulous

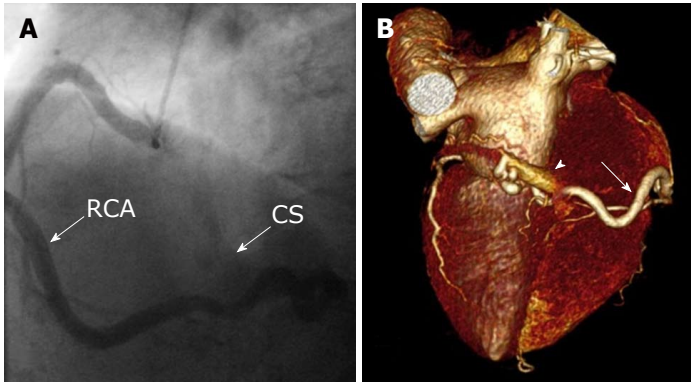


Figure 6 Unilateral fistula and computed tomography coronary angiography. A: Unilateral fistula originating from the right coronary artery (RCA) terminating into the coronary sinus (CS) with single origin, pathway and termination with dilated RCA and enlarged CS; B: Computed tomography coronary angiography: Coronary artery fistula originating from the distal segment of RCA (arrow) and terminating into the coronary sinus. Volume-rendered three-dimensional image reconstruction demonstrating fistulous vessel located posterior connected with the CS (arrowhead). RAC: Right coronary artery; CS: Coronary sinus.

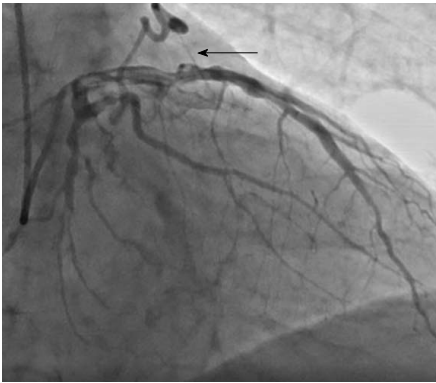


Figure 7 A fistulous connection between the left anterior descending coronary artery and pulmonary artery with single origin, pathway and termination with a single jet ending into the pulmonary artery (arrow).

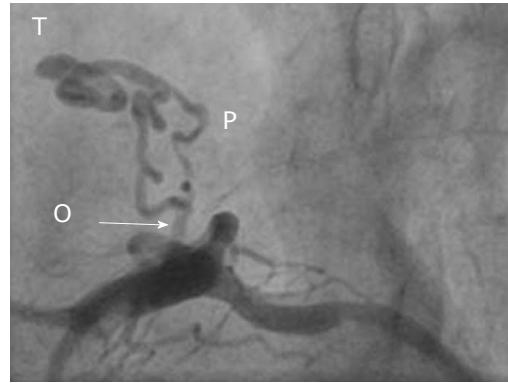


Figure 9 Left lateral frame demonstrating a fistula with multiple origin (arrow) and pathway from the proximal left anterior descending coronary artery ending to the pulmonary artery with a single termination. O: Origin; P: Pathway; T: Termination.



Figure 8 Right anterior oblique view shows the fistulous vessel between the left anterior descending coronary artery and the pulmonary artery with multiple origin, pathway and termination with small aneurysmal formation (arrow).



Figure 10 Left anterior oblique view shows a fistula between proximal left circumflex coronary artery (arrow) with multiple origin, pathway and termination with outflow to the pulmonary artery.

vessels, thereby avoiding the need for occlusion of the fistula.

The interventions included leaving a small fistula without percutaneous or surgical intervention; surgical ligation (SL) of the fistula in combination with CABG (patient 2); percutaneous closure of the fistulous tract

(LCx to PA) and percutaneous coronary intervention (PCI) of the LAD due to chest pain and dyspnea upon exertion (patient 3); PCI of the OM branch of the LCx and coiling of the fistula (LAD to PA) in a patient (patient 5) with non-sustained ventricular tachycardia; and transcatheter obliteration of the fistula secondary to

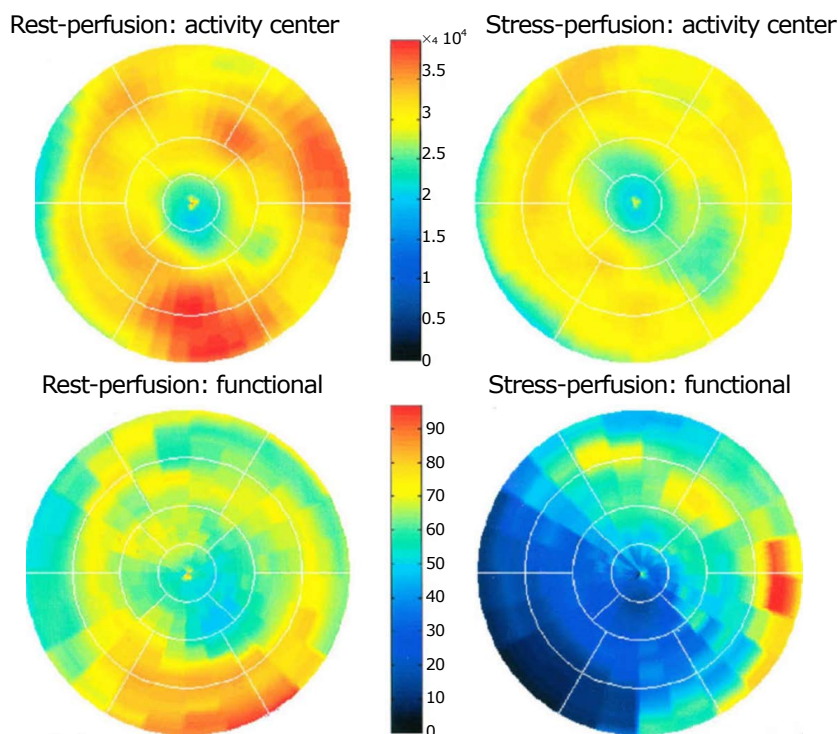


Figure 11 Positron emission tomography computed tomography scanning demonstrating normal findings on the rest ¹³N-ammonia polar map (left panel) and normal perfusion on adenosine ¹³N-ammonia polar map (right panel). Myocardial perfusion was assessed at rest and during vasodilator pharmacological stress induced by adenosine, using 400 MBq of ¹³N-ammonia as the perfusion radiotracer.

angina pectoris (patient 10).

Treatment and management of the fistula included CMM in seven patients, PTE in three patients and SL combined with coronary artery bypass grafting (CABG) in one patient. Of the patients who underwent adenosine stress/rest ¹³N-ammonia PET-CT, PTE was performed in only one patient (patient 3). This patient showed high flow in the LCx, which was the fistula-related vessel, and PTE was successfully performed with angiographic documentation. In the other four patients (patients 4, 7, 8 and 11), PET-CT showed no flow restrictions, indicating CMM and avoiding the need for fistula closure.

Five patients had known CAD (one vessel disease in four patients and three vessel diseases in one patient). Of these patients, three underwent PCI procedures, one patient was managed with optimal medical treatment, and one patient underwent CABG in combination with fistula ligation.

DISCUSSION

In this study, we describe congenital CAFs that were incidentally found in 11 adult patients during routine CAG. To investigate the functional characteristics of these fistulas, PET-CT was performed at rest and after adenosine pharmacological stress in five subjects. To date, the role of PET-CT has not been extensively studied in adult patients with congenital CAFs.

Congenital CAFs are usually asymptomatic in many

adult patients and are usually incidentally detected during routine CAG for suspected CAD. Over the past century, congenital CAFs associated with continuous cardiac murmur have often been confused with patent ductus arteriosus Botalli^[28,29]. More recently, congenital CAFs have been misdiagnosed as a right atrial myxoma^[30].

Coronary artery vascular and cameral fistulas are increasingly found during echocardiography^[3,31,32], CTCA^[2,33] and diagnostic CAG procedures^[1]. One study reported the diagnosis of a small coronary-pulmonary fistula (CPF) by echocardiography in asymptomatic dizygotic twin infant brothers^[31], suggesting a possible genetic cause of CAFs. Invasive CAG is considered the gold standard for the detection and diagnosis of congenital CAFs; however, non-invasive imaging techniques such as contrast echocardiography^[34], 2D and color Doppler echocardiography, cardiovascular MRI and CTCA provide valuable complementary data for the visualization of fistula components (origin, pathway and termination sites) that are not visible on the CAG^[20,35-37].

FFR

The value of FFR has been emphasized by several authors. Ouyang *et al.*^[38] reported deferral of treatment of the fistula-related artery and tandem intermediate stenosis in a patient with a huge CAF originating from the LAD and draining into the PA based on the findings of FFR. In the case of an adult subject assessed by both FFR and intravascular ultrasound, PCI was performed

for significant stenosis of the LAD, which was the fistula-related artery (LAD-PA), but the congenital fistula remained untouched due to the absence of myocardial ischemia^[18]. In congenital CAFs, the steal phenomenon has been demonstrated by FFR^[17]. Few reports have been published regarding the functional assessment of congenital CAFs (left main PA) in which FFR was used to guide clinical decision-making for intervention. In one of these reports, normal FFR was observed for a patient with concomitant moderate coronary artery stenosis, which led to the deferral of surgical or transcatheter interventions^[39]. Furthermore, Hollenbeck *et al*^[40] demonstrated ischemic changes due to the combination of a moderate LAD stenosis and CVF, which was relieved by PCI. Oh *et al*^[41] assessed the hemodynamic significance of congenital multiple micro-fistulas and coronary cameral fistulas by FFR, which ruled out ischemia. In 2014, Sasi *et al*^[42] assessed CAF using coronary flow reserve (CFR) and FFR. The LCx FFR and CFR were 0.97 and 2.33, respectively, and the LAD FFR of 0.86 was associated with a CFR of 1.56. This patient was treated medically. In 2016, Ito *et al*^[43] successfully performed FFR-guided PCI of an intermediate LAD stenosis associated with CAFs, and the fistula was treated conservatively. Bi-directional flow in the fistula may occur in the left ventricle^[44] and the right ventricle^[45]; however, none of our patients demonstrated bi-directional fistulous flow.

Radionuclide examinations and MPI

In the 1990s, myocardial perfusion scintigraphy SPECT using Tl-201 was performed in some patients to determine fistula-related ischemia. A report by Gupta *et al*^[46] in 1991, followed by Glynn *et al*^[47] in 1994, reported the first case studies documenting the use of thallium-201 perfusion imaging for physiological assessment of CAF (LAD-PA) and as the cause of an exercise-induced reversible thallium-201 perfusion defect in an adult patient^[46,47]. The pharmacological stress MPI SPECT technique may indicate segmental perfusion defects in patients with congenital CPF in the absence of CAD^[11]. In a patient series evaluated by Lee *et al*^[11], 35% of patients with congenital CPF without CAD developed perfusion defects, but the findings were only clinically relevant in 12%.

Adenosine stress-induced ¹³N-ammonia PET-CT uptake in the myocardium is related to perfusion and may offer better assessment of myocardial ischemia. Adenosine stress ¹³N-ammonia PET-CT has several advantages over SPECT, such as higher spatial resolution and sensitivity, absolute quantification, better counting efficiency and improved attenuation correction^[11,24]. In 2011, a report described the application of adenosine ¹³N-ammonia PET-CT in congenital CAFs for the first time^[19].

Adenosine ¹³N-ammonia PET-CT scanning is routinely applied to assess the functional status and quantify flow in patients with CAD^[26,48], which could also be used

in subjects with congenital coronary artery anomalies of origin (*i.e.*, single coronary artery^[49]) and termination (*i.e.*, CAFs^[19]).

Quantification of myocardial perfusion facilitates the high-performance detection and localization of perfusion abnormalities. In the same patient with CAF, PET-CT was reported to show greater areas of ischemic change than ^{99m}Tc-sestamibi scintigraphy^[50]. In a comparative study by Kong *et al*^[20], adenosine stress ¹³N-ammonia PET-CT imaging was shown to have higher diagnostic sensitivity (91% vs 65%) and specificity (89% vs 82%) compared with SPECT using Tc-99m sestamibi, providing better assessment of myocardial perfusion. Thus, MPI may guide decisions regarding which patients will benefit from invasive treatment. Adenosine ¹³N-ammonia PET-CT may prove to be valuable in clinical decision-making for whether to close the fistulous communication based on the presence or absence of distribution abnormalities^[51]. Successful SL of the fistula and reconstruction of the CS was performed in an adult male with a congenital RCA-CS fistula, which was associated with aneurysmal dilatation of the CS and stenosis of the CS ostium^[3]. In the patient series reported by Zhang *et al*^[52], SL of isolated congenital CAFs was related to lower morbidity and mortality associated with residual shunt in 8/47 (17%) patients, two of whom required PTE. Based on the findings of adenosine ¹³N-ammonia PET-CT in our five patients, transcatheter or surgical intervention was avoided in four subjects. In the current series, treatment and management of the fistula included CMM in seven patients, PTE in three patients and SL in one patient.

In conclusion, adenosine ¹³N-ammonia PET-CT is a useful technique that provides additional information for diagnosis and decision-making related to the management of incidentally detected congenital CAFs. The technique may also be useful for determining the functional status of the fistula and may add some clues for clinical decision-making in adult patients with congenital CAFs. Further prospective studies with a large number of patients are warranted.

Limitations of the study

Firstly, the study was retrospective in nature, with patients collected from different cardiac catheterization laboratories in the Netherlands. Secondly, this study contained a small sample size, involving a limited number of patients collected from three centers which used different diagnostic modalities. There is increasing need for a prospective international registry.

ARTICLE HIGHLIGHTS

Research background

Congenital coronary artery fistulas (CAFs) are uncommon coronary artery vascular anomalies which are often incidentally found during coronary angiography (CAG) performed for suspected atherosclerotic coronary artery disease (CAD). Moreover, most asymptomatic patients are diagnosed with CAFs during evaluation for cardiac murmur. Nowadays, congenital

CAFs are increasingly detected due to the widespread use of non-invasive techniques such as echocardiography and computed tomography coronary angiography (CTCA). Functional assessment and determination of the clinical significance of CAFs is of great importance for therapeutic decision-making. The choice of treatment strategy depends on the size and location of the fistula, the magnitude of left-to-right shunt and the characteristics of the fistulous tract. Many diagnostic modalities are currently used to evaluate the functional characteristics of the fistula, including non-invasive methods such as Doppler echocardiography, CTCA and radionuclide angiography, and invasive methods such as right heart catheterization and fractional flow reserve (FFR), among others. In the current study, the role of positron emission tomography computed tomography (PET-CT) is described in an observational setting. We aimed to determine the impact of the fistula on the clinical status of the patient, in addition to whether PET-CT can be used to assess the functional status of the fistula. This information was used to determine the best therapeutic strategy, which included monitoring, conservative medical management (CMM), transcatheter catheter embolization or surgical ligation (SL). In general, echocardiography represents the first diagnostic imaging approach, but it may be limited by an inappropriate acoustic window. Modern echocardiography equipment has greater sensitivity, which explains why congenital CAFs are frequently diagnosed by this method. Echocardiography can be used to diagnose and evaluate the hemodynamic significance, anatomy and physiopathology of CAFs. CTCA is a widely used technique that can be used for morphological and functional analyses, as well as for perfusion studies of CAFs. CTCA allows for comprehensive cardiac evaluation, providing morphological and functional data on coronary circulation and myocardial perfusion status, as well as anatomical images. Electrocardiography (ECG)-gated cardiovascular computed tomography may play an important role in the evaluation of the origin, pathway, termination and morphology of the fistula in relation to the adjacent anatomical structures, as well as cardiac morphology and contractility. Cardiovascular magnetic resonance does not use ionizing radiation and plays a crucial role in determining myocardial wall viability, characterizing the myocardial tissue and its morphology, as well as providing detailed data related to cardiac function, estimated blood flow within the fistula and the anatomical characteristics. Myocardial perfusion imaging (MPI) is used to identify abnormalities in cardiac and pulmonary circulation, providing the Qp:Qs ratio is required to diagnose and quantify left-to-right shunt, and to assess myocardial perfusion defects that occur as a result of segmental hypoperfusion caused by the fistula-bearing vessel. Myocardial perfusion single-photon emission computed tomography (SPECT) is used to detect myocardial ischemia and to stratify the risk of experiencing a cardiac event in patients with CAFs. The hemodynamic significance of this modality remains unclear. The closure technique for congenital CAFs will be chosen after thorough diagnostic imaging and functional investigation has been performed to assess the hemodynamic and functional significance of the fistula, its anatomical morphology, and its impact on the clinical status of the patient.

Research motivation

The aim of this study was to review and present the current data on non-invasive and invasive diagnostic methods used to evaluate the anatomical morphology and functional significance of CAFs. Medical imaging is important for assessing the location and size of CAFs.

Research objectives

We assessed the hemodynamic impact of CAFs using ^{13}N -ammonia PET-CT imaging under pharmacological adenosine-induced stress and at rest. Future research in a larger group of symptomatic and asymptomatic patients with a greater magnitude of left-to-right shunt is warranted.

Research methods

This was an observational study of 11 subjects with congenital CAFs that had been incidentally found during CAG performed for suspected atherosclerotic CAD. In all patients, physical examination, ECG, echocardiography, chest X-ray and laboratory investigation were performed. The patients were collected from three non-academic hospitals in the West and East regions of the Netherlands. FFR was not measured due to a lack of interventional cardiology facilities in these non-interventional hospitals. Different fistula characteristics were delineated using coronary angiographic imaging techniques. Five subjects underwent pharmacological adenosine stress/rest ^{13}N -ammonia PET-CT to

assess the hemodynamic impact of the fistula. PET-CT was performed in a different academic center. PET-CT is considered a superior diagnostic modality as it provides data on the metabolic status of the myocardial tissue.

Research results

The patients involved in this study had a variety of clinical presentations, including limited posterior non-ST-elevation myocardial infarction (MI), angina pectoris and chest pain ($n = 6$), dyspnea upon exertion ($n = 3$), and an asymptomatic presentation with abnormal resting electrocardiogram ($n = 1$). One patient presented with palpitation, ischemic cerebrovascular accident, paroxysmal atrial fibrillation and non-sustained ventricular tachycardia. Another patient presented with exercise-induced non-sustained ventricular tachycardia. Previous MI was reported in two patients. The physical examination was unremarkable in seven patients. Apical systolic murmur was heard in one patient, and systolic ejection murmur was heard in the second intercostal space in three other patients. Although continuous cardiac murmur is usually present in patients with CAF, no continuous murmur was heard in the current group of patients. In this case series, the body mass index of subjects ranged between 21.1 to 33.4 kg/m², with four patients classified as normal weight, five as overweight and two as obese. The electrocardiogram demonstrated sinus rhythm in 10 patients and permanent atrial fibrillation in one patient. Echocardiography revealed dilated coronary sinus in one patient. None of the patients showed pulmonary hypertension, with normal results for right ventricular systolic pressure. There were 10 single-sided and one double-sided fistulas. All fistulas were of the coronary vascular type, terminating into the pulmonary artery ($n = 11$) or coronary sinus ($n = 1$), and originating from the LAD ($n = 8$), right coronary artery (RCA, $n = 2$) or left circumflex coronary artery (LCx, $n = 2$). In regard to the characteristics of the fistula (origin, pathway and termination), the origin and pathway of the fistulous vessels was plural in most fistulas (8/12, 67% and 9/12, 75%, respectively). Multiplicity was common among the different fistula components (22/36, 61%). In contrast, single (7/12, 58%) termination of the fistulous vessels was more common than multiple (5/12, 42%) termination of fistulous vessels. The termination was equally distributed between single (6/12, 50%) and multiple (6/12, 50%) fistulous vessels. Multiplicity was common among the different fistula components (23/36, 64%). Tortuosity of the pathway was found in eight fistulas (8/12, 67%). A dilated RCA was found in one patient, and large and small aneurysmal formation was present in two patients. The presence of tortuosity and multiplicity of the fistulous tract meant that percutaneous intervention would be very challenging. In patient 2, who had symptomatic significant CAD, SL of the fistula was performed in combination with coronary artery bypass grafting. The characteristics of the fistula components in this patient were multiple origin and termination with multiple-tortuous pathways, which meant the percutaneous approach could not be used. In four patients (patients 4, 7, 8 and 11), PET-CT showed no flow restrictions. Thus, CMM could be implemented, avoiding the need for fistula closure either transcatheter or surgically. The adenosine stress/rest ^{13}N -ammonia PET-CT performed in five subjects demonstrated homogenous distribution of perfusion in two patients, and no perfusion defects in two patients. One patient showed diffuse, reversible reduction in perfusion in the apical and antero-septal regions, and also partly in the basal anterior segment. In another patient, perfusion of the left anterior descending coronary artery (LAD) area was slightly lower than the inferior segment, but it was equal to the lateral wall. Normal perfusion with reduced left ventricular ejection fraction (rest 33%, stress 39%) was probably underestimated in one patient. In these five patients, the mean global stress/rest ratio was 2.9 (range 2.33-3.90). The mean regional stress/rest ratio was 3.0 for the LAD (range 2.35-4.50), 2.9 for the RCA (range 2.49-3.60) and 2.8 for the LCx (range 2.36-3.20). Blood flow through the LAD was slightly higher than through the RCA and LCx. Absolute flow quantification revealed normal myocardial perfusion with high flow in the LCx, which was the fistula-related vessel, compared to the flow of the RCA and the LAD, indicating successful PTE closure procedure of the fistulous vessel. On the other hand, semi-quantitative analysis revealed normal perfusion in two patients and a reduction in diffuse perfusion in the other two patients.

Research conclusions

The hemodynamic characteristics of incidentally found CAFs are of great importance to guide decision-making for whether to treat patients or perform periodic monitoring. Pharmacological adenosine stress/rest ^{13}N -ammonia PET-CT in patients with incidentally found congenital CAFs provided adequate

and clear information regarding the hemodynamic burden of the fistula in this small patient population. For better diagnosis of incidentally found congenital CAFs, pharmacological adenosine stress/rest ^{13}N -ammonia PET-CT should be performed as part of the diagnostic imaging work-up. However, this needs to be confirmed in a large, prospective, international study or registry. In the current study, pharmacological adenosine stress/rest ^{13}N -ammonia PET-CT was performed in a limited number of adult patients with incidentally found congenital CAFs. This test is achievable in patients with congenital CAFs. That pharmacological adenosine stress-rest ^{13}N -ammonia PET-CT in incidentally found congenital CAFs is currently, in this patient population, can provide adequate and clear answer regarding the hemodynamic burden of the fistula and guiding the clinical decision making. For patients with CAFs, multiple imaging modalities are required to assess the anatomical morphology, hemodynamic significance and behavior of the fistula in order to assist in the choice of therapeutic strategy. Angiographic characterization of the individual fistula components (origin, pathway and termination) may help guide the selection of closure technique, either percutaneously or surgically.

Research perspectives

Further studies on a larger number of patients with congenital CAFs (small or large, symptomatic or asymptomatic, treated or untreated) are required to determine the prospective incidence and other characteristics, such as history and long-term outcomes. In 2018-2019, we are planning to initiate an international registry on CAFs (Euro-CAF Survey) to address the diagnostic and therapeutic issues.

ACKNOWLEDGEMENTS

The authors would like to thank the members and staff of the catheterization unit of the Department of Cardiology and the Department of Nuclear Medicine, as well as Mr. Jeroen Geerdink, Hospital System Integrator, for his assistance during the preparation of the manuscript.

REFERENCES

- Karazisi C, Eriksson P, Dellborg M. Coronary Artery Fistulas: Case Series and Literature Review. *Cardiology* 2017; **136**: 93-101 [PMID: 27577264 DOI: 10.1159/000447445]
- Ghaffari S, Akbarzadeh F, Pourafkari L. Aneurysmal coronary arteriovenous fistula closing with covered stent deployment: a case report and review of literature. *Cardiol J* 2011; **18**: 556-559 [PMID: 21947993 DOI: 10.5603/CJ.2011.0013]
- Pu L, Li R, Yang Y, Liu G, Wang Y. Right coronary artery coronary sinus fistula with coronary sinus ostium stenosis. *Echocardiography* 2017; **34**: 1102-1104 [PMID: 28517107 DOI: 10.1111/echo.13559]
- Bittencourt MS, Seltman M, Achenbach S, Rost C, Ropers D. Right coronary artery fistula to the coronary sinus and right atrium associated with giant right coronary enlargement detected by transthoracic echocardiography. *Eur J Echocardiogr* 2011; **12**: E22 [PMID: 21186199 DOI: 10.1093/ejehocardiography/jeq180]
- Green T, Crilley J. Endocarditis and coronary artery fistula: a case report. *Eur Heart J* 2018; 1-4 [DOI: 10.1093/ehjcr/ety023]
- Scansen BA. Coronary Artery Anomalies in Animals. *Vet Sci* 2017; **4**: pii: E20 [PMID: 29056679 DOI: 10.3390/vetsci4020020]
- Villa AD, Sammut E, Nair A, Rajani R, Bonamini R, Chiribiri A. Coronary artery anomalies overview: The normal and the abnormal. *World J Radiol* 2016; **8**: 537-555 [PMID: 27358682 DOI: 10.4329/wjrv.v8.i6.537]
- Magro V, Cacciapuoti F, Cacciapuoti F, Lama D. An unexpected finding in a diabetic patient studied with transthoracic echocardiography. *MOJ Gerontol Ger* 2017; **2**: 00041 [DOI: 10.15406/mojgg.2017.02.00041]
- Zhang P, Cai G, Chen J, Wang Y, Duan S. Echocardiography and 64-multislice computed tomography angiography in diagnosing coronary artery fistula. *J Formos Med Assoc* 2010; **109**: 907-912 [PMID: 21195889 DOI: 10.1016/S0929-6646(10)60138-6]
- Iskandrian AS, Kimbiris D, Bemis CE, Segal BL. Coronary artery to pulmonary artery fistulas. *Am Heart J* 1978; **96**: 605-609 [PMID: 263393 DOI: 10.1016/0002-8703(78)90196-5]
- Lee SK, Jung JI, O JH, Kim HW, Youn HJ. Coronary-to-pulmonary artery fistula in adults: Evaluation with thallium-201 myocardial perfusion SPECT. *PLoS One* 2017; **12**: e0189269 [PMID: 29216309 DOI: 10.1371/journal.pone.0189269]
- Jani L, Mester A, Hodas R, Kovacs I, Benedek T, Bajka B, Benedek I. Computed tomography assessment of coronary fistulas. *J Interdisc Med* 2017; **2**: 155-159 [DOI: 10.1515/jim-2017-0052]
- Detorakis EE, Foukarakis E, Karavolias G, Dermitzakis A. Cardiovascular magnetic resonance and computed tomography in the evaluation of aneurysmal coronary-cameral fistula. *J Radiol Case Rep* 2015; **9**: 10-21 [PMID: 26629294 DOI: 10.3941/jrcr.v9i7.2305]
- Siddiqi MS, Sharma AK, Sharma J. Giant left circumflex artery aneurysm with coronary artery fistula. *Open Access J Surg* 2016; **1**: 555-572 [DOI: 10.19080/OAJS.2016.01.555572]
- Challoumas D, Pericleous A, Dimitrakaki IA, Danelatos C, Dimitrakakis G. Coronary arteriovenous fistulae: a review. *Int J Angiol* 2014; **23**: 1-10 [PMID: 24940026 DOI: 10.1055/s-0033-1349162]
- Sunil Roy TN, Sajeev CG, Francis J, Krishnan MN, Venugopal K. Three major coronary artery-to-left ventricular fistula: an unusual cause of a diastolic murmur at the apex. *J Am Soc Echocardiogr* 2006; **19**: 1402.e1-1402.e4 [PMID: 17098147 DOI: 10.1016/j.echo.2006.07.013]
- Härle T, Kronberg K, Elsässer A. Coronary artery fistula with myocardial infarction due to steal syndrome. *Clin Res Cardiol* 2012; **101**: 313-315 [PMID: 22212517 DOI: 10.1007/s00392-011-0405-1]
- Ouyang F, Chen M, Yi T, Wu M, Peng H, Huang H, Huang H, Zhou S. Successful percutaneous coronary intervention for multivessel stenosis complicated by a huge coronary artery fistula with the combined physiology and intracoronary anatomy techniques. *Int J Cardiol* 2015; **192**: 70-71 [PMID: 26000465 DOI: 10.1016/j.ijcard.2015.05.026]
- Said SA, Nijhuis RL, Op den Akker JW, Kimman GP, Van Houwelingen KG, Gerrits D, Huisman AB, Slart RH, Nicastia DM, Koomen EM, Tans AC, Al-Windy NY, Sonker U, Slagboom T, Pronk AC. Diagnostic and therapeutic approach of congenital solitary coronary artery fistulas in adults: Dutch case series and review of literature. *Neth Heart J* 2011; **19**: 183-191 [PMID: 22020997 DOI: 10.1007/s12471-011-0088-2]
- Kong EJ, Cho IH, Chun KA, Won KC, Lee HW, Park JS, Shin DG, Kim YJ, Shim BS. Comparison of clinical usefulness between N-13 ammonia PET/CT and Tc-99m sestamibi SPECT in coronary artery disease. *Nucl Med Mol Imaging* 2008; **5**: 354-361
- Knuuti J. Integrated positron emission tomography/computed tomography (PET/CT) in coronary disease. *Heart* 2009; **95**: 1457-1463 [PMID: 19684196 DOI: 10.1136/hrt.2008.151944]
- Beanlands RS, Chow BJ, Dick A, Friedrich MG, Gulenchyn KY, Kiess M, Leong-Poi H, Miller RM, Nichol G, Freeman M, Bogaty P, Honos G, Hudon G, Wisenberg G, Van Berkem J, Williams K, Yoshinaga K, Graham J; Canadian Cardiovascular Society; Canadian Association of Radiologists; Canadian Association of Nuclear Medicine; Canadian Nuclear Cardiology Society; Canadian Society of Cardiac Magnetic Resonance. CCS/CAR/CANM/CNCS/CanSCMR joint position statement on advanced noninvasive cardiac imaging using positron emission tomography, magnetic resonance imaging and multidetector computed tomographic angiography in the diagnosis and evaluation of ischemic heart disease—executive summary. *Can J Cardiol* 2007; **23**: 107-119 [PMID: 17311116 DOI: 10.1016/S0828-282X(07)70730-4]
- Herzog BA, Husmann L, Valenta I, Gaemperli O, Siegrist PT, Tay FM, Burkhard N, Wyss CA, Kaufmann PA. Long-term prognostic value of ^{13}N -ammonia myocardial perfusion positron emission tomography added value of coronary flow reserve. *J Am Coll Cardiol* 2009; **54**: 150-156 [PMID: 19573732 DOI: 10.1016/j.jacc.2009.02.069]
- Siegrist PT, Husmann L, Knabenhans M, Gaemperli O, Valenta I, Hoefflinghaus T, Scheffel H, Stolzmann P, Alkadhi H, Kaufmann PA. (13)N-ammonia myocardial perfusion imaging with a PET/CT

- scanner: impact on clinical decision making and cost-effectiveness. *Eur J Nucl Med Mol Imaging* 2008; **35**: 889-895 [PMID: 18057933 DOI: 10.1007/s00259-007-0647-3]
- 25 **Dilsizian V**, Bacharach SL, Beanlands RS, Bergmann SR, Delbeke D, Gropler RJ, Knuuti J, Schelbert HR, Travin MI. PET myocardial perfusion and metabolism clinical imaging. *J Nucl Cardiol* 2009; **16**: 651 [DOI: 10.1007/s12350-009-9094-9]
 - 26 **Tio RA**, Dabeshlim A, Siebelink HM, de Sutter J, Hillege HL, Zeebregts CJ, Dierckx RA, van Veldhuisen DJ, Zijlstra F, Slart RH. Comparison between the prognostic value of left ventricular function and myocardial perfusion reserve in patients with ischemic heart disease. *J Nucl Med* 2009; **50**: 214-219 [PMID: 19164219 DOI: 10.2967/jnumed.108.054395]
 - 27 **Germano G**, Kiat H, Kavanagh PB, Moriel M, Mazzanti M, Su HT, Van Train KF, Berman DS. Automatic quantification of ejection fraction from gated myocardial perfusion SPECT. *J Nucl Med* 1995; **36**: 2138-2147 [PMID: 7472611]
 - 28 **Bogers AJ**, Quaegebeur JM, Huysmans HA. Early and late results of surgical treatment of congenital coronary artery fistula. *Thorax* 1987; **42**: 369-373 [PMID: 3660291 DOI: 10.1136/thx.42.5.369]
 - 29 **Biorck G**, Crafoord C. Arteriovenous aneurysm on the pulmonary artery simulating patent ductus arteriosus botalli. *Thorax* 1947; **2**: 65-74 [PMID: 20252393 DOI: 10.1136/thx.2.2.65]
 - 30 **Wen B**, Yang J, Jiao Z, Fu G, Zhao W. Right coronary artery fistula misdiagnosed as right atrial cardiac myxoma: A case report. *Oncol Lett* 2016; **11**: 3715-3718 [PMID: 27284376 DOI: 10.3892/ol.2016.4457]
 - 31 **Caputo S**, Sorice N, Sansone R, Simeone D, Caruso V, Russo R, Cicchella N, Izzo A, Saviano C, Casani A, Ciampi Q, Villari B. Echocardiographic diagnosis of coronary artery fistula in both dizygotic twin brothers: environmental mechanism? *J Cardiovasc Med (Hagerstown)* 2017; **18**: 378-380 [PMID: 20404741 DOI: 10.2459/JCM.0b013e328336b5b7]
 - 32 **Ganji JL**, Click RL, Najib MQ, Schaff HV, Chaliki HP. Coronary arteriovenous fistula in a patient with aortic valve regurgitation. *Echocardiography* 2013; **30**: E85-E86 [PMID: 23336353 DOI: 10.1111/echo.12072]
 - 33 **Pursnani A**, Jacobs JE, Saremi F, Levisman J, Makaryus AN, Capuñay C, Rogers IS, Wald C, Azmoon S, Stathopoulos IA, Srichai MB. Coronary CTA assessment of coronary anomalies. *J Cardiovasc Comput Tomogr* 2012; **6**: 48-59 [PMID: 22264632 DOI: 10.1016/j.jcct.2011.06.009]
 - 34 **Hong SM**, Yoon SJ, Rim SJ. Contrast echo-a simple diagnostic tool for a coronary artery fistula. *Korean Circ J* 2012; **42**: 205-207 [PMID: 22493617 DOI: 10.4070/kcj.2012.42.3.205]
 - 35 **Latson LA**. Coronary artery fistulas: how to manage them. *Catheter Cardiovasc Interv* 2007; **70**: 110-116 [PMID: 17420995 DOI: 10.1002/ccd.21125]
 - 36 **Cademartiri F**, Malagò R, La Grutta L, Alberghina F, Palumbo A, Maffei E, Brambilla V, Pugliese F, Runza G, Midiri M, Mollet NR, Krestin GP. Coronary variants and anomalies: methodology of visualisation with 64-slice CT and prevalence in 202 consecutive patients. *Radiol Med* 2007; **112**: 1117-1131 [PMID: 18080097 DOI: 10.1007/s11547-007-0210-0]
 - 37 **Black IW**, Loo CK, Allan RM. Multiple coronary artery-left ventricular fistulae: clinical, angiographic, and pathologic findings. *Cathet Cardiovasc Diagn* 1991; **23**: 133-135 [PMID: 2070401 DOI: 10.1002/ccd.1810230216]
 - 38 **Ouyang F**, Wu M, Peng H, Zhang M, Huang H, Chen M, Huang H, Zhou S. Fractional flow reserve, an effective preoperative guideline to a patient with a huge coronary artery fistula and tandem stenosis. *Int J Cardiol* 2015; **199**: 333-334 [PMID: 26233901 DOI: 10.1016/j.ijcard.2015.06.135]
 - 39 **Yew KL**, Ooi PS, Law CS. Functional assessment of sequential coronary artery fistula and coronary artery stenosis with fractional flow reserve and stress adenosine myocardial perfusion imaging. *J Saudi Heart Assoc* 2015; **27**: 283-285 [PMID: 26557747 DOI: 10.1016/j.jsha.2015.03.008]
 - 40 **Hollenbeck RD**, Salloum JG. Sequential moderate coronary artery fistula and moderate coronary artery stenosis causing ischemia demonstrated by fractional flow reserve and relieved following percutaneous coronary intervention. *Catheter Cardiovasc Interv* 2014; **83**: 443-447 [PMID: 24038764 DOI: 10.1002/ccd.25170]
 - 41 **Oh JH**, Lee HW, Cha KS. Hemodynamic significance of coronary cameral fistula assessed by fractional flow reserve. *Korean Circ J* 2012; **42**: 845-848 [PMID: 23323123 DOI: 10.4070/kcj.2012.42.12.845]
 - 42 **Sasi V**, Nemes A, Forster T, Ungi I. Functional assessment of a left coronary-pulmonary artery fistula by coronary flow reserve. *Postępy Kardiologii Interwencyjnej* 2014; **10**: 141-143 [PMID: 25061466 DOI: 10.5114/pwki.2014.43526]
 - 43 **Ito T**, Murai S, Fujita H, Tani T, Ohte N. Fractional flow reserve-guided percutaneous coronary intervention for an intermediate stenosis complicated by a coronary-to-pulmonary artery fistula. *Heart Vessels* 2016; **31**: 816-818 [PMID: 25643760 DOI: 10.1007/s00380-015-0641-9]
 - 44 **Chen JP**, Rodie J. Bi-directional flow in coronary-to-left ventricular fistula. *Int J Cardiol* 2009; **133**: e41-e42 [PMID: 18155306 DOI: 10.1016/j.ijcard.2007.08.126]
 - 45 **Ono M**, Otake S, Fukushima N, Sawa Y, Ichikawa H, Kagisaki K, Matsuda H. Huge right ventricle-right coronary artery fistula compromising right ventricular function in a patient with pulmonary atresia and intact ventricular septum: a case report. *J Thorac Cardiovasc Surg* 2001; **122**: 1030-1032 [PMID: 11689814 DOI: 10.1067/mtc.2001.116466]
 - 46 **Gupta NC**, Beauvais J. Physiologic assessment of coronary artery fistula. *Clin Nucl Med* 1991; **16**: 40-42 [PMID: 1999055 DOI: 10.1097/00003072-199101000-00010]
 - 47 **Glynn TP Jr**, Fleming RG, Haist JL, Huntman RK. Coronary arteriovenous fistula as a cause for reversible thallium-201 perfusion defect. *J Nucl Med* 1994; **35**: 1808-1810 [PMID: 7965162]
 - 48 **Hasbak P**, Kjær A. 82 Rubidium PET to replace myocardial scintigraphy. *Ugeskr Laeger* 2011; **173**: 567-572 [PMID: 21333256]
 - 49 **Said SA**, de Voogt WG, Bulut S, Han J, Polak P, Nijhuis RL, Op den Akker JW, Slootweg A. Coronary artery disease in congenital single coronary artery in adults: A Dutch case series. *World J Cardiol* 2014; **6**: 196-204 [PMID: 24772259 DOI: 10.4330/wjc.v6.i4.196]
 - 50 **Said SA**, Nijhuis RL, Akker JW, Takechi M, Slart RH, Bos JS, Hoorntje CR, Houwelingen KG, Bakker-de Boo M, Braam RL, Vet TM. Unilateral and multilateral congenital coronary-pulmonary fistulas in adults: clinical presentation, diagnostic modalities, and management with a brief review of the literature. *Clin Cardiol* 2014; **37**: 536-545 [PMID: 25196980 DOI: 10.1002/clc.22297]
 - 51 **Said SA**, Oortman RM, Hofstra JH, Verhorst PM, Slart RH, de Haan MW, Eerens F, Crijns HJ. Coronary artery-bronchial artery fistulas: report of two Dutch cases with a review of the literature. *Neth Heart J* 2014; **22**: 139-147 [PMID: 24464641 DOI: 10.1007/s12471-014-0518-z]
 - 52 **Zhang W**, Hu R, Zhang L, Zhu H, Zhang H. Outcomes of surgical repair of pediatric coronary artery fistulas. *J Thorac Cardiovasc Surg* 2016; **152**: 1123-1130.e1 [PMID: 27245418 DOI: 10.1016/j.jtcvs.2016.04.093]

P- Reviewer: Altarabsheh SE, Barik R, Korosoglou G, Petix NR, Uehara Y, Vermeersch P **S- Editor:** Ji FF
L- Editor: A **E- Editor:** Wu YXJ



Undiscovered pathology of transient scaffolding remains a driver of failures in clinical trials

Alexander N Kharlamov

Alexander N Kharlamov, Department of Interventional Cardiovascular Biomedicine, De Haar Research Foundation, Amsterdam 1069CD, The Netherlands.

Alexander N Kharlamov, Research Division, Transfiguration Clinic, Yekaterinburg 620078, Russia

ORCID number: Alexander N Kharlamov (0000-0003-4631-1261).

Author contributions: Kharlamov AN was the only author who comprehensively contributed to the analysis and writing.

Conflict-of-interest statement: The author does not have any conflict of interest to report.

Open-Access: This article is an open-access article, which was selected by an in-house editor and fully peer-reviewed by external reviewers. It is distributed in accordance with the Creative Commons Attribution Non-Commercial (CC BY-NC 4.0) license, which permits others to distribute, remix, adapt, build upon this work non-commercially, and license their derivative works on different terms, provided the original work is properly cited and the use is non-commercial. See: <http://creativecommons.org/licenses/by-nc/4.0/>

Manuscript source: Invited manuscript

Correspondence to: Alexander N Kharlamov, MD, Academic Research, Doctor, Lecturer, Department of Interventional Cardiovascular Biomedicine, De Haar Research Foundation, Keurenplein 41, Box G9950, 1069CD Amsterdam, The Netherlands. akharlamov@dhfrpro.com
Telephone: +31-87-7842273

Received: March 27, 2018

Peer-review started: March 28, 2018

First decision: May 2, 2018

Revised: May 21, 2018

Accepted: August 26, 2018

Article in press: August 27, 2018

Published online: October 26, 2018

Abstract

AIM

To statistically examine the released clinical trials and

meta-analyses of polymeric bioresorbable scaffolds resuming the main accomplishments in the field with a translation to the routine clinical practice.

METHODS

The statistical power in clinical trials such as ABSORB Japan, ABSORB China, EVERBIO II, AIDA, and few meta-analyses by the post hoc odds ratio-based sample size calculation, and the patterns of artery remodeling published in papers from ABSORB A and B trials were evaluated.

RESULTS

The phenomenal admiration from the first ABSORB studies in 2006-2013 was replaced by the tremendous disappointment in 2014-2017 due to reported relatively higher rates of target lesion failure (a mean prevalence of 9.16%) and device thrombosis (2.38%) in randomized controlled trials. Otherwise, bioresorbable vascular scaffold (BVS) performs as well as the metallic drug-eluting stent (DES) with a trend toward some benefits for cardiac mortality [risk ratio (RR), 0.58-0.94, $P > 0.05$]. The underpowered design was confirmed for some studies such as ABSORB Japan, ABSORB China, EVERBIO II, AIDA trials, and meta-analyses of Polimeni, Collet, and Mahmoud with some unintentional bias (judged by the asymmetrical Funnel plot). Scaffold thrombosis rates with Absorb BRS were comparable with DES performed with a so-called strategy of the BVS implantation with optimized pre-dilation (P), sizing (S) and post-dilation (P) (PSP) implantation (RR, PSP vs no PSP 0.37) achieving 0.35 per 100 patient-years, which is comparable to the RR 0.49 with bare-metal stents and the RR 1.06 with everolimus DES. Both ABSORB II and ABSORB III trials were powered enough for a five-year follow-up, but the results were not entirely conclusive due to the mostly non-significant fashion of data. The powered meta-analyses were built mostly on statistically poor findings.

CONCLUSION

The misunderstanding of the pathology of transient

scaffolding drives the failures of the clinical trials. More bench studies of the vascular response are required. Several next-generation BVS including multifunctional electronic scaffold grant cardiology with a huge promise to make BVS technology great again.

Key words: Bioresorbable scaffold; Device thrombosis; Clinical outcomes; Statistics; Intravascular imaging; Arterial remodeling; Transient scaffolding

© **The Author(s) 2018.** Published by Baishideng Publishing Group Inc. All rights reserved.

Core tip: The high rates of target lesion failure and device thrombosis in randomized controlled trials caused confusion in the international interventional community with a decline of the technology in routine practice. The provided statistical analysis confirms the underpowered design of some clinical studies and meta-analyses of bioresorbable scaffolds. The misunderstanding of the pathobiology of the transient scaffolding drives the failures of the clinical trials. More bench studies of the vascular response are required to verify the leading mechanism of the device failure. Several next-generation scaffolds including multifunctional electronic scaffold grant cardiology with a huge promise to make this technology great again.

Kharlamov AN. Undiscovered pathology of transient scaffolding remains a driver of failures in clinical trials. *World J Cardiol* 2018; 10(10): 165-186 Available from: URL: <http://www.wjgnet.com/1949-8462/full/v10/i10/165.htm> DOI: <http://dx.doi.org/10.4330/wjc.v10.i10.165>

INTRODUCTION

The groundbreaking news of September 8, 2017 delivered by Abbott Vascular (Santa Clara, CA; <https://www.vascular.abbott/>) outlined that “due to low commercial sales, Abbott will stop selling the first-generation Absorb bioresorbable vascular scaffold (BVS)”. The reassuring point was that Abbott will continue work on a next-generation 99 μ m bioresorbable device. This was the end of the device thrombosis story that reached its climax this year when the United States Food and Drug Administration (FDA) on March 18, 2017 (and then on October 31, 2017 after release of ABSORB II 4-year, ABSORB III 3-year, and ABSORB IV 30-d results at TCT 2017 in Denver, CO, United States) informed^[1] health care providers who are managing patients with Absorb GT1 BVS that there is a high rate of major adverse cardiac events (MACE) or correctly target lesion failure (TLF) registered in patients receiving BVS when compared to metallic XIENCE drug-eluting stent (DES). This alert was initially provoked by the release of the two-year data from the ABSORB III trial (a paper was not published yet) showing^[2] an 11% rate of MACE in patients treated

with BVS ($n = 1322$) at two years compared with 7.9% ($n = 686$) in XIENCE DES ($P = 0.03$). This study also demonstrated a 1.9% rate of scaffold thrombosis (ST) within the BVS vs 0.8% within the XIENCE stent at two years ($P > 0.05$, NS). These observed higher MACE rates in BVS patients were more likely when the device was implanted in small heart vessels (< 2.25 mm). Almost immediately after the United States, the European Union restricted BVS^[3] to the sites of clinical registries (valid as of May 31, 2017). The CE Mark of approval remains in place, but only centers participating in formal registries (about 12 registries across Europe covering 114 hospitals) should be using BVS for now. Furthermore, the Australian Therapeutic Goods Administration (TGA) on May 2, 2017^[4] issued a hazard alert as well and recalled all BVS from medical centers not studying the device. These reactions^[5-15] of the healthcare authorities amid few recently published meta-analyses^[16-25] wreck confusion^[26-37] among physicians^[38-45] about when and if they will ever be using the device again, jeopardizing the future of BVS and further development of bioresorbable devices. Notwithstanding, did we clear the situation with causes of these trends toward increased MACE and ST in the case of BVS? What is going on with cardiac mortality after BVS? Can we trust these data? Can we propose a solution and optimize our approaches for BVS implantation to prevent these complications and secure the technology? Do we understand the pathology of transient scaffolding? Should we first complete the bench studies and clear the vascular pathobiology of the BVS implantation?

Certainly, we face a real phenomenon of the elevated TLF and ST after implantation of BVS, which is very confusing and disappointing for physicians even for the fathers of technology such as Professor Patrick W Serruys, MD, PhD (Erasmus MC, Rotterdam, The Netherlands; Imperial College, London, United Kingdom) who said that “It’s not what we were expecting...That’s the reality!...Of course, we’re still in the first generation...” (a report to TCTMD on Oct 30, 2016 at TCT2016, Washington, DC, United States). We must mind the fact that this is a first-generation technology, and as Professor Gregg Stone, MD (Columbia University, NY, United States) said once, “If science stopped with every challenge for first gen devices, we would have no PCI devices!” (Twitter, @GreggWStone, Apr 16th, 2017). Meanwhile, the Colombo’s concept of the plastic jacket (a team of Professor Antonio Colombo, MD, San Raffaele Scientific Institute, Milan, Italy)^[10], recently reported positive results of the European registries (German GABI-R, Italian IT-DISAPPEARS, Italian RAI, Swedish SCAAR, British Absorb United Kingdom, and French France Absorb) and Asian randomized controlled trials (RCT)^[11] (ABSORB China, ABSORB Japan) are very reassuring and promising with relatively low rates of both TLF (3.9%-9.9% by one year) and ST ($< 1.7\%$) even in complex lesions due to optimized accurate technique of the implantation (a high-pressure post-dilation in some

registries was performed in 96.8% of cases with full PSP strategy in > 65.8% of lesions).

The running fourth industrial revolution^[23-38] supports us with the remarkable idea of the transient scaffolding^[39-51] and a dream of the vascular restoration therapy^[25] of coronary atherosclerosis that has a potential to revolutionize cardiology providing physicians with a tackle for both to revitalize a circulation^[20-36] in the coronary pool tailoring atheroregression^[37-52]. Since 2006 the multimodality imaging studies of ABSORB^[31] and ABSORB B^[53-56] clinical trials that examined BVS have crashed to perform significant regression of atherosclerosis but with a trend toward absolute reduction of the percent atheroma volume (PAV) at 60 mo (at least -2.62%), which claims further research efforts.

The goal of this systematic review was to evaluate the accomplishments of the clinical trials, and patterns of pathology with trends of the artery remodeling in patients who underwent transient scaffolding with polymeric BVS within 60 mo after implantation with the grey-scale (GS) and virtual histology (VH) intravascular ultrasound (IVUS) imaging, quantitative coronary angiography (QCA), multislice computed tomography (MSCT) angiography, and optical coherence tomography (OCT). This review must answer the question about both the reasons for unsuccessful experience in clinical trials and the potential of BVS for regression of atherosclerosis with its further introduction into the routine clinical practice.

MATERIALS AND METHODS

The available sources of the information published in PubMed/MEDLINE (primary electronic database), Google Scholar, ResearchGate, ClinicalTrials.Gov, and SCOPUS with the key words BVS, BRS, regression of atherosclerosis, imaging, artery remodeling, and atherosclerosis through the last 20 years with a focus on polymeric BVS and particularly ABSORB trials were investigated. The estimated observations comprised mean and/or median numbers of the variables reported by the authors of the original papers without access to the detailed patient-by-patient matrix of the evaluated studies. This systematic review (without meta-analysis) was accomplished by two reviewers who independently analyzed abstracts, extract data, and calculate the risk of bias. The received data have a different quality and potential of comparability but provide the most recent information. The risk of bias of each included trial was tested with the Cochrane Collaboration's tool and elaborated with the information about expert imaging analysis and a methodology of the statistical estimation.

We have selected some trials for the further in-depth analysis including special subanalysis of the published results from ABSORB A and B trials. The study design of ABSORB A (NCT00300131) and B (NCT00856856) trials with a description of the study population, study device, study procedure, and definitions^[31-43] were previously reported^[44-56]. Briefly, the Absorb BVS device (Abbott Vascular, Santa Clara, CA, United States) was examined

in the single-group, prospective, open-label study (A), with safety and imaging endpoints, 30 patients were enrolled at four participating sites between March 7, and July 18, 2006. The BVS was tested in 101 patients of the ABSORB Cohort B study, which was subdivided into two subgroups of patients: the first group (B1) underwent invasive imaging with QCA, IVUS grey-scale, and OCT at 6, 24, and 60 mo ($n = 45$), whereas the second group (B2) underwent invasive imaging at 12, 36, and 60 mo ($n = 56$).

Statistical analysis

For binary variables, percentages were calculated. Continuous variables are performed as the mean and standard deviation (SD) with a median (m) and 95% confidential interval (CI). The overall comparison of serial measurement was assessed by applying the Friedman test, and pairwise comparisons between post-procedure, and follow-up was calculated by a Wilcoxon signed-rank test adjusted by the Bonferroni method. The unpaired *t*-test was applied in cases when the matrix of datasets was unavailable. To assess the changes of imaging variables over time, the longitudinal repeated measurement analysis using a mixed effect model with five follow-up visits (at post-procedure, 6 mo, 1 year, 2 years, and 3 years) was performed in the SAS procedure PROC MIXED by pooling two cohorts (B1 and B2), as these two groups of patients were comparable in baseline characteristics. Compound symmetry covariance structure was used in the mixed model. In fact, there is no additional random effect beyond the residual error in this analysis. As no formal hypothesis examination was scheduled for assessing the success of the study, no statistical adjustment was proceeded. *P* values presented are exploratory analyses only and should therefore be interpreted cautiously. The estimated *P* value for the plaque burden (PB) in the ABSORB cohort A and B trials was adjusted by the maximum *P* value calculated originally for numerator or denominator at the formula of the PAV due to unavailability of the datasets with a frame-by-frame and patient-by-patient analysis. The *P* value was interpreted as non-significant (NS, > 0.05) in the case if historically assessed *P* value of either numerator or denominator was above 0.05. Statistical analysis was completed with SPSS 20.0 software (SPSS Inc., Chicago, IL, United States).

RESULTS

Determination of whether recent trials were underpowered

Current RCTs are being conducted with an under-powered design. In our previous analysis^[12], we concluded that the meta-analyses were built on the non-significant data. Only a combo analysis of ABSORB III and ABSORB IV has a chance to clear those trends with ST in the near future (one-year results of ABSORB IV trial are expected before Spring 2018). We intentionally conducted the brief analysis (Table 1) in order to cal-

Table 1 The results of post hoc odds-ratio-based sample size calculations for randomized controlled trials and meta-analyses of the bioresorbable vascular scaffold

| Trial | No. patients with BVS (ad hoc sample size) | No. patients with metallic DES (ad hoc sample size) | Total TLF | TLF, rate in BVS patients | TLF, RR (BVS/DES), P value | TV-MI | ID-TLR | ST (definite/probable), RR, P value | ST (definite/probable), rate in BVS patients | Estimated (post hoc) minimal sample size for groups BVS:DES (by TLF), (eOR) | Estimated (post hoc) minimal sample size for groups BVS:DES (by ST), (eOR) | Post-dilation, percent of patients | Full PSP, estimated maximum, percent of patients | Small vessels, QCA RVD maximum, (< 2.25 mm), percent of patients |
|---|--|---|-------------------------------|---------------------------|----------------------------|-------------------------------|-------------------------------|-------------------------------------|--|---|--|------------------------------------|--|--|
| BVS randomized controlled trials | | | | | | | | | | | | | | |
| ABSORB II, by 3 yr ^[31] | 335 | 166 | 2.11 ^S P = 0.04 | 10.5% | 0.5 P = 0.40 | 5.20 ^S P = 0.01 | 1.65 P = 0.56 | Nul P = 0.03 | 2.8% | 324:162 eOR = 2.23 | NA | Approximately 60% | NA | NA |
| ABSORB II, by 4 yr ^{UD[43]} | 289 | 139 | 2.04 ^S P = 0.05 | 11.1% | NA | NA | NA | NA | 3.0% | 293:141 ^{UD} eOR = 2.04 | NA | NA | NA | NA |
| ABSORB III, by 1 yr (13 mo) ^[21] | 1313 | 677 | 1.28 P = 0.16 | 7.8% ² | 4.12 P = 0.29 | 1.31 P = 0.18 | 1.21 P = 0.5 | 2.08 P = 0.13 | 1.5% | 1236:637 eOR = 1.31 | 1285:666 eOR = 2.09 | 66% | 66% | 19% |
| ABSORB III, by 2 yr (25 mo) ^[21] | 1322 | 686 | 1.39 ^S P = 0.03 | 11.0% | 1.83 P = NS | 1.49 ^S P = 0.04 | 1.23 P = NS | 2.38 P = NS | 1.9% | 1291:669 eOR = 1.45 | 1215:630 eOR = 2.52 | 66% | 66% | 19% |
| ABSORB III, by 3 yr ^{UD[43]} | 1322 | 686 | 1.31 P = 0.06 | 13.4% | 1.17 P = 0.71 | 1.47 ^S P = 0.03 | 1.23 P = 0.27 | 3.12 ^S P = 0.01 | 2.3% | 1262:655 eOR = 1.23 | 1375:714 ^{UD} eOR = 3.16 | NA | NA | 18.8% |
| ABSORB IV, by 1 yr (13 mo) ^[21] | 1273 | 1273 (1500) ¹ | NA | NA | NA | NA | NA | NA | 0.5% | NA | NA | 83% | 83% | 4% |
| A B S O R B Japan, by 3 yr ^{UD[11]} | 258 | 128 | 1.62 P = 0.23 | 8.9% | Nul P = 1.00 | 1.74 P = 0.31 | 1.79 P = 0.23 | 2.25 P = 0.35 | 3.6% | 260:130 ^{UD} eOR = 1.69 | 248:124 eOR = 2.28 | Approximately 80% (low pressure) | NA | NA |
| A B S O R B China, by 3 yr ^{UD[11,27]} | 234 | 229 | 1.17 P = 0.71 | 5.5% | 0.33 P = 0.31 | 2.97 P = 0.16 | 1.64 P = 0.33 | Nul P = 0.16 | 0.9% | 231:231 ^{UD} eOR = 1.19 | NA | 16.9% | 13.5% | 18.1% |
| EVERBIO II, by 9 mo ^{UD[28]} | 78 | 160 | 1.33 P = 0.60 | 12% | Nul P = 0.33 | NA | 1.11 P = 0.83 | Nul P = 0.33 | 1% | 83:170 ^{UD} eOR = 1.26 | NA | 34% | 34% | NA |
| AIDA, by 2 yr ^{UD[29]} | 924 | 921 | 1.17 P = 0.31 | 10.3% | 0.78 P = 0.43 | 1.60 ^S P = 0.04 | 1.33 P = 0.15 | 3.87 ^S P < 0.001 | 3.5% | 941:941 ^{UD} eOR = 1.17 | 898:898 eOR = 4.09 | 74% | 74% | 19% |
| DES trials and BVS registry comparators | | | | | | | | | | | | | | |
| RESOLUTE All-Comers, by 1 yr ^{UD[13]} | 1140 | 1152 | 1.01 P = 0.94 | 8.3% ² | 1.75 P = 0.08 | 0.98 P = 0.92 | 0.87 P = 0.50 | 2.29 P = NS | 1.6% | 1132:1132 eOR = 1.00 | 1152:1152 ^{UD} eOR = 2.26 | NA | NA | NA |
| RESOLUTE All-Comers, by 5 yr ^{UD[13]} | 1140 | 1152 | 1.05 P = 0.61 | 17.0% | 1.14 P = 0.48 | 1 P = 1.00 | 1.09 P = 1.58 | 1.41 P = 0.24 | 2.4% | 2632:2632 ^{UD} eOR = 0.43 | 1133:1133 eOR = 2.03 | NA | NA | NA |
| S C A A R Registry, by 2 yr ^{UD[11]} | 810 | 67099 | NA | NA | NA | NA | NA | 2.5 P = 0.006 | 1.5% ² | NA | 826:68308 ^{UD} eOR = 2.47 | NA | NA | Nul |
| Recent meta-analyses of BVS | | | | | | | | | | | | | | |
| Polimeni <i>et al</i> ^[6] , at 2 yr ^{UD} | 3079 | 2140 | 1.33 ^S P = 0.01 | 9.4% | 0.94 P = 0.80 | 1.66 ^S P < 0.01 | 1.32 P = 0.05 | 3.22 ^S P < 0.0001 | 2.3% | 2708:1881 eOR = NA | 3214:2234 ^{UD} eOR = NA | > 61% | 61% | NA |
| Collet <i>et al</i> ^[7] , at 2 yr ^{UD} | 996 | 696 | 1.48 P = 0.09 | 8.2% | 0.69 P = 0.35 | 2.25 P = 0.09 | 1.89 ^S P = 0.02 | 2.93 ^S P = 0.01 | 2.2% | 616:437 eOR = NA | 2759:1930 ^{UD} eOR = NA | NA | NA | NA |
| Ha <i>et al</i> ^[18] , mostly at 2 yr ³ | 1379 | 1095 | 1.31 P = 0.12 | 7.7% | 0.58 P = 0.23 | 2.59 ^S P = 0.02 | 1.70 ^S P = 0.04 | 2.35 ^S P = 0.02 | 2.6% | 1233:987 eOR = NA | 1374:1082 eOR = NA | > 36% | 36% | NA |

| | | | | | | | | | | | | | | |
|--|------|------|---------------------------------------|---------------------------|--------------------------|---------------------------------------|---------------------------------------|--|--------------------------|-------------------------------------|--------------------------------------|-------|-----|---------|
| Mahmoud <i>et al</i> ^[5] , at 2 yr ^{UD} | 3166 | 2226 | 1.32 ^S <i>P</i> < 0.01 | 10.90% | 0.75 <i>P</i> = 0.21 | 1.65 ^S <i>P</i> < 0.001 | 1.39 ^S <i>P</i> = 0.01 | 3.22 ^S <i>P</i> < 0.0001 | 2.40% | 3206;2258 ^{UD} eOR= 1.4 | 3174;2235 ^{UD} eOR= 3.58 | > 34% | 34% | NA |
| Sorrentino <i>et al</i> ^[9] , mostly at 2 yr | 3261 | 2322 | 1.32 ^S <i>P</i> < 0.01 | 9.60% | 0.89 <i>P</i> = 0.63 | 1.62 ^S <i>P</i> < 0.001 | 1.40 ^S <i>P</i> = 0.007 | 3.15 ^S <i>P</i> < 0.0001 | 2.40% | 3118;2227 eOR= 1.38 | 3241;2315 eOR= 3.49 | > 34% | 34% | NA |
| Ali <i>et al</i> ^[35] , at 2 yr ^S | 3261 | 2322 | 1.29 ^S <i>P</i> < 0.01 | 9.40% | 0.9 | 1.64 ^S <i>P</i> < 0.001 | 1.39 ^S <i>P</i> = 0.009 | 2.99 ^S <i>P</i> < 0.0001 | 2.30% | 3054;2183 eOR= 1.32 | 3207;2296 eOR= 3.32 | 67% | 56% | < 51.8% |
| Zhang <i>et al</i> ^[36] , at > 1 yr ^{UD} | 3257 | 2303 | 1.37 ^S <i>P</i> < 0.01 | 9.96% (7.3%) ⁴ | 0.92 <i>P</i> = 0.711 | 1.63 ^S <i>P</i> < 0.001 | 1.31 ^S <i>P</i> = 0.027 | 3.40 ^S <i>P</i> < 0.001 | 2.5% (1.8%) ⁴ | 2968;2116 eOR= NA | 3470;2469 ^{UD} eOR= NA | NA | NA | NA |
| Ali <i>et al</i> ^[39] , at 3 yr ^{UD} | 2096 | 1189 | 1.37 ^S <i>P</i> = 0.01 | 11.70% | 0.9 <i>P</i> = 0.77 | 1.68 ^S <i>P</i> = 0.001 | 1.41 ^S <i>P</i> = 0.03 | 2.83 ^S <i>P</i> = 0.01 | 2.40% | 2083;1177 ^{UD} eOR= 1.5 | 2068;1162 eOR= 4.1 | NA | NA | NA |
| Kang <i>et al</i> ^[45] , at > 2 yr ^{UD} | 3179 | 2239 | 1.39 ^S <i>P</i> < 0.001 | 12.50% | 0.86 <i>P</i> = 0.49 | 1.67 ^S <i>P</i> < 0.001 | 1.46 ^S <i>P</i> = 0.004 | 3.59 ^S <i>P</i> < 0.001 | 2.60% | 2957;2083 eOR= NA | 3297;2322 ^{UD} eOR= NA | NA | NA | NA |

¹Enrollment is not completed yet (2546/3000 subjects in ABSORB IV trial were allocated in March 2017; presented data are preliminary); ²Primary end-point; ³Odds ratio (OR) was provided by the author instead of RR (estimated OR was calculated from the data provided by the author in the article if applicable); ⁴Pooled incidence of definite or probable stent thrombosis at longest follow-up in patients receiving BVS^[36]; ⁵D + L, DerSimonian and Laird random-effect model. The OR, confidence level and relevant sample size were determined with a validated online calculator of Select Statistical Services ([https://select-statistics.co.uk/calculators/sample-size-calculator-odds-ratio/](https://select-statistics.co.uk/calculators/confidence-interval-calculator-odds-ratio/); Exeter, United Kingdom) with a 95% CI, estimated relative precision (calculated as a percentage by which the lower limit for the confidence interval is less than the estimated odds ratio) and the known prevalence of the variables. The estimated odds ratio (eOR), which was calculated from the data that were provided by the author in the original article, represents the odds that an outcome will occur given a particular exposure, compared to the odds of the outcome occurring in the absence of that exposure. Either P value or OR presented inside the cells below the numbers. Cells with "g" depict data with a statistically significant P value (*P* < 0.05, addressing the question of whether the intervention effect is precisely nil). Cells with "UD" indicate variables with underpowered design by sample size (when the estimated post hoc sample size is bigger than ad hoc one). If not mentioned, the data from meta-analyses presented are from the Fixed effects model.

ulate a posthoc sample size by the odds ratio (OR) and estimate the statistical power for each available RCT comparing BVS with DES. The documented high resemblance between ad hoc and post hoc sample size calculations confirms the presence of bias due to the very confusing tailored fashion of their appearance. The OR-based sample size calculation that we used in our analysis is one of the most simple and reliable. It is sensitive to a relative precision, a prevalence, an OR, and a presence to absence ratio. Both ABSORB II and ABSORB III were specifically designed and powered for a five-year supervision. However, RESOLUTE All-Comers^[13] became dramatically underpowered beyond the primary end-point by the five-year follow-up. Both ABSORB China and ABSORB Japan were not powered enough either: ABSORB China lost statistical power by the second year of the trial, and ABSORB Japan lost statistical power at three years. Regretfully, EVERBIO II and AIDA RCTs, available registries with DES, and few meta-analyses^[6,7,36], were not optimally powered either (Table 1). Regretfully, ABSORB II^[42] and ABSORB III^[43] became underpowered by four years and three years, respectively. Moreover, in cases with truly powered research, all the outcomes with *P* values > 0.05 must be interpreted as false, which means that we can only trust the higher rates of TLF driven by the target vessel myocardial infarction (TV-MI).

Determination of bias

Results of the recently published (Mahmoud *et al*^[5]) meta-analysis (six RCTs with 5392 patients including ABSORB III, ABSORB China, ABSORB Japan, AIDA, ABSORB II, EVERBIO II; mean follow-up was 25 mo) were rather ambiguous. BVS had a higher rate of TLF [risk ratio (RR), 1.32, *P* = 0.002] with the worst results in ABSORB II (34/335 vs 8/166) compared with metallic DES run by the higher rates of TV-MI (RR, 1.65, *P* < 0.0001) and ischemia-driven target lesion revascularization (ID-TLR; RR, 1.39, *P* = 0.01). The risk of definite or probable ST (RR, 3.22, *P* < 0.0001) and very late ST (> one year; RR, 4.78, *P* = 0.004) was higher with BVS. This is a very tricky meta-analysis with a sophisticated statistical adjustment, which is totally undermining benefits of BVS for cardiac (RR, 0.75; *P* = 0.21) and all-cause mortality (RR, 0.79, *P* = 0.36). The better outcomes with BVS were observed in ABSORB China (cardiac mortality RR = 0.33, all-cause mortality RR = 0.17) and ABSORB II (cardiac mortality RR = 0.50, all-cause mortality RR = 0.66). The worst performance of BVS was documented in ABSORB Japan. Six meta-analyses from the teams of Collet *et al*^[7], Ha *et al*^[8], Sorrentino *et al*^[9], Ali *et al*^[35,39], Zhang *et al*^[36], and Kang *et al*^[45] released in 2017 with the latest findings demonstrate very similar numbers. The high-quality seven-study meta-analysis of Ali *et al*^[35,39] demonstrated the inferiority of Absorb BVS vs metallic DES in randomized trials where BVS consorted with elevated rates of composite device-oriented and

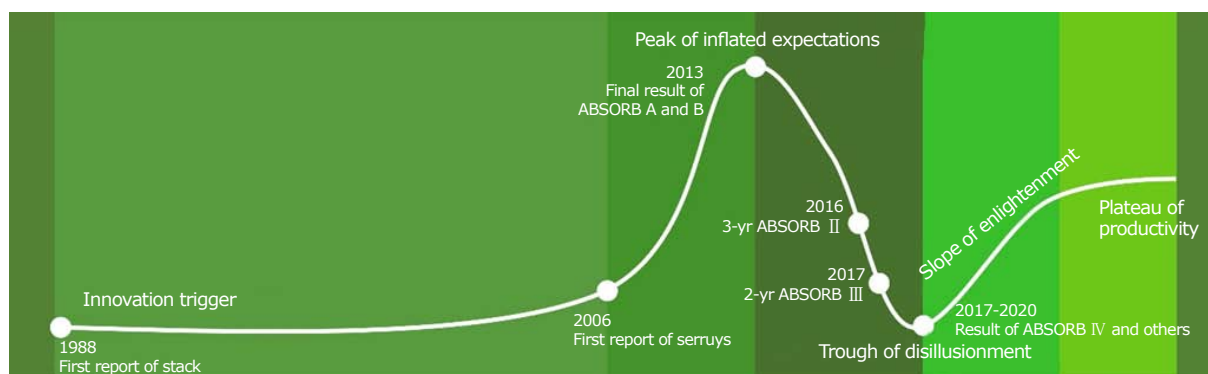


Figure 1 Performance of bioresorbable vascular scaffolds in the market. A schematic representation of the Gartner Hype Cycle for the bioresorbable vascular scaffold.

patient-oriented adverse events at both two- and three-year follow-up compared with DES, with a certain risk of adverse events between one and three years. The pooled meta-analysis of Zhang *et al.*^[36] with the longest follow-up findings from both observational and randomized trials exposed the incidence of definite or probable ST after BVS of 1.8% (95%CI: 1.5% to 2.2%, $n = 21884$), and the incidence of TLF of 7.3% (CI: 5.9% to 8.8%, $n = 19998$).

BVS is as good as DES by the rates of cardiac mortality with a trend toward more benefits from BVS for survival. Statistically, it is quite a challenging scenario to draw any conclusions from the data with no strong evidence that the intervention has an effect (with $P > 0.05$). The best evidence synthesis with only methodologically sound studies must be included in a meta-analysis to avoid any kind of bias. If the RCTs alone failed to demonstrate statistically significant data for ST, sources of bias by the method in such a meta-analysis of the weak studies cannot be controlled. Clinically, it is of paramount importance to detect any number of severe adverse events associated with the intervention in order to protect patients, but we must be honest with the correct interpretation of the findings and further conclusions.

Our previous analysis^[12] with a Funnel plot of the existing observational and randomized trials demonstrated that there is an unintentional bias with a lack of data from patients with metallic DES in order to compare and judge BVS properly. The meta-analysis of Polimeni *et al.*^[6] (five RCTs with 5219 patients) and Sorrentino *et al.*^[9] (seven RCTs with 5583 patients) observed similar trends of clinical outcomes and another Funnel plot analysis. Unfortunately, the authors ignored clear asymmetry in the Funnel plots especially in the case of TV-MI, cardiac death, and ST where we can exclude a publication bias (due to negative Egger or Harbord test with $P > 0.05$). There are at least three studies with small sample sizes, which means it produces less precise estimated effects^[14]. The ultimate assessment is very subjective but difficult because the number of trials is not large (less than ten). This "asymmetrical" bias can occur because of the poor methodological design in the trials, which

is typical for a relatively small sample size trial because it can lead to spuriously inflated estimated treatment effects. It is challenging to specify the nature of the bias, and the only way to overcome it is to conduct a well-powered statistically harmonized RCT.

A tailored strategy

The story of BVS looks like a curve of the Gartner Hype Cycle^[34] (Figure 1). The innovation trigger of BVS technology began in 1988 when the team of Professor Richard S Stack from Duke University (Durham, NC) first reported in the American Journal of Cardiology about a PLLA bioabsorbable stent. There were no usable products, but it brought us to the next stage^[34], Gartner's peak of inflated expectations. This stage started in 2006 with the first publication in the Journal of Catheterization and Cardiovascular Interventions from the team of Professor Patrick W Serruys from Erasmus MC (Rotterdam, The Netherlands). The third scientific compendium of 2013 included 72 articles (mostly pre-clinical studies, clinical ABSORB cohorts A and B trial, ABSORB EXTEND) covering all the challenging options related to transient scaffolding. This was a stage according to Gartner when early publicity was producing a number of success stories accompanied by scores and minor failures. The story became different with a new stage of the so-called trough of disillusionment in 2013 when the first paper with a design of ABSORB II trial was released in the American Heart Journal. The three-year (TCT 2016, Washington, DC) and four-year (TCT 2017, Denver, CO) results of ABSORB II, and then the two-year (ACC 2017, Washington, DC) and three-year (TCT 2017, Denver, CO) reports of ABSORB III trial destroyed all the previous illusions warning about concerns of a higher prevalence of TLF and ST in BVS patients. It is standard at this stage to continue investments to improve the products to the satisfaction of early adopters. In the future, a slope of enlightenment with more clearance about how technology can be beneficial and become more widely understood. Likely, the results of the ABSORB IV trial and further meta-analyses will resolve the situation with trends during 2017-2020. We predict that the second- and third-generation BVS (with thinner struts below 100

µm) will result in a plateau of productivity and finally the adoption of the technology.

Device thrombosis in interventional studies: Preparation is the only solution

ST rates with Absorb BRS were comparable with DES^[44] performed with a lesion preparation or so-called PSP implantation^[24] (RR, PSP vs no PSP 0.37) achieving 0.35 per 100 patient-years, which is comparable to the RR 0.49 with bare-metal stents, the RR 1.06 with everolimus DES, the RR 0.44 with paclitaxel DES, the RR 0.60 with sirolimus DES, and the RR 0.70 with zotarolimus DES.

From clinical outcomes to arterial remodeling: A pooled analysis of plaque burden in selected ABSORB A and B trials

The pathobiological mechanism responsible for failures of BVS in clinical trials and to assess patterns of the arterial remodeling have been investigated. A total of 30 patients were enrolled in the ABSORB A trial (a revision 1.0 of BVS) between March 7 and July 28, 2006^[31,57], and 101 patients were assigned to the ABSORB Cohort B study (a revision 1.1 of BVS) from March 19 to November 6, 2009^[53,55,56]. Baseline characteristics were published elsewhere. The main clinical outcomes and adverse events were previously reported^[31,53,55-57].

Figure 2 and Table 2 show the pooled data of PB and mean plaque area (MPA) collected with IVUS and MSCT. Between 6 and 60 mo of follow-up, there were 25 (A), 21 (B1), and 30 (B2) serial IVUS measurements. At five years, 18 patients took MSCT as an optional investigation that was performed at three of four centers. Quantitative analysis of the scaffolded segment was feasible in all patients. The insignificant increase of PB was documented in ABSORB cohort A and B1 trials at 6, 24, and 60 mo (if applicable). The absolute growth of PB was +7.52% (*P* value is not applicable, NA; *n* = 25) at 6 mo (a +13.72% relative increase), and +1.63% (*P* value is NA) at 24 mo (a relative +2.97% from baseline) in ABSORB A trial (*n* = 29), and +2.47% (*P* < 0.02, *n* = 33) at 6 mo (a +4.62% relative increase), +1.89% (NA, *n* = 33) at 24 mo (+3.53%) with a -2.46% (estimated *P* value < 0.06, *n* = 21) reduction at 60 mo (a -4.59% relative decrease) in ABSORB cohort B1 trial (*n* = 45). A +1.60% increase of PB (*P* value is NA, *n* = 45) registered at 12 mo (a +2.94% relative increase) with a further -1.10% reduction at 36 mo (a -2.02% relative decrease from baseline, *P* = 0.05, *n* = 45), and a -2.62% decrease at 60 mo (a -4.88% relative decrease, estimated *P* value < 0.22, *n* = 30) in ABSORB cohort B2 trial (*n* = 56).

In order to evaluate the quality of the data, the accuracy of the imaging modalities in ABSORB cohort B1 trial was estimated. The length of the scaffolded region was measured in patients who underwent QCA, IVUS, VH-IVUS, MSCT, and OCT and then compared with the nominal size of the scaffold, which was equal to 18 mm in all cases (Figure 3). The accuracy (a trueness by ISO

57251) was highest for OCT imaging (96.6%) with very good precision (estimated by 95%CI of a trueness; the length of the scaffold was correct in 13.1% of cases). The lowest accuracy assessed in MSCT analysis with a 62.0% trueness and poor precision (the length was overestimated in 93.2% of observations). The moderate accuracy with relatively poor precision attested for QCA (82.7%, totally underestimated), IVUS, and VH-IVUS (82.9% and 84.3%, respectively, the length was mostly overestimated).

Plaque burden and lesion composition in ABSORB cohort B1 trial

The GS IVUS analysis of 32 patients (72.73% of the cohort) with serial imaging examination established the statistically significant increase in PB at 6 mo (a +2.73% absolute increase, *P* = 0.05) with a further light decrease between 6 mo and 2 years (a +2.54% absolute increase from baseline, *P* = 0.08) with similar dynamic edges (Table 2 and Figure 4). Eight patients proved a -2.67% absolute abatement of PB at 24 mo (*P* = 0.28). The VH-IVUS assessments (Figure 4) substantiated a 0.12-fold increase in the number of VH-thin-cap fibroatheromas (VH-TCFA) from post-procedure to 24-mo follow-up as a manifestation of the natural history of atherosclerosis and significant area enlargement of the fibrous tissue (+48.52%, *P* = 0.02, *n* = 32) in the lesions without any powered (*P* > 0.05) distinction of the other plaque components. The patients with reduction of PB (*n* = 8) had a composition of the lesion at the scaffold region pre-procedure (one observation) with less pronounced depositions of calcium (*P* > 0.05) and a higher value of fibrous tissue (*P* > 0.05), which was very similar to the composition of the lesions that were documented in both edges (*P* > 0.05) compared to 24 patients (three observations) with increased PB at 24 mo. Post-procedure, the general tendency for reduction of the dense calcium was shown (*P* = 0.10) in all observations, which was related to the degradation of the scaffold that sometimes imitates calcium in VH-IVUS. A -0.11-fold decrease in the number of VH-TCFA per patient with a trend toward change of the percentages of necrotic core (a -11.10% relative decrease, *P* = 0.13) and fibrous tissue (a +20.12% relative increase, *P* = 0.11) with a significant increase of fibro-fatty tissue (a 0.91-fold increase, *P* = 0.04) at 24 mo was argued in observations (*P* = 8) to be "regression of atherosclerosis".

Currently, it is unclear whether the plaque regression is a true phenomenon due to the disappearance of the scaffold, which is ultimately replaced by connective tissue^[56]. The documented trend toward a reversal of atherosclerosis, lumen enlargement, and progressive hyaline arteriosclerosis^[58] (mediating so-called OCT-phenomenon of the "golden tubes"^[59]) after placement of BVS resembles the previously delineated histologic findings in animals^[59-62] and human autopsies^[63].

The curve of the PB draws a four-phase regression of

Table 2 Serial imaging analysis of the artery remodeling in ABSORB cohort A and B trials

| Variable | Post-procedure (baseline) | 6 mo | 12 mo | 24 mo | 36 mo | 60 mo | Friedman <i>P</i> value |
|--|---------------------------|---|---|---|---|---|-------------------------|
| Intravascular ultrasound, 60-mo results of ABSORB cohort B (B1, <i>n</i> = 21, and B2, <i>n</i> = 30) trial | | | | | | | |
| Mean vessel area in mm ² , mean ± SD (<i>n</i>), BL-to-FUP <i>P</i> value | 14.56 ± 3.82 (21) | 14.92 ± 3.78 (21), 0.3925 | | 15.88 ± 4.02 (21), 0.0014 ^s | | 15.28 ± 4.53 (21), 2.1371 | 0.0193 ^s |
| | 13.61 ± 2.40 (30) | | 14.15 ± 2.61 (30), 0.2140 | | 14.25 ± 2.57 (30), 0.0788 | 13.23 ± 2.70 (28), 0.2701 | 0.0337 ^s |
| Mean lumen area in mm ² , mean ± SD (<i>n</i>), BL-to-FUP <i>P</i> value | 6.75 ± 1.19 (21) | 6.59 ± 1.20 (21), 0.0610 | | 7.24 ± 1.91 (21), 0.1995 | | 7.46 ± 2.45 (21), 0.0851 | 0.0626 |
| | 6.31 ± 0.86 (30) | | 6.31 ± 1.01 (30), 0.5131 | | 6.70 ± 1.48 (30), 0.0858 | 6.48 ± 1.50 (30), 0.5666 | 0.2221 |
| Plaque burden in %, mean ± estimated SD (<i>n</i>) ¹ , BL-to-FUP <i>P</i> value | 53.64 ± 14.08 (21) | 55.83 ± 14.15 (21), < 0.39 ² | | 54.41 ± 14.35 (21), < 0.20 ² | | 51.18 ± 16.81 (21), < 2.14 ² | < 0.06 ² |
| | 53.64 ± 9.46 (30) | | 55.41 ± 10.22 (30), < 0.51 ² | | 52.98 ± 11.70 (30), < 0.09 ² | 51.02 ± 11.81 (30), < 0.56 ² | < 0.22 ² |
| Mean plaque area in mm ² , mean ± SD (<i>n</i>), BL-to-FUP <i>P</i> value | 7.81 ± 2.98 (21) | 8.33 ± 2.88 (21), 0.0660 | | 8.64 ± 2.85 (21), 0.0004 ^s | | 7.75 ± 2.62 (21), 4.4007 | 0.0025 ^s |
| | 7.30 ± 1.85 (30) | | 7.84 ± 1.92 (30), 0.0220 ^s | | 7.55 ± 1.58 (30), 0.8121 | 6.79 ± 1.90 (28), 0.0108 ^s | < 0.0001 ^s |
| Intravascular ultrasound, 36-mo results of ABSORB cohort B (B1, <i>n</i> = 33, and B2, <i>n</i> = 45) trial | | | | | | | |
| Mean vessel area in mm ² , mean ± SD (<i>n</i>), BL-to-FUP <i>P</i> value | 14.04 ± 3.80 (33) | 14.44 ± 3.82 (33), 0.008 ^s | | 15.35 ± 4.05 (33), < 0.001 ^s | | NA | NA |
| | 13.79 ± 2.37 (45) | | 14.43 ± 2.64 (45), 0.03 ^s | | 14.58 ± 2.67 (45), 0.002 ^s | NA | 0.18 |
| Mean lumen area in mm ² , mean ± SD (<i>n</i>), BL-to-FUP <i>P</i> value | 6.53 ± 1.24 (33) | 6.36 ± 1.18 (33), 0.02 ^s | | 6.85 ± 1.78 (33), 0.35 | | NA | NA |
| | 6.29 ± 0.90 (45) | | 6.35 ± 1.17 (45), NS | | 6.81 ± 1.62 (45), 0.05 ^s | NA | 0.007 ^s |
| Plaque burden in %, mean ± estimated SD (<i>n</i>) ¹ , BL-to-FUP <i>P</i> value | 53.49 ± 14.48 (33) | 55.96 ± 14.80 (33), < 0.02 ^s | | 55.37 ± 14.61 (33), < 0.35 | | NA | NA |
| | 54.39 ± 9.35 (45) | | 55.99 ± 10.32 (45), NS | | 53.29 ± 12.68 (45), < 0.05 ^s | NA | NA |
| Mean plaque area in mm ² , mean ± SD (<i>n</i>), BL-to-FUP <i>P</i> value | 7.52 ± 2.84 (33) | 8.08 ± 2.87 (33), < 0.001 ^s | | 8.49 ± 2.89 (33), < 0.001 ^s | | NA | NA |
| | 7.50 ± 1.82 (45) | | 8.08 ± 1.94 (45), < 0.001 ^s | | 7.77 ± 1.73 (45), NS | NA | 0.004 |
| Intravascular ultrasound, 24-mo (<i>n</i> = 25), and MSCT, 60 mo (<i>n</i> = 18), results of ABSORB cohort A trial | | | | | | | |
| Mean vessel area in mm ² , mean ± SD (<i>n</i>), BL-to-FUP <i>P</i> value | 13.49 ± 3.74 (25) | 13.79 ± 3.84 (25), 0.98 | NA | 12.75 ± 3.43 (19), 0.68 | NA | NA | NA |
| | NA | NA | NA | 13.17 (18) (18 mo baseline) | NA | 11.93 (18), 0.26 | NA |
| Mean lumen area in mm ² , mean ± SD (<i>n</i>), BL-to-FUP <i>P</i> value | 6.04 ± 1.12 (25) | 5.19 ± 1.33 (25), < 0.0001 ^s | NA | 5.47 ± 2.11 (19), 0.12 | NA | NA | NA |
| | NA | NA | NA | 4.47 (18) (18 mo baseline) | NA | 4.29 (18), 0.11 | NA |
| Plaque burden in %, mean ± estimated SD (<i>n</i>) ¹ , BL-to-FUP <i>P</i> value | 55.23 ± 15.31 (25) | 62.36 ± 17.37 (25), < 0.98 | NA | 57.10 ± 22.02 (19), < 0.68 | NA | NA | NA |
| | NA | NA | NA | 66.06 (18) (18 mo baseline) | NA | 64.04 (18), < 0.26 | NA |
| Mean plaque area in mm ² , mean ± SD (<i>n</i>), BL-to-FUP <i>P</i> value | 7.44 ± 2.83 (25) | 8.60 ± 2.85 (25), < 0.0001 ^s | NA | 7.10 ± 2.02 (19), 0.80 | NA | NA | NA |
| | NA | NA | NA | 8.23 (18) (18 mo baseline) | NA | 7.10 (18), 0.23 | NA |

Numbers are expressed in mean ± SD or *n*. ¹The SD cannot be directly calculated due to unavailability of the patient-by-patient matrix of the ABSORB trial, and presented as either a 5% deviation or adjusted by the maximum deviation for both numerator and denominator; ²The *P* value cannot be directly calculated due to unavailability of the patient-by-patient matrix of ABSORB trial, and performed as an estimated *P* value adjusted by the maximum *P* value in either numerator or denominator. The cells with “S” performed statistically significant changes (*P* < 0.05) of the variables. NS: Non-significant (*P* value > 0.05); NA: Non-available or not applicable.

atherosclerosis. First, the polymeric struts are covered by a fibromuscular neointima (first 6-12 mo, or “reactive” phase) with an inflammatory “swelling” (a foreign body reaction, including multinucleated giant cells, macrophages, and lymphocytes) of the artery wall (slowly shrinking inflammatory infiltrate with macrophages and

lymphocytes mostly observed between 12 and 36 mo, maximum of 42 mo)^[60,61]. The increase of the necrotic area post-procedure in VH-IVUS definitely consorted with the fibrinoid necrosis in the scaffolded lesion, but this fact demands a special investigation to discern the hyalinosis whereas the association of the necrotic core

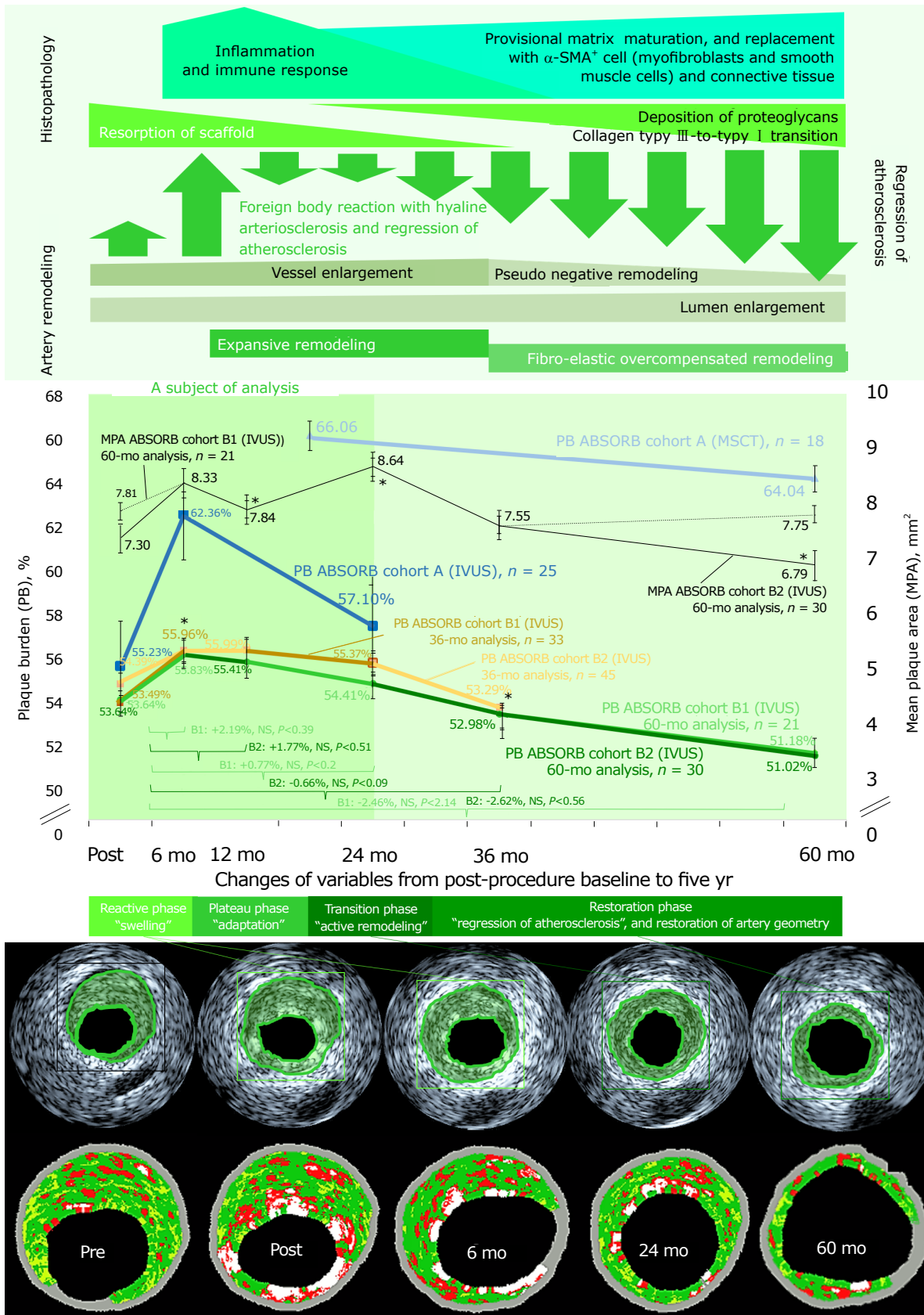


Figure 2 Plaque burden in patients of ABSORB cohort A and B trials at 60 mo. The top panel outlines the acute/subacute and chronic inflammatory/immune response to the implantation of the BVS, which is ongoing during the first 24-36 mo. The middle panel renders a pooled analysis of the plaque burden (PB) and mean plaque area (MPA) in the selected ABSORB phase I / II trials and different multimodality imaging analyses through the five years of the study. The bottom panel shows an example of the grey scale- and virtual histology-IVUS analyses in the five-year time-frame of the ABSORB trial highlighting a clear reduction of the plaque area and artery remodeling with the lumen enlargement and positive expansive remodeling of the vessel at least until 24 mo with the further constrictive-like remodeling. The figure was adapted from reference [34].

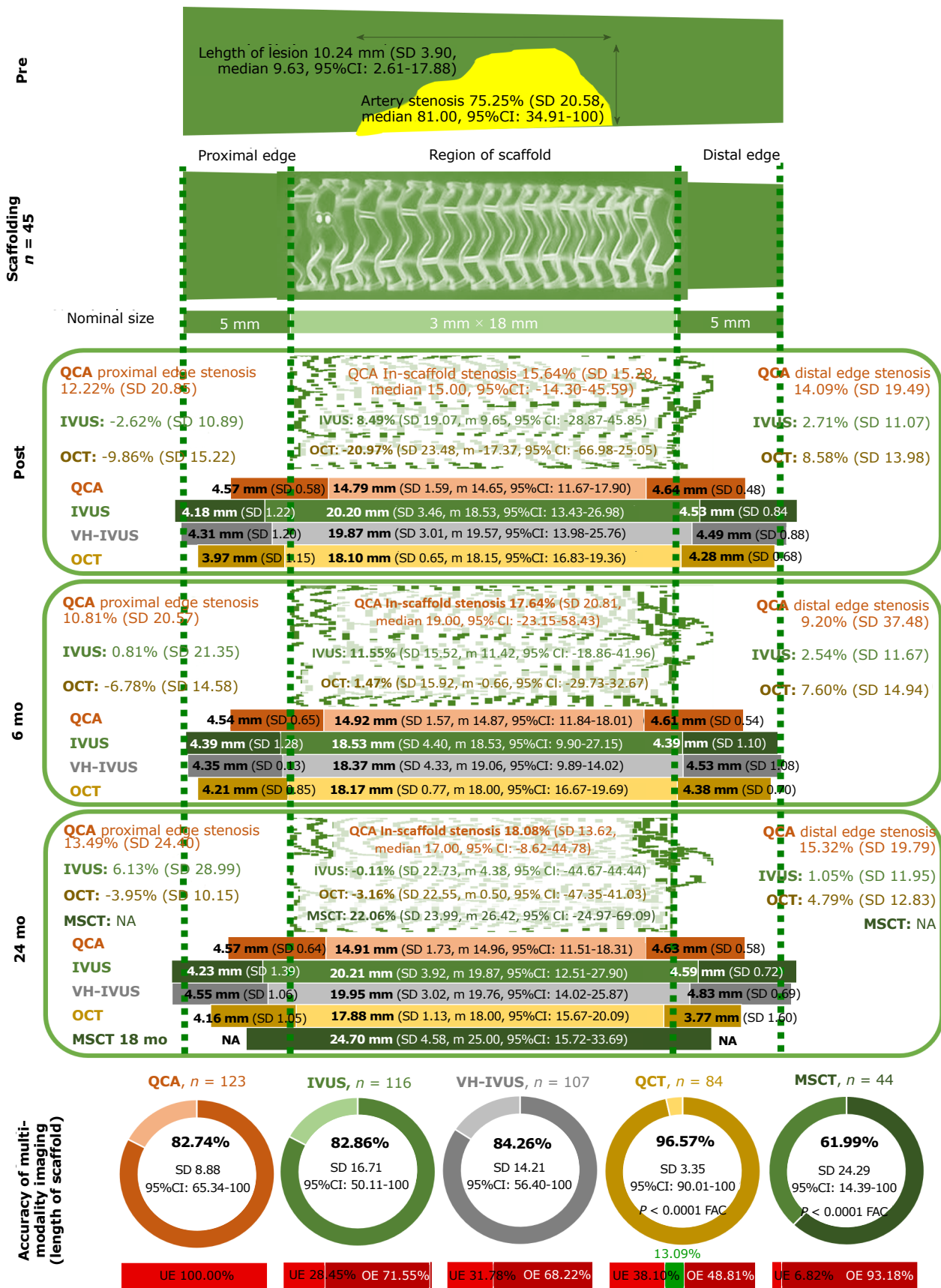


Figure 3 The accuracy of multimodality imaging analysis. The analysis of accuracy (trueness and precision) administered with quantitative coronary angiography, intravascular ultrasound, virtual histology-IVUS, multislice computed tomography, and optical coherence tomography by the nominal length of the scaffold, which was 18 mm in all cases. The panel defines the spread-out-vessel graphics (axial resolution of 200 μ m) with the appearance of the scaffolded and edge regions pre- and post-procedure at 6 mo and 24 mo. The figure was adapted from ref. [34]. UE: Underestimated (observations with the length of the scaffolded region less than 18 mm); OE: overestimated (the examined scaffolded region was more than 18 mm). QCA: quantitative coronary angiography; IVUS: intravascular ultrasound; VH-IVUS: virtual histology-intravascular ultrasound; OCT: optical coherence tomography; MSCT: multislice computed tomography.

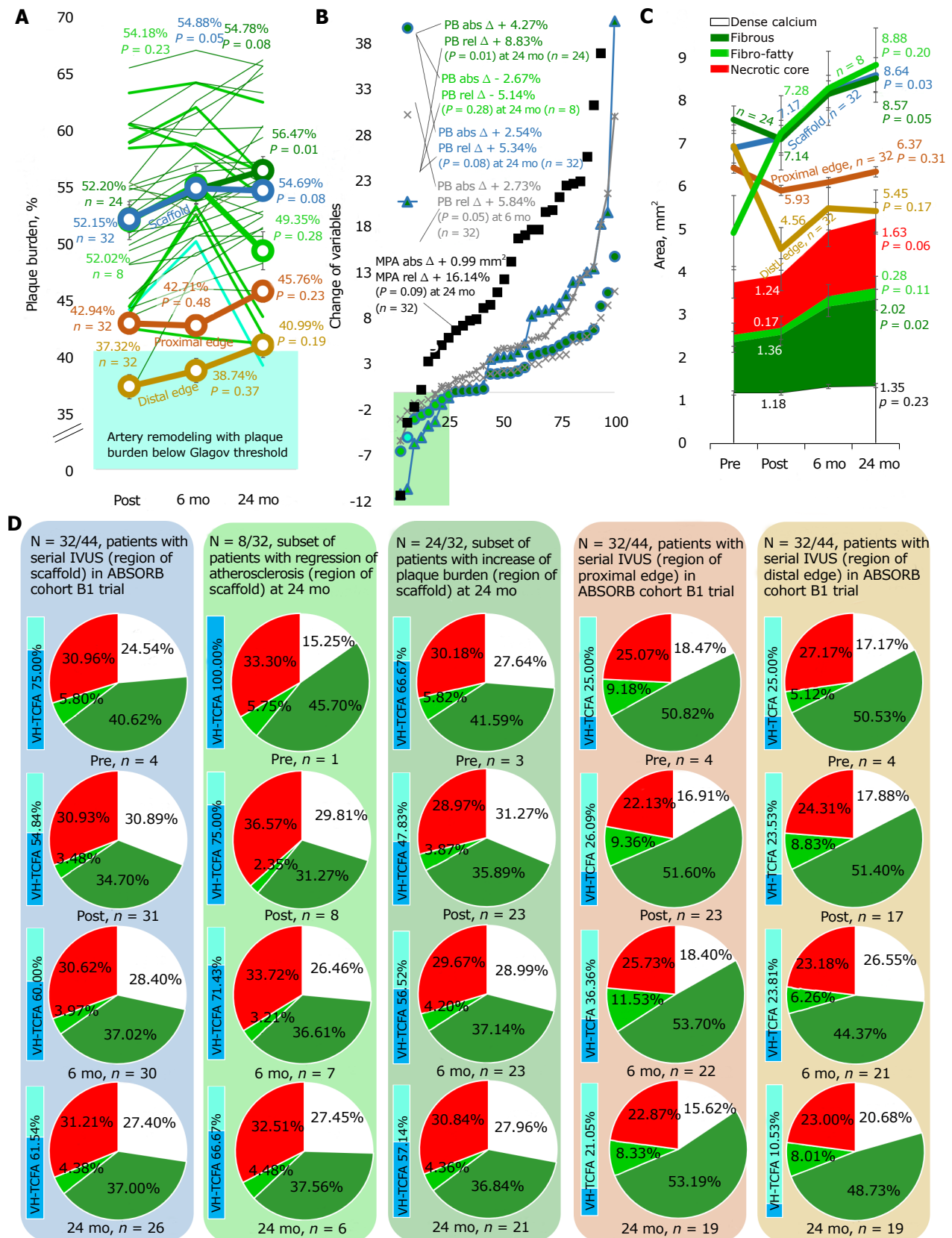


Figure 4 The artery remodeling in ABSORB cohort B1 trial. A, B: The plaque burden (%) in 44 patients of cohort B1 trial (panel A with the changes at panel B); C, D: The proportion between the lesion components, which was computed by virtual histology-intravascular ultrasound imposed for each patient, but the percentage of each plaque component did not differ significantly between baseline and 24 mo. The depicted results mounted as the mean of the estimated proportions. The figure was adapted from ref. [34]. n: Number of patients; MPA: Mean plaque area; abs: Absolute; rel: Relative; VH-TCFA: Virtual histology-thin-cap fibroatheroma; PB: plaque burden; VH-IVUS: virtual histology-intravascular ultrasound.

is based on the value of the cholesterol deposits (VH-IVUS fibro-fatty component). Second, struts and artery are of stable morphology through 18 mo (a “plateau phase” with an adaptation of the artery wall to the altered hemodynamics/shear stress and a foreign body in the grip of inflammation and a “frame” of the scaffold). Third, the struts become replaced by proteoglycan matrix (arterial hyalinosis)^[58] at 24 mo (a “transition” phase with an active compensatory artery remodeling that starts at 12 mo with a peak at 18 mo)^[60,61], which corresponds to resorption of BVS (morphological changes in the scaffold resorption sites begin at 18 mo) with a light calcification of the vessel wall and increasing eosinophilia (30 mo). These changes are linked to the absorption and inspissation of proteins (presence of proteinaceous material including albumin being a manifestation of the Vroman effect^[64,65]). The precipitation of calcium phosphate might be the result of a benign, localized drop in pH caused by acidic polymer degradants at the strut-tissue interface. Fourth, the strut sites are eventually composed of a provisional matrix (mostly, proteoglycan) that matures from collagen type III integration (36 mo) to eventual replacement by α -SMA⁺ cells (myofibroblasts and smooth muscle cells) and collagen type I at 42 to 48 mo (hyaline-associated arteriosclerosis with an excess of the dense connective tissue at the sites of the struts replacement, which looks like a fibrous tissue at VH-IVUS), demonstrating an augmenting integration of scaffold into the arterial tissue (a “restoration” phase). Strictly speaking, the process of “bioresorption” finishes by 24 mo with the consequent “integration” of the struts within the arterial wall. The debris of the scaffold can be pinpointed until 36 mo. The drawbacks (increased stenosis and greater neointimal thickness) of the BVS seen at early time points were no longer pertinent at 36 mo^[61]. Meanwhile, the MPA in IVUS exhibits a biphasic change with an increase until 12-24 mo and a plaque reduction until 24-36 mo^[55], which is relevant to the above-mentioned findings, but different from the dynamics of PB.

The process of the PB reduction or “regression of atherosclerosis” starts at 12 mo and turns substantial with a relatively slow pace after 36 mo. However, the histopathologic signs of the excessive extracellular matrix production (including VH-IVUS signs of the fibrous metamorphosis in the lesion) with the “hardening” hyaline arteriosclerosis cause debate for a potential of the transient scaffolding for the “restoration” of the artery wall. Frankly, a hyaline deposition in the middle-size arteries is typical for aging and very benign in elderly patients^[22,23]. The nature and structure of hyaline (nonfibrillar glycoprotein) in the case of the transient scaffolding is not entirely clear. However, the accumulation of the extracellular matrix in tissue might be evidence for a reversal of atherogenesis. Moreover, such a phenomenon with a lumen enlargement (as a result of the transient scaffolding) could be the only way to settle on atherosclerosis protecting the arteries, which necessitates further long-term studies.

The scaffold-induced hyaline arteriosclerosis managed by the complex immune response is typical for the foreign body (biomaterial-induced) reaction^[60,61,64,65]. The mTOR-inhibition with everolimus devaluates the immune response to the scaffold. However, in human autopsies^[62], macrophage and granulocyte activation where the limus drugs are not effective enough are observed. The complement system, a major host defense system, conserves clotting and inflammation, which is the most critical for the rate of ST and any adverse events^[64,65]. Such an immune hurricane amid the post-intervention healing of the vessel wall has a potential to catalyze specific artery remodeling with a lumen enlargement, certain atheroprotective patterns, and hyaline arteriosclerosis as an outcome of the foreign body reaction to BVS partly adjusted with mTOR-inhibition.

The decrease in the number of TCFA lesions in the tested cohort of patients with “regression of atherosclerosis” is further evidence of the BVS benefits promising the prevention of MACE merely because it is known^[59,66,67] that VH-IVUS can identify plaques at increased risk of subsequent events, and VH-TCFA are strongly linked with MACE (VIVA trial, 2011). Historically BVS (since 2006 in at least five studies: ABSORB II, ABSORB-Japan, ABSORB-China, ABSORB III, and ABSORB-Extend) substantiated the excellent clinical profile^[20-54] with the proper safety (relatively low rate of TLF) that with the reduction of PB is able to significantly shift the management of atherosclerosis.

The benign adaptive artery remodeling with the lumen enlargement and vessel wall thinning of atherogenesis (the ABSORB B trial confirmed the strong trend toward reduction of PB through 60 mo without signs of the “natural” progression of atherosclerosis) with a potential to become a magic bullet in order to ultimately overpower atherosclerosis.

The window of external elastic membrane enlargement and Glagov-Pasterkamp artery remodeling in ABSORB trials

The multiple linear and polynomial regression analysis of the different degrees (Figure 5) in both scaffold (Figure 5A) and edge (Figure 5B) regions (290 observations) in ABSORB cohort B1 trial authenticated the existence of the window of external elastic membrane (EEM) enlargement with the boundaries between 30.26% and 50.01% where EEM slows down without compromised lumen geometry. The number of observations with PB below 30.26% was not high enough to ultimately clarify the lower limit ($P = 0.06$), but box-and-whisker analysis certified the statistically significant difference between three distributions above 30.26%, in particular between 30.26%-40.00% and 40.00%-50.01% ($P = 0.02$), which denotes that the Glagov threshold of a 40% PB is a real phenomenon but with the broader boundaries when lumen becomes narrow if PB achieves 50.01% ($P < 0.02$). These findings were corroborated at the analysis of associations between IVUS PB and artery stenosis. The

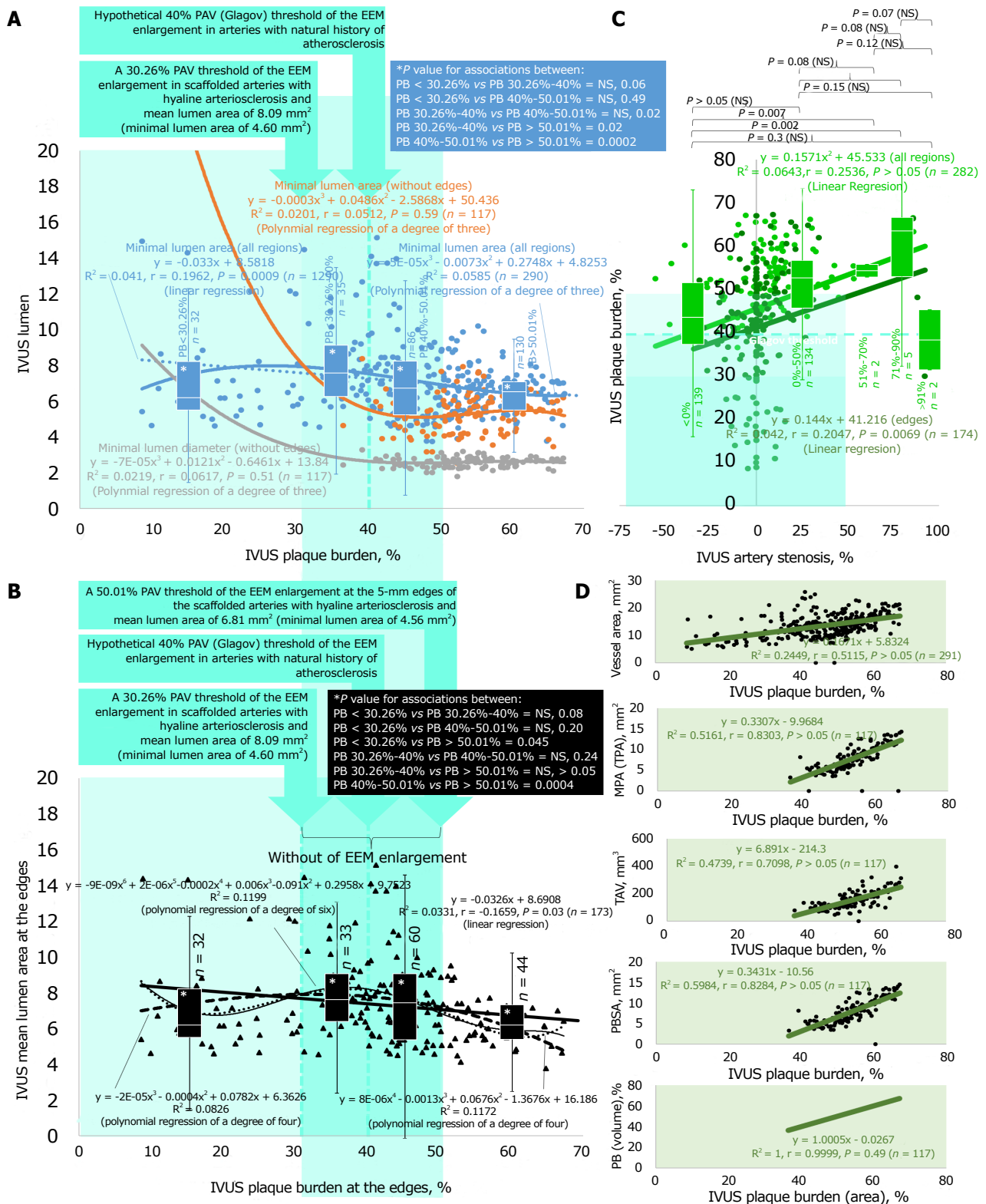


Figure 5 The external elastic membrane enlargement and Glagovian artery remodeling. A, B: Character regression analysis of the associations between plaque burden (PB) and lumen geometry verified by intravascular ultrasound (IVUS). The linear and polynomial regression of the different degrees at the regions of scaffold and edges bared two boundaries (30.26% and 50.01%) of the phenomenon of the external elastic membrane (EEM) enlargement (shown with a vertical stripe). The further box-and-whisker analysis was from four PB distributions (PB < 30.26%, PB 30.26%-40%, PB 40%-50.01%, and PB > 50.01%) to assess patterns of the Glagovian artery remodeling; C, D: The comparison of PB with artery stenosis (adjusted by the mean reference area) with a five-distribution box-and-whisker analysis (artery stenosis < 0%, 0%-50%, 51%-70%, 71%-90%, and > 91%); The upper boundary of the window of the EEM enlargement where artery stenosis was no more than 45% (C). The associations between IVUS PB and other variables characterizing the lesion geometry were estimated (D). The P value was calculated for comparison of one or two variables in order to either examine the means of two groups (paired or unpaired *t* test) or test statistical consistency for regression. The figure was adapted from ref. [34]. *n*: Number of observations; PAV: Percent atheroma volume; R²: Coefficient of determination; *r*: Pearson correlation (for linear regression); IQR: Interquartile range; NS: Non-significant (*P* > 0.05); PBSA: Plaque behind stent area; TAV: Total atheroma volume; MPA: Mean plaque area.

artery stenosis was below 0% until the threshold of a 45.76% PB in all regions (including scaffold and edges), and a 40.34% PB in edges (beyond the scaffold). The upper boundary of a 50.01% PB was associated with a 33.85% IVUS artery stenosis in all regions and a 45.09% in edges that is relevant to data of the box-and-whisker analysis that did not reveal any significant difference in PB if match artery stenosis was below 0% and 0%-50%. The VH-IVUS examination (Figure 6, top right panel) of PB supported a 32.07%-49.13% window of EEM enlargement for all regions ($P > 0.05$ for all comparisons, FAC) vs a 32.07%-54.86% window for 12 observations in naïve pre-procedure arteries ($P > 0.05$, FAC).

Eight BVS patients in the ABSORB B1 trial had a 2.67% decrease of PB at 24 mo ($P = 0.28$). The phenomenon of the window of EEM enlargement with a PB of 30.26%-54.86% was disclosed in the population, but only one patient had a PB reduction below a 40% Glagovian threshold. At 24 mo, 15/32 patients achieved PB within a window of EEM enlargement a vs 19 patients at baseline without cases below a lower end of the interval. Implantation of BVS in ABSORB II trial^[17,68,69] was defined by more pronounced sub- and decompensated arterial remodeling when compared with stenting (Figure 7). There was documented positive remodeling with lumen enlargement and plaque decrease (OR, 0.23, 95%CI: 0.14, 0.38, $P < 0.02$) with more stable arterial geometry in the metallic jacket, subcompensated expansive remodeling (OR, 3.13, 95%CI: 1.74, 5.65, NS), and constrictive remodeling (OR, 3.24, 95%CI: 1.67, 6.28, NS). Transient scaffolding was labeled by tremendous regression of atherosclerosis in 6.9% of BVS patients vs 1.5% after stenting (OR, 4.95, 95%CI: 1.13, 21.77, $P = 0.02$) when compared with DES XIENCE.

The evaluated patterns of the Glagovian artery remodeling^[50,51] play a role in the estimation of the existing CV risks in real clinical practice. A large PB of $> 70\%$ is related to higher risk of MACE being a predictor of events. Half of these events were related to nonculprit lesions (PROSPECT trial, 2011)^[22,23]. The knowledge about the window of the EEM enlargement ("Glagov threshold"^[23,50,51]) might be pivotal in the selection of the optimal strategy as a target for the reduction of PB. The decrease of PAV below that threshold or upper boundary bonds the restoration of the artery geometry and local circulation amid atheroprotective reorganization of the lesion and benign progressive hyalinosis. This was validated in 4/8 patients (one patient committed PB reduction below a 40% PB) of the ABSORB cohort B1 trial with a reversed atherogenesis at 24 mo with a similar trend in the entire population of the ABSORB B trial at 60 mo. Meanwhile, the PB in the Cath Lab might be assessed with the moderate accuracy by IVUS or VH-IVUS (to evaluate a composition of the lesion) and poor accuracy by MSCT^[57]. However, accuracy analysis in the study was impaired by the progress of bioresorption with discontinuation and dismantling^[16] of the scaffold as well as technical difficulties of the imaging^[19-35], which were

released previously^[36-52,59].

Associations between components of lesion and artery geometry in ABSORB cohort B1 trial

The PB by the artery dimensions can be evaluated by correlation (Pearson's R^2 and r) between PAV, artery stenosis, lumen area and others (Figure 5C and D, and Figure 6) with the available multi-modality imaging tools. A low heterogeneity of data was appropriate for assessment of correlation and regression ($P > 0.05$ if not mentioned) to see how two variables vary together. The moderate correlation was validated ($P > 0.05$, FAC) for associations between PB and artery stenosis ($r = 0.25$ in all regions; $r = 0.20$ in edges, $P = 0.007$), vessel area ($r = 0.51$), and total atheroma volume (TAV) ($r = 0.71$) with high correlation between PB, plaque behind stent area (PBSA) ($r = 0.83$), and MPA ($r = 0.83$). There was no difference ($P > 0.05$ FAC) between PB calculated by either area or volume in IVUS ($R^2 = r = 1.0$) with the minimal distinction between PB measured by IVUS and VH-IVUS ($r = 0.94$). MSCT was less accurate (Figure 6, top left panel) and overestimated PB when compared to IVUS ($r = 0.22$, $P = 0.08$).

To test comparability of the imaging modalities (Figure 6, middle panel), the variables were performed in IVUS with QCA, VH-IVUS, and OCT at the post-procedure baseline, 6 mo, and 24 mo. Then they were compared with the MSCT measurements at 18 mo, which were received at the inflammatory phase of the BVS resorption and resemble those at 24 mo. The IVUS mean lumen area (MLA) had the highest correlation (Figure 6, middle panel) with VH-IVUS ($r = 0.94$), moderate with QCA ($r = 0.62$) and MSCT ($r = 0.40$, $P = 0.003$), and lowest surprisingly with OCT ($r = 0.04$) with similar associations for artery stenosis ($P > 0.05$, FAC, if not mentioned). Measuring a degree of the association between IVUS PB and the lumen area, which was evaluated with other imaging modalities, we revealed a moderate correlation with MSCT ($r = 0.38$, $P = 0.005$), but not with others ($r < 0.12$, $P > 0.05$).

The estimation of the lesion's components (Figure 6, bottom panel) verified a trend toward correlation between VH-IVUS PB and the size of necrotic core ($r = 0.78$) as well as deposits of dense calcium ($r = 0.75$, $P > 0.05$ FAC). However, MLA had the highest but moderate correlation with fibrous ($r = 0.25$, $P = 0.0001$) and fibro-fatty tissue ($r = 0.42$, $P > 0.05$). The strongest association between different components vindicated for necrotic core and calcium ($r = 0.85$, $P > 0.05$), fibrous and fibro-fatty tissue ($r = 0.75$, $P > 0.05$), necrotic core and fibrous tissue ($r = 0.63$, $P > 0.05$), and necrotic core and fibro-fatty tissue ($r = 0.20$, $P = 0.004$).

DISCUSSION

Impact of the findings on daily practice

The most critical point for the first-generation BVS remains unpredictable prognosis. The modern-day transient scaffolding means a 36-48-mo biodegrada-

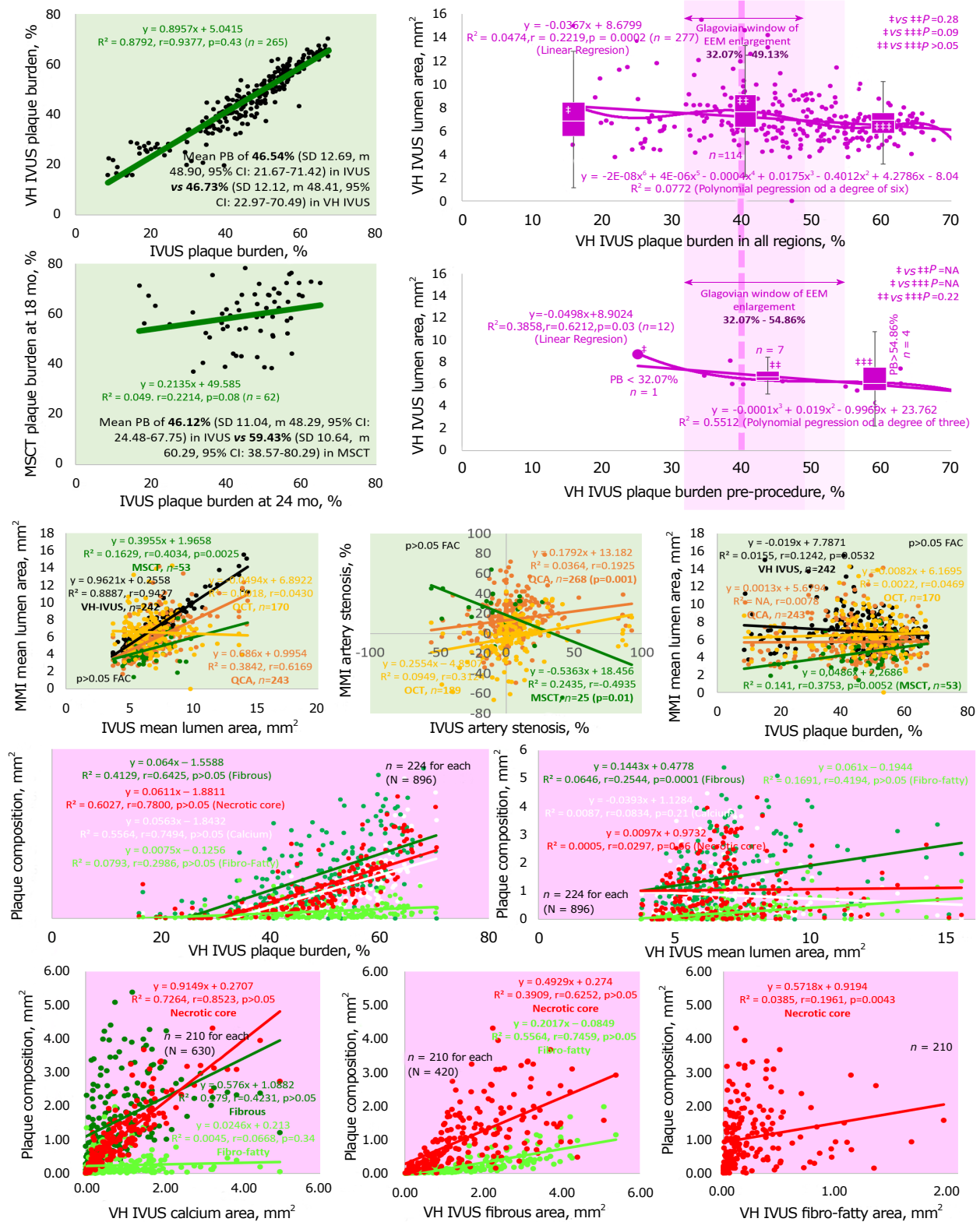


Figure 6 The association between the components of the lesion and artery layers. The correlation between plaque burden (PB) assessed by intravascular ultrasound (IVUS) and virtual histology (VH)-IVUS was strong with relatively weak association with PB evaluated by multislice computed tomography (MSCT) (top left panel). The three-distribution (PB < 32.07%, PB 32.07%-49.13%, and PB > 49.13%) box-and-whisker analysis (top right panel separately for all regions and pre-procedure) of the VH-IVUS-examined correlation between PB and lumen area vindicated existence of the window of the external elastic membrane (EEM) enlargement between 32.07% and 49.13%. The pre-procedure evaluation in naïve arteries with a broader size of the window between 32.07% and 54.86%. The middle and bottom panels set out correlations between plaque burden, lumen, vessel wall dimensions, and components of the lesion examined by the various imaging modalities. The P value was calculated for comparison of one or two variables in order to either estimate the means of two groups (paired or unpaired t test) or appreciate statistical consistency for regression. The figure was adapted from ref. [34]. n : Number of observations; N : Total number of observations at the screened population; R^2 : Coefficient of determination; r : Pearson correlation (for linear regression); IQR: Interquartile range; NS: Non-significant ($P > 0.05$); NA: Not applicable.

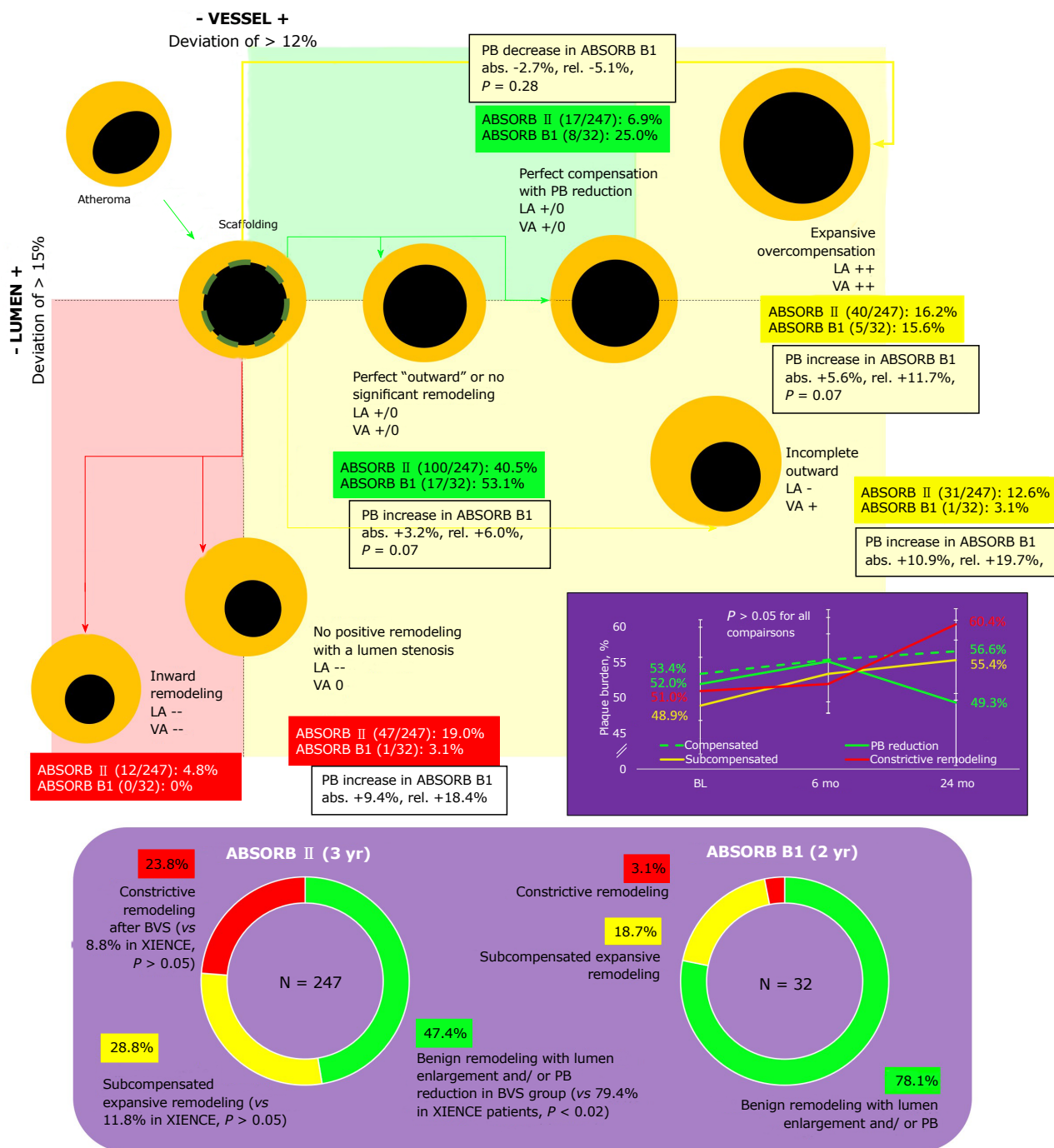


Figure 7 Arterial remodeling in coronary arteries after transient scaffolding with Absorb bioresorbable vascular scaffold. Patterns of Pasterkamp remodeling demonstrated at the top panel with a percent of patients in RCT ABSORB II and observational ABSORB B1 trials with a plaque burden (PB) change in ABSORB cohort B1 trial. The bottom panel demonstrates a percentage of the different types of the arterial remodeling in Absorb bioresorbable vascular scaffold patients. The middle dark purple panel shows dynamics of PB in patients of ABSORB cohort B1 trial. Mean PB in subsets failed to achieve Glagovian threshold of a 40% PB in all scenarios. $P < 0.05$ if compared with XIENCE.

tion with compromised local shear stress^[15], a risk of malapposition, uncovered struts, fractures, and discontinuation^[16]. The immune and inflammatory response, hyaline arteriosclerosis (sometimes with abundance of the connective tissue which appears as an OCT-phenomenon of the "golden tubes")^[17,34,35], and a foreign body-like reaction drive the biological retaliation of the vessel to the implanted scaffold with a pronounced risk of thrombosis and decompensated artery remodeling. At

least 19% of the lesions after BVS develop progressive atherosclerosis but without a clear impact on clinical outcomes^[17,34,35].

Lower affordability (with budget constraints especially in case of PSP scenario with advanced multi-modality imaging), poor availability of BVS sizes, clinical concerns, and awareness due to confusing results from RCT tremendously restrict a broad utilization of BVS in real-world cardiology despite the phenomenal success

of BVS in the first observational studies (ABSORB A, ABSORB B, and others since 2006).

Attributes of BVS trials

BVS has a good clinical and research profile with a tremendous number of patients^[5-9,17,19-21]. More than 150000 patients were treated, and more than 30000 patients were studied in 12 RCTs and 20 registries in more than 100 countries. The procedural success was tested in REPARA and GABI-R trials. Healing success comparable to the most advanced modern-day DES was confirmed in TROFI, II, and ESTROFA-BVS trials. Effectiveness and safety comparable to DES was documented in ABSORB III, ABSORB Japan, ABSORB China, ABSORB FIRST, and GHOST-EU trials. Event rates comparable to DES were observed in ABSORB II and ASSURE trials. Low long-term event rates were shown in the ABSORB EXTEND trial. Stable lumen area (OCT-documented compensated lumen enlargement) including a partial restoration of the vasomotor function was performed in the ABSORB cohort B trial^[17,23,25]. A phenomenon of the vessel wall thinning was also shown. This is a kind of regression of atherosclerosis below a threshold of the 40% PB in accordance with the concepts of artery remodeling developed by Glagov and Pasterkamp^[17,22,23]. Only 23.1% of patients had expansive remodeling of the artery with lumen enlargement and plaque decrease^[11,17,24].

Transient scaffolding is challenging because the scaffold failure remains an Achilles' heel of the technology. It is mostly associated with extensive malapposition and further secondary evaginations (9%), late discontinuity (8%), peri-strut low intensity area (5%), uncovered strut with delayed endothelialization (4%), under-deployment (4%), incomplete lesion coverage (4%), recoil with a decrease of radial strength including scaffold fracture and collapse, acute disruption of struts and overlapping struts (3%), restenosis (2%), neoatherosclerosis with severe inflammation (1%), bifurcation concerns (1%), and non-specific imaging findings including acute and chronic inflammatory responses, and increased thrombogenicity (1%)^[26,27]. These points require some clinical awareness despite confusing statistics (an underpowered fashion at least for some variables in RCTs such as ABSORB China and Japan, EVERBIO II^[28], and AIDA^[29] and no optimized design of a few meta-analyses with a lack of statistical power from the teams of Polimeni, Collet, Mahmoud, Ali, Zhang, and Kang; Table 1) and relevant efforts to prevent the aforementioned complications.

Concerns from the European task force

There are several concerns to consider in real clinical practice with BVS (according to the ESC-EAPCI Task Force, not yet published, announced in May 2017 at EuroPCR, Paris, France)^[30] and therefore must overcome to protect patients and harmonize intervention remain: (1) optimization of the implantation by the PSP scheme (pre-dilation with a residual stenosis < 30% (under

IVUS imaging ideally), correct sizing (excluding patients with a vessel size < 2.25 mm and > 3.5 mm), post-dilation (balloon diameter/scaffold diameter = 1:1; balloon diameter < scaffold diameter + 0.5 mm) with a non-compliant balloon pressure > 18 atm (under OCT imaging ideally) to prevent malapposition and injury of BVS); (2) fractures and discontinuities (could be managed by the harmonized implantation); (3) duration of the anti-thrombotic therapy (> 18 mo) until the disappearance of the uncovered struts, which means hypothetically that some protection (for instance, with a prophylactic dose of oral anticoagulants) is necessary even for 48 mo^[6]; and (4) optimal sites of intervention avoiding complex lesions (left main, bifurcations, long lesions, chronic total occlusions, calcification) and small vessels (< 2.25 mm)^[7] excluding CHIP patients (at least for the moment due to absence of the strong evidence for any clinical benefit of the strategy). However, according to the ESC/EAPCI Task Force report^[30] and an academic collaboration analysis^[40], pre-dilation in ABSORB studies (ABSORB II^[31], ABSORB III^[2], ABSORB China, ABSORB Japan, ABSORB EXTEND^[11]; pooled 2973 patients) was performed in 99.8% of cases, but high-pressure post-dilation in only 12.7%. Taking into account a number of patients (82.3%)^[40] with optimal sizing (2.25 mm < RVD < 3.5 mm), a percentage of cases with full PSP were not higher than 10.4%^[30], which means it is difficult to judge clinical outcomes in these RCTs.

Accomplishments of the ABSORB trials

The serial multi-imaging approach of the prospective, single-group, open-label study displayed that the transient scaffolding with BVS can beget a reduction of PB below the baseline in coronary arteries at 24 mo. Atherosclerosis was first described when Leonardo da Vinci autopsied a centenarian man. Leonardo theorized that the cause of the degeneration of the vessels were very close to the understanding of the role of cholesterol in atherosclerosis^[46]. However, it was not described again until 1904 when Marchand first introduced the term, and in 1912 when Anichkov *et al*^[47] effectuated lesions by adding pure cholesterol to rabbit food.

The latter part of the century was spent understanding the pathology and the reversal of atherosclerosis^[47]. The first interventional study was published by Friedman *et al*^[48] in 1957. Then the angiographic paradox was studied in the 1960s^[49,50]. The first retrospective analysis with statins that found the benefits of low-density lipoprotein-cholesterol (LDL-C) in reducing coronary calcium-volume score was reported in 1998^[51] with a series of further intravascular imaging studies of the lipid-lowering strategies^[19,22] manifesting the strides of the third industrial revolution in biomedicine with a maximum 1.22% absolute reduction of PB under intensive statin therapy (ASTEROID trial, 2006; SATURN, 2011; IBIS-4, 2015; and STABLE, 2016)^[22]. Four Japanese trials (ESTABLISH, 2004; JAPAN-ACS, 2009; COSMOS, 2009;

and TWINS, 2009) demonstrated a dramatic 10.4% absolute reduction of PAV. However, statin therapy did not reduce mortality^[22,66-69]. Unfortunately, statin trials such as REVERSAL (2004), CAMELOT (2004), A-PLUS (2004), ACTIVATE (2006), PERISCOPE (2008), ILLUSTRATE (2007), STRADIVARIUS (2008), IBIS-2 (2008), TOGETHAR (2010), and YELLOW (2013) did not successfully reduce atherosclerosis^[22]. Novel lipid-lowering agents (combination of ezetimibe and statins) in ZEUS (2014) and PRECISE-IVUS (2015) showed a 2.39% decrease of PB, but results of the trials testing the PCSK9 (proprotein convertase subtilisin kexin 9) inhibitors are not yet available^[22].

Fully bioresorbable BVS is a novel approach for the treatment of coronary stenosis that supplies a transient vessel support with drug delivery advocating the increases of the fourth industrial revolution with the potential to pave the way for a reduction in atherosclerosis^[19-25].

Limitations

The analyzed ABSORB and some other BVS studies, with a small number of patients and moderate accuracy were unpowered to detect changes in the imaging endpoints from baseline to follow-up. It is infeasible to determine the impact of both transient scaffolding and statin therapy on atherosclerosis in the absence of any baseline or follow-up data with LDL-C. More than 60% of patients enrolled in ABSORB A and B trials have had hyperlipidemia-requiring medication, but the levels of LDL-C were never reported, which does not allow us to estimate a contribution of statin drugs or other interventions to the size of the coronary atherosclerotic lesions.

Future perspective

Unfortunately, all BVS in development today are of the same first generation. Due to smaller struts, which are the key and the only point of the modern-day innovators that can optimize re-endothelialization and prevent the phenomenon of the uncovered struts attenuating biological response and slightly reducing the rate of complications. Notwithstanding, it is not solving mechanical concerns including options of integrity, radial strength, durability, duration of bioresorption, and implantation-associated troubles causing malapposition and ST. Both the optimization of the BVS implantation^[24,44,68] and introduction of drug-coated balloons^[38] after the implantation have the potential to dramatically harmonize short- and long-term outcomes. Recently published results of the BIOFLOW V randomized trial^[32] demonstrated superiority of the ultrathin (60 μ m) bioresorbable polymer sirolimus-eluting stent over the durable polymer everolimus-eluting stent, which means that this direction is quite promising. These findings are totally relevant to the BIONICS study (not yet published, TCT 2016 in Washington, DC, United States) of the ridaforolimus-eluting cobalt-chromium stent with

the narrowest struts made of a combination of 40 μ m struts with 72 μ m supportive struts (a rate of ST was low at 0.4%). At least two BVS with thinner struts below 100 μ m are in translational development today as well as early phase clinical trials (a courtesy of Amaranth Medical and Abbott Vascular on October 31, 2017 at TCT 2017 in Denver, CO, United States). Meanwhile, the biology and pathology of the transient scaffolding (including specific options of acute fracture, chronic recoil, and late intraluminal scaffold dismantling) remain largely unknown. That is why we cannot expect any breakthrough in this field until success in translational research including biology and pathology of arterial remodeling, immune response, foreign body reaction, and inflammatory feedback of the coronary, adventitial and perivascular adipose tissue (the last one is feasible with a PET/CT). The absence of the broad financial support for in-depth science and an expectant strategy of the industry including a pressure over editors and editorial content at the leading journals^[41] compromise scientific findings and discourage progress in the field. A decision of Boston Scientific that halted the project of the Renuvia scaffold in July 2017 (courtesy of TCTMD, August 1, 2017) 3 mo prior to the release of the positive clinical outcomes at TCT 2017 jeopardized the future of the bioresorbable medical device technology. Potentially, the development of new polymers, exploration of the polymer biodegradation, and examination of the vascular biology and pathology of the transient scaffolding as well as immune response to the BVS implantation could shift BVS to a new level. The possibilities for BVS are exciting with the development of an electronic multi-tasking BVS^[33] that has the potential to revolutionize this technology with an optimized mechanical profile and applied nanotechnologies able to measure blood flow (including shear stress) and temperature, release drugs, and dissolve when it is necessary.

Furthermore, large-scale randomized trials are necessary to evaluate associations between documented patterns of the artery remodeling (lumen enlargement with a PB reduction) within the Glasgowian concept of atherogenesis and long-term clinical outcomes (including adverse events, in particular, MACE, restenosis, device thrombosis, complications of the device discontinuation, etc) of the transient scaffolding. The histopathological study of the hyaline arteriosclerosis in the middle-size coronary arteries could shed light on the physiology of transient scaffolding, clinical importance, and prognosis of patients who underwent implantation of BVS.

The pathology of transient scaffolding remains largely unknown. What is known has prevented further development of the technology because the controversial results are confusing, and therefore it has destroyed optimization of clinical approaches. The current study uncovered some of the flaws of the clinical trials. Many of these observations are clinically relevant and have to potential to advance the strategies for both imaging and treatment of progressive atherosclerosis.

ARTICLE HIGHLIGHTS

Research background

Bioresorbable vascular scaffold (BVS) initially had incredible success in the first ABSORB studies in 2006-2013, but was consequently deemed a failure due to reported relatively higher rates of target lesion failure (TLF) and device thrombosis in randomized controlled trials. However, BVS performs as well as the metallic drug-eluting stent (DES) with a trend toward some benefits for cardiac mortality.

Research motivation

The exploration of the insights in statistics of the relevant studies has a potential to discover the main obstacles of the BVS research and development preventing major cardiovascular events and therefore improving clinical outcomes adapting the technology in routine clinical practice.

Research objectives

The overarching objective was to supplant the perils of the current standard of care with the polymeric bioresorbable scaffolds.

Research methods

We evaluated the statistical power in clinical trials such as ABSORB Japan, ABSORB China, EVERBIO II, AIDA, and meta-analyses by the post hoc OR-based sample size calculation, and the patterns of artery remodeling published in papers from ABSORB A and B trials.

Research results

The underpowered design was confirmed for some studies such as ABSORB Japan, ABSORB China, EVERBIO II, AIDA trials, and meta-analyses of Polimeni, Collet, and Mahmoud with some unintentional bias (judged by the asymmetrical Funnel plot). ST rates with Absorb BRS were comparable with DES performed with a strategy of the BVS implantation with optimized predilation (P), sizing (S), and post-dilation (P) (PSP) implantation achieving 0.35 per 100 patient-years, which is comparable to the RR 0.49 with bare-metal stents and the RR 1.06 with everolimus DES. Both ABSORB II and ABSORB III trials were powered enough for a five-year follow-up, but the results were not entirely conclusive due to the mostly non-significant fashion of data. The powered meta-analyses were built mostly on statistically poor findings.

Research conclusions

The misunderstanding of the pathology of transient scaffolding drives the failures of the clinical trials. More bench studies of the vascular response are required. Several next-generation BVS including multifunctional electronic scaffold grant cardiology with a huge promise to make BVS technology great again.

Research perspectives

The biology of transient scaffolding remains mostly unknown. The thin-strut scaffolds and stents with advanced mechanical features are able to partly solve the problem of device thrombosis. Nevertheless, the unclear mechanism of related complications challenges the further development of the technology. Future research must be focused on both bench and bedside studies of vascular biology and pathology of the transient scaffolding in order to understand which mechanism is a leading source of the troubles that we face in routine clinical practice with bioresorbable scaffolds.

REFERENCES

- 1 **U.S. Food and Drug Administration.** MedWatch Safety Alerts for Human Medical Products. [cited June 1 2017]. Available from: URL: <https://www.fda.gov/safety/medwatch/safetyinformation/safetyalertsforhumanmedicalproducts/default.htm>
- 2 **Ellis SG, Kereiakes DJ.** A Bioresorbable Everolimus-Eluting Scaffold Versus a Metallic Everolimus-Eluting Stent III - ABSORB III. Presented by Ellis SG and Kereiakes DJ. American College of Cardiology Annual Scientific Session (ACC 2017). [cited June 1 2017]. Available from: URL: <http://www.acc.org/latest-in-cardiology/clinical-trials/2015/10/10/21/09/absorb-iii#sthash.GJEbjNK.dpuf>
- 3 **O'Riordan M.** Absorb in Europe: When, How, and by Whom the Beleaguered BVS Is Being Used After Restrictions. [cited June 1 2017]. Available from: URL: <https://www.tctmd.com/news/absorb-europe-when-how-and-whom-beleaguered-bvs-being-used-after-restrictions>
- 4 **Therapeutic Goods Administration.** Absorb Bioresorbable Vascular Scaffold System. [cited June 1 2017]. Available from: URL: <https://www.tga.gov.au/alert/absorb-bioresorbable-vascular-scaffold-system>
- 5 **Mahmoud AN, Barakat AF, Elgendy AY, Schneibel E, Mentias A, Abuzaid A, Elgendy IY.** Long-Term Efficacy and Safety of Everolimus-Eluting Bioresorbable Vascular Scaffolds Versus Everolimus-Eluting Metallic Stents: A Meta-Analysis of Randomized Trials. *Circ Cardiovasc Interv* 2017; **10**: pii: e005286 [PMID: 28468954 DOI: 10.1161/CIRCINTERVENTIONS.117.005286]
- 6 **Polimeni A, Anadol R, Münzel T, Indolfi C, De Rosa S, Gori T.** Long-term outcome of bioresorbable vascular scaffolds for the treatment of coronary artery disease: a meta-analysis of RCTs. *BMC Cardiovasc Disord* 2017; **17**: 147 [PMID: 28592227 DOI: 10.1186/s12872-017-0586-2]
- 7 **Collet C, Asano T, Miyazaki Y, Tenekecioglu E, Katagiri Y, Sotomi Y, Cavalcante R, de Winter RJ, Kimura T, Gao R, Puricel S, Cook S, Capodanno D, Onuma Y, Serruys PW.** Late thrombotic events after bioresorbable scaffold implantation: a systematic review and meta-analysis of randomized clinical trials. *Eur Heart J* 2017; **38**: 2559-2566 [PMID: 28430908 DOI: 10.1093/eurheartj/ehx155]
- 8 **Ha FJ, Nerlekar N, Cameron JD, Bennett MR, Meredith IT, West NE, Brown AJ.** Midterm Safety and Efficacy of ABSORB Bioresorbable Vascular Scaffold Versus Everolimus-Eluting Metallic Stent: An Updated Meta-Analysis. *JACC Cardiovasc Interv* 2017; **10**: 308-310 [PMID: 28183474 DOI: 10.1016/j.jcin.2016.11.054]
- 9 **Sorrentino S, Giustino G, Mehran R, Kini AS, Sharma SK, Faggioni M, Farhan S, Vogel B, Indolfi C, Dangas GD.** Everolimus-Eluting Bioresorbable Scaffolds Versus Everolimus-Eluting Metallic Stents. *J Am Coll Cardiol* 2017; **69**: 3055-3066 [PMID: 28412389 DOI: 10.1016/j.jacc.2017.04.011]
- 10 **Tanaka A, Jabbour RJ, Mitomo S, Latib A, Colombo A.** Hybrid Percutaneous Coronary Intervention With Bioresorbable Vascular Scaffolds in Combination With Drug-Eluting Stents or Drug-Coated Balloons for Complex Coronary Lesions. *JACC Cardiovasc Interv* 2017; **10**: 539-547 [PMID: 28335892 DOI: 10.1016/j.jcin.2016.12.285]
- 11 **PCRONline.** BVS/BRS trial updates and registries. Session comprising selected EuroPCR 2017 late-breaking trial submissions. [cited 1 June 2017]. Available from: URL: <https://www.pcronline.com/Cases-resources-images/Resources/Course-videos-slides/2017/BVS-BRS-trial-updates-and-registries>
- 12 **Kharlamov AN.** Scaffold thrombosis: Exaggerated illusion, or when statistics rules. *Int J Cardiol* 2016; **209**: 206-209 [PMID: 26896624 DOI: 10.1016/j.ijcard.2016.02.054]
- 13 **Iqbal J, Serruys PW, Silber S, Kelbaek H, Richardt G, Morel MA, Negoita M, Buszman PE, Windecker S.** Comparison of zotarolimus- and everolimus-eluting coronary stents: final 5-year report of the RESOLUTE all-comers trial. *Circ Cardiovasc Interv* 2015; **8**: e002230 [PMID: 26047993 DOI: 10.1161/CIRCINTERVENTIONS.114.002230]
- 14 **Sedgwick P, Marston L.** How to read a funnel plot in a meta-analysis. *BMJ* 2015; **351**: h4718 [PMID: 26377337 DOI: 10.1136/bmj.h4718]
- 15 **Tenekecioglu E, Sotomi Y, Torii R, Bourantas C, Miyazaki Y, Collet C, Crake T, Su S, Onuma Y, Serruys PW.** Strut protrusion and shape impact on endothelial shear stress: insights from pre-clinical study comparing Mirage and Absorb bioresorbable scaffolds. *Int J Cardiovasc Imaging* 2017; **33**: 1313-1322 [PMID: 28365819 DOI: 10.1007/s10554-017-1124-0]
- 16 **Onuma Y, Serruys PW, Muramatsu T, Nakatani S, van Geuns RJ, de Bruyne B, Dudek D, Christiansen E, Smits PC, Chevalier**

- B, McClean D, Koolen J, Windecker S, Whitbourn R, Meredith I, Garcia-Garcia HM, Veldhof S, Rapoza R, Ormiston JA. Incidence and imaging outcomes of acute scaffold disruption and late structural discontinuity after implantation of the absorb Everolimus-Eluting fully bioresorbable vascular scaffold: optical coherence tomography assessment in the ABSORB cohort B Trial (A Clinical Evaluation of the Bioabsorbable Everolimus Eluting Coronary Stent System in the Treatment of Patients With De Novo Native Coronary Artery Lesions). *JACC Cardiovasc Interv* 2014; **7**: 1400-1411 [PMID: 25523532 DOI: 10.1016/j.jcin.2014.06.016]
- 17 **Serruys PW**, Katagiri Y, Sotomi Y, Zeng Y, Chevalier B, van der Schaaf RJ, Baumbach A, Smits P, van Mieghem NM, Bartorelli A, Barragan P, Gershlick A, Kornowski R, Macaya C, Ormiston J, Hill J, Lang IM, Egred M, Fajadet J, Lesiak M, Windecker S, Byrne RA, Räber L, van Geuns RJ, Mintz GS, Onuma Y. Arterial Remodeling After Bioresorbable Scaffolds and Metallic Stents. *J Am Coll Cardiol* 2017; **70**: 60-74 [PMID: 28662808 DOI: 10.1016/j.jacc.2017.05.028]
- 18 **Kharlamov AN**. Cardiovascular burden and percutaneous interventions in Russian Federation: systematic epidemiological update. *Cardiovasc Diagn Ther* 2017; **7**: 60-84 [PMID: 28164014 DOI: 10.21037/cdt.2016.08.10]
- 19 **Muramatsu T**, Onuma Y, Zhang YJ, Bourantas CV, Kharlamov A, Diletti R, Farooq V, Gogas BD, Garg S, Garcia-Garcia HM, Ozaki Y, Serruys PW. Progress in treatment by percutaneous coronary intervention: the stent of the future. *Rev Esp Cardiol (Engl Ed)* 2013; **66**: 483-496 [PMID: 24776051 DOI: 10.1016/j.rec.2012.12.009]
- 20 **Kharlamov AN**. Phenomenon of elongated struts: is optical coherence tomography accurate enough to analyze scaffold area? *Int J Cardiol* 2013; **168**: 4280-4284 [PMID: 23701927 DOI: 10.1016/j.ijcard.2013.04.201]
- 21 **Kharlamov AN**. Can we adapt histological injury score for optical coherence tomography of coronaries? *Int J Cardiol* 2013; **168**: 4322-4324 [PMID: 23701930 DOI: 10.1016/j.ijcard.2013.04.168]
- 22 **Kharlamov AN**. Why do we fail to achieve Glagovian atheroregression in lipid-lowering trials? *Interv Cardiol* 2015; **7**: 469-482 [DOI: 10.2217/ica.15.37]
- 23 **Kharlamov AN**. Bioresorbable Scaffolds for Atheroregression: Understanding of Transient Scaffolding. *Curr Cardiol Rev* 2016; **12**: 66-82 [PMID: 26818488 DOI: 10.2174/1573403X1201160126125853]
- 24 **Serruys PW**, Onuma Y. Dmax for sizing, PSP-1, PSP-2, PSP-3 or OCT guidance: interventionalist's jargon or indispensable implantation techniques for short- and long-term outcomes of Absorb BRS? *EuroIntervention* 2017; **12**: 2047-2056 [PMID: 28246059 DOI: 10.4244/EIJY17M02_01]
- 25 **Onuma Y**, Muramatsu T, Kharlamov A, Serruys PW. Freeing the vessel from metallic cage: what can we achieve with bioresorbable vascular scaffolds? *Cardiovasc Interv Ther* 2012; **27**: 141-154 [PMID: 22569783 DOI: 10.1007/s12928-012-0101-8]
- 26 **Sotomi Y**, Onuma Y, Collet C, Tenekecioglu E, Virmani R, Kleiman NS, Serruys PW. Bioresorbable Scaffold: The Emerging Reality and Future Directions. *Circ Res* 2017; **120**: 1341-1352 [PMID: 28408454 DOI: 10.1161/CIRCRESAHA.117.310275]
- 27 **Räber L**, Brugaletta S, Yamaji K, O'Sullivan CJ, Otsuki S, Koppa T, Taniwaki M, Onuma Y, Freixa X, Eberli FR, Serruys PW, Joner M, Sabaté M, Windecker S. Very Late Scaffold Thrombosis: Intracoronary Imaging and Histopathological and Spectroscopic Findings. *J Am Coll Cardiol* 2015; **66**: 1901-1914 [PMID: 26493663 DOI: 10.1016/j.jacc.2015.08.853]
- 28 **Puricel S**, Arroyo D, Corpataux N, Baeriswyl G, Lehmann S, Kallinikou Z, Muller O, Allard L, Stauffer JC, Togni M, Goy JJ, Cook S. Comparison of everolimus- and biolimus-eluting coronary stents with everolimus-eluting bioresorbable vascular scaffolds. *J Am Coll Cardiol* 2015; **65**: 791-801 [PMID: 25720622 DOI: 10.1016/j.jacc.2014.12.017]
- 29 **Wykrzykowska JJ**, Kraak RP, Hofma SH, van der Schaaf RJ, Arkenbout EK, IJsselmuiden AJ, Elias J, van Dongen IM, Tijssen RYG, Koch KT, Baan J Jr, Vis MM, de Winter RJ, Piek JJ, Tijssen JGP, Henriques JPS; AIDA Investigators. Bioresorbable Scaffolds versus Metallic Stents in Routine PCI. *N Engl J Med* 2017; **376**: 2319-2328 [PMID: 28402237 DOI: 10.1056/NEJMoa1614954]
- 30 **Byrne RA**, Stefanini GG, Capodanno D, Onuma Y, Baumbach A, Escaned J, Haude M, James S, Joner M, Juni P, Kastrati A, Oktay S, Wijns W, Serruys PW, Windecker S. Report of an ESC-EAPCI Task Force on the evaluation and use of bioresorbable scaffolds for percutaneous coronary intervention: executive summary. *EuroIntervention* 2018; **13**: 1574-1586 [PMID: 28948934 DOI: 10.4244/EIJ20170912-01]
- 31 **Serruys PW**, Chevalier B, Sotomi Y, Cequier A, Carrié D, Piek JJ, Van Boven AJ, Dominici M, Dudek D, McClean D, Helqvist S, Haude M, Reith S, de Sousa Almeida M, Campo G, Iñiguez A, Sabaté M, Windecker S, Onuma Y. Comparison of an everolimus-eluting bioresorbable scaffold with an everolimus-eluting metallic stent for the treatment of coronary artery stenosis (ABSORB II): a 3 year, randomised, controlled, single-blind, multicentre clinical trial. *Lancet* 2016; **388**: 2479-2491 [PMID: 27806897 DOI: 10.1016/S0140-6736(16)32050-5]
- 32 **Kandzari DE**, Mauri L, Koolen JJ, Massaro JM, Doros G, Garcia-Garcia HM, Bennett J, Roguin A, Gharib EG, Cutlip DE, Waksman R; BIOFLOW V Investigators. Ultrathin, bioresorbable polymer sirolimus-eluting stents versus thin, durable polymer everolimus-eluting stents in patients undergoing coronary revascularisation (BIOFLOW V): a randomised trial. *Lancet* 2017; **390**: 1843-1852 [PMID: 28851504 DOI: 10.1016/S0140-6736(17)32249-3]
- 33 **Son D**, Lee J, Lee DJ, Ghaffari R, Yun S, Kim SJ, Lee JE, Cho HR, Yoon S, Yang S, Lee S, Qiao S, Ling D, Shin S, Song JK, Kim J, Kim T, Lee H, Kim J, Soh M, Lee N, Hwang CS, Nam S, Lu N, Hyeon T, Choi SH, Kim DH. Bioresorbable Electronic Stent Integrated with Therapeutic Nanoparticles for Endovascular Diseases. *ACS Nano* 2015; **9**: 5937-5946 [PMID: 25905457 DOI: 10.1021/acs.nano.5b00651]
- 34 **Kharlamov AN**, Feinstein JA, Cramer JA, Boothroyd JA. WITHDRAWN: What exactly, regression of atherosclerosis or foreign body reaction with hyaline arteriosclerosis, drives transient scaffolding of coronary arteries? A pooled analysis of observational ABSORB studies with a serial multimodality imaging substudy of ABSORB cohort B1 trial. *Int J Cardiol* 2017; pii: S0167-5273(16)32984-9 [PMID: 28629625 DOI: 10.1016/j.ijcard.2017.05.134]
- 35 **Ali ZA**, Serruys PW, Kimura T, Gao R, Ellis SG, Kereiakes DJ, Onuma Y, Simonton C, Zhang Z, Stone GW. 2-year outcomes with the Absorb bioresorbable scaffold for treatment of coronary artery disease: a systematic review and meta-analysis of seven randomised trials with an individual patient data substudy. *Lancet* 2017; **390**: 760-772 [PMID: 28732815 DOI: 10.1016/S0140-6736(17)31470-8]
- 36 **Zhang XL**, Zhu QQ, Kang LN, Li XL, Xu B. Mid- and Long-Term Outcome Comparisons of Everolimus-Eluting Bioresorbable Scaffolds Versus Everolimus-Eluting Metallic Stents: A Systematic Review and Meta-analysis. *Ann Intern Med* 2017; **167**: 642-654 [PMID: 29049539 DOI: 10.7326/M17-1101]
- 37 **Xu B**, Yang Y, Han Y, Huo Y, Wang L, Qi X, Li J, Chen Y, Kuo HC, Ying SW, Cheong WF, Zhang Y, Su X, Popma JJ, Gao R, Stone G. Comparison of everolimus-eluting bioresorbable vascular scaffolds and metallic stents: three-year clinical outcomes from the ABSORB China randomised trial *EuroIntervention* 2017; pii: EIJ-D-17-00796 [PMID: 29235306 DOI: 10.4244/EIJ-D-17-00796]
- 38 **Elwany M**, Latini RA, Di Palma G, Orrego PS, Cortese B. First experience of drug-coated balloons for treatment of bioresorbable vascular scaffold restenosis. *Cardiovasc Revasc Med* 2017; **18**: 482-486 [PMID: 28385555 DOI: 10.1016/j.carrev.2017.03.020]
- 39 **Ali ZA**, Gao R, Kimura T, Onuma Y, Kereiakes DJ, Ellis SG, Chevalier B, Vu MT, Zhang Z, Simonton CA, Serruys PW, Stone GW. Three-Year Outcomes With the Absorb Bioresorbable Scaffold: Individual-Patient-Data Meta-Analysis From the ABSORB Randomized Trials. *Circulation* 2018; **137**: 464-479 [PMID: 29089314 DOI: 10.1161/CIRCULATIONAHA.117.031843]
- 40 **Stone GW**, Abizaid A, Onuma Y, Seth A, Gao R, Ormiston J, Kimura T, Chevalier B, Ben-Yehuda O, Dressler O, McAndrew T, Ellis SG, Kereiakes DJ, Serruys PW. Effect of Technique on

- Outcomes Following Bioresorbable Vascular Scaffold Implantation: Analysis From the ABSORB Trials. *J Am Coll Cardiol* 2017; **70**: 2863-2874 [PMID: 29100704 DOI: 10.1016/j.jacc.2017.09.1106]
- 41 **Liu JJ**, Bell CM, Matelski JJ, Detsky AS, Cram P. Payments by US pharmaceutical and medical device manufacturers to US medical journal editors: retrospective observational study. *BMJ* 2017; **359**: j4619 [PMID: 29074628 DOI: 10.1136/bmj.j4619]
 - 42 **Chevalier B**, Cequier A, Dudek D, Haude M, Carrie D, Sabaté M, Windecker S, Reith S, de Sousa Almeida M, Campo G, Iñiguez A, Onuma Y, Serruys PW. Four-year follow-up of the randomised comparison between an everolimus-eluting bioresorbable scaffold and an everolimus-eluting metallic stent for the treatment of coronary artery stenosis (ABSORB II Trial). *EuroIntervention* 2018; **13**: 1561-1564 [PMID: 29094677 DOI: 10.4244/EIJ-D-17-00873]
 - 43 **Kereiakes DJ**, Ellis SG, Metzger C, Caputo RP, Rizik DG, Teirstein PS, Litt MR, Kini A, Kabour A, Marx SO, Popma JJ, McGreevy R, Zhang Z, Simonton C, Stone GW; ABSORB III Investigators. 3-Year Clinical Outcomes With Everolimus-Eluting Bioresorbable Coronary Scaffolds: The ABSORB III Trial. *J Am Coll Cardiol* 2017; **70**: 2852-2862 [PMID: 29100702 DOI: 10.1016/j.jacc.2017.10.010]
 - 44 **Bangalore S**, Bezerra HG, Rizik DG, Armstrong EJ, Samuels B, Naidu SS, Grines CL, Foster MT, Choi JW, Bertolet BD, Shah AP, Torguson R, Avula SB, Wang JC, Zidar JP, Maksoud A, Kalyanasundaram A, Yakubov SJ, Chehab BM, Spaedy AJ, Potluri SP, Caputo RP, Kondur A, Merritt RF, Kaki A, Quesada R, Parikh MA, Toma C, Matar F, DeGregorio J, Nicholson W, Batchelor W, Gollapudi R, Korngold E, Sumar R, Chrysant GS, Li J, Gordon JB, Dave RM, Attizzani GF, Stys TP, Gigliotti OS, Murphy BE, Ellis SG, Waksman R. The State of the Absorb Bioresorbable Scaffold: Consensus From an Expert Panel. *JACC Cardiovasc Interv* 2017; **10**: 2349-2359 [PMID: 29216997 DOI: 10.1016/j.jcin.2017.09.041]
 - 45 **Kang SH**, Gogas BD, Jeon KH, Park JS, Lee W, Yoon CH, Suh JW, Hwang SS, Youn TJ, Chae IH, Kim HS. Long-term safety of bioresorbable scaffolds: insights from a network meta-analysis including 91 trials. *EuroIntervention* 2018; **13**: 1904-1913 [PMID: 29278353 DOI: 10.4244/EIJ-D-17-00646]
 - 46 **Boon B**. Leonardo da Vinci on atherosclerosis and the function of the sinuses of Valsalva. *Neth Heart J* 2009; **17**: 496-499 [PMID: 20087455 DOI: 10.1007/BF03086311]
 - 47 **Williams KJ**, Feig JE, Fisher EA. Rapid regression of atherosclerosis: insights from the clinical and experimental literature. *Nat Clin Pract Cardiovasc Med* 2008; **5**: 91-102 [PMID: 18223541 DOI: 10.1038/npcardio1086]
 - 48 **Friedman M**, Byers SO, Rosenman RH. Resolution of aortic atherosclerotic infiltration in the rabbit by phosphatide infusion. *Proc Soc Exp Biol Med* 1957; **95**: 586-588 [PMID: 13453516 DOI: 10.3181/00379727-95-23300]
 - 49 **Brown BG**, Zhao XQ, Sacco DE, Albers JJ. Lipid lowering and plaque regression. New insights into prevention of plaque disruption and clinical events in coronary disease. *Circulation* 1993; **87**: 1781-1791 [PMID: 8504494 DOI: 10.1161/01.CIR.87.6.1781]
 - 50 **Glagov S**, Weisenberg E, Zarins CK, Stankunavicius R, Kolettis GJ. Compensatory enlargement of human atherosclerotic coronary arteries. *N Engl J Med* 1987; **316**: 1371-1375 [PMID: 3574413 DOI: 10.1056/NEJM198705283162204]
 - 51 **Callister TQ**, Raggi P, Cooil B, Lippolis NJ, Russo DJ. Effect of HMG-CoA reductase inhibitors on coronary artery disease as assessed by electron-beam computed tomography. *N Engl J Med* 1998; **339**: 1972-1978 [PMID: 9869668 DOI: 10.1056/NEJM199812313392703]
 - 52 **Wada H**, Mattson PC, Iwata H. Stent or Scaffold Thrombosis: Past, Current and Future Perspectives. *EMJ* 2017; **5**: 55-61
 - 53 **Ormiston JA**, Serruys PW, Onuma Y, van Geuns RJ, de Bruyne B, Dudek D, Thuesen L, Smits PC, Chevalier B, McClean D, Koolen J, Windecker S, Whitbourn R, Meredith I, Dorange C, Veldhof S, Hebert KM, Rapoza R, Garcia-Garcia HM. First serial assessment at 6 months and 2 years of the second generation of absorb everolimus-eluting bioresorbable vascular scaffold: a multi-imaging modality study. *Circ Cardiovasc Interv* 2012; **5**: 620-632 [PMID: 23048057 DOI: 10.1161/CIRCINTERVENTIONS.112.971549]
 - 54 **Brugaletta S**, Garcia-Garcia HM, Garg S, Gomez-Lara J, Diletti R, Onuma Y, van Geuns RJ, McClean D, Dudek D, Thuesen L, Chevalier B, Windecker S, Whitbourn R, Dorange C, Miquel-Hebert K, Sudhir K, Ormiston JA, Serruys PW. Temporal changes of coronary artery plaque located behind the struts of the everolimus eluting bioresorbable vascular scaffold. *Int J Cardiovasc Imaging* 2011; **27**: 859-866 [PMID: 20941544 DOI: 10.1007/s10554-010-9724-y]
 - 55 **Serruys PW**, Onuma Y, Garcia-Garcia HM, Muramatsu T, van Geuns RJ, de Bruyne B, Dudek D, Thuesen L, Smits PC, Chevalier B, McClean D, Koolen J, Windecker S, Whitbourn R, Meredith I, Dorange C, Veldhof S, Hebert KM, Rapoza R, Ormiston JA. Dynamics of vessel wall changes following the implantation of the absorb everolimus-eluting bioresorbable vascular scaffold: a multi-imaging modality study at 6, 12, 24 and 36 months. *EuroIntervention* 2014; **9**: 1271-1284 [PMID: 24291783 DOI: 10.4244/EIJV9I11A217]
 - 56 **Serruys PW**, Ormiston J, van Geuns RJ, de Bruyne B, Dudek D, Christiansen E, Chevalier B, Smits P, McClean D, Koolen J, Windecker S, Whitbourn R, Meredith I, Wasungu L, Ediebah D, Veldhof S, Onuma Y. A Polylactide Bioresorbable Scaffold Eluting Everolimus for Treatment of Coronary Stenosis: 5-Year Follow-Up. *J Am Coll Cardiol* 2016; **67**: 766-776 [PMID: 26892411 DOI: 10.1016/j.jacc.2015.11.060]
 - 57 **Onuma Y**, Dudek D, Thuesen L, Webster M, Nieman K, Garcia-Garcia HM, Ormiston JA, Serruys PW. Five-year clinical and functional multislice computed tomography angiographic results after coronary implantation of the fully resorbable polymeric everolimus-eluting scaffold in patients with de novo coronary artery disease: the ABSORB cohort A trial. *JACC Cardiovasc Interv* 2013; **6**: 999-1009 [PMID: 24156961 DOI: 10.1016/j.jcin.2013.05.017]
 - 58 **Karanasos A**, Simsek C, Serruys P, Ligthart J, Witberg K, van Geuns RJ, Sianos G, Zijlstra F, Regar E. Five-year optical coherence tomography follow-up of an everolimus-eluting bioresorbable vascular scaffold: changing the paradigm of coronary stenting? *Circulation* 2012; **126**: e89-e91 [PMID: 22891170 DOI: 10.1161/CIRCULATIONAHA.112.110122]
 - 59 **Onuma Y**, Serruys PW, Perkins LE, Okamura T, Gonzalo N, Garcia-Garcia HM, Regar E, Kamberi M, Powers JC, Rapoza R, van Beusekom H, van der Giessen W, Virmani R. Intracoronary optical coherence tomography and histology at 1 month and 2, 3, and 4 years after implantation of everolimus-eluting bioresorbable vascular scaffolds in a porcine coronary artery model: an attempt to decipher the human optical coherence tomography images in the ABSORB trial. *Circulation* 2010; **122**: 2288-2300 [PMID: 20975003 DOI: 10.1161/CIRCULATIONAHA.109.921528]
 - 60 **Kharlamov AN**, Krams R, Fayad Z, Matter C, Gabinsky JL. Understanding of the transient scaffolding: new frontiers in vascular interventional medicine for atheroregression. *Treatment Strategies: Interventional Cardiology* 2013; **3**
 - 61 **Otsuka F**, Pacheco E, Perkins LE, Sakakura K, Yahagi K, Ladich E, Kolodgie FD, Rapoza R, Joner M, Virmani R. Detailed morphologic characterization of the strut composition following Absorb scaffold placement in a porcine coronary artery model through 48 months. *J Am Coll Cardiol* 2014; **64**: B179-B179 [DOI: 10.1016/j.jacc.2014.07.680]
 - 62 **Otsuka F**, Pacheco E, Perkins LE, Lane JP, Wang Q, Kamberi M, Frie M, Wang J, Sakakura K, Yahagi K, Ladich E, Rapoza R, Kolodgie FD, Virmani R. Long-term safety of an everolimus-eluting bioresorbable vascular scaffold and the cobalt-chromium XIENCE V stent in a porcine coronary artery model. *Circ Cardiovasc Interv* 2014; **7**: 330-342 [PMID: 24895447 DOI: 10.1161/CIRCINTERVENTIONS.113.000990]
 - 63 **Kraak RP**, de Boer HH, Elias J, Ambarus CA, van der Wal AC, de Winter RJ, Wykrzykowska JJ. Coronary Artery Vessel Healing Pattern, Short and Long Term, After Implantation of the Everolimus-Eluting Bioresorbable Vascular Scaffold. *J Am Heart Assoc* 2015; **4**: pii: e002551 [PMID: 26553215 DOI: 10.1161/JAHA.115.002551]

- 64 **Anderson JM**, Rodriguez A, Chang DT. Foreign body reaction to biomaterials. *Semin Immunol* 2008; **20**: 86-100 [PMID: 18162407 DOI: 10.1016/j.smim.2007.11.004]
- 65 **Kourtzelis I**, Rafail S, DeAngelis RA, Foukas PG, Ricklin D, Lambris JD. Inhibition of biomaterial-induced complement activation attenuates the inflammatory host response to implantation. *FASEB J* 2013; **27**: 2768-2776 [PMID: 23558338 DOI: 10.1096/fj.12-225888]
- 66 **Hobbs FD**, Banach M, Mikhailidis DP, Malhotra A, Capewell S. Is statin-modified reduction in lipids the most important preventive therapy for cardiovascular disease? A pro/con debate. *BMC Med* 2016; **14**: 4 [PMID: 26769594 DOI: 10.1186/s12916-016-0550-5]
- 67 **Calvert PA**, Obaid DR, O'Sullivan M, Shapiro LM, McNab D, Densem CG, Schofield PM, Braganza D, Clarke SC, Ray KK, West NE, Bennett MR. Association between IVUS findings and adverse outcomes in patients with coronary artery disease: the VIVA (VH-IVUS in Vulnerable Atherosclerosis) Study. *JACC Cardiovasc Imaging* 2011; **4**: 894-901 [PMID: 21835382 DOI: 10.1016/j.jcmg.2011.05.005]
- 68 **Steinvil A**, Rogers T, Torguson R, Waksman R. Overview of the 2016 U.S. Food and Drug Administration Circulatory System Devices Advisory Panel Meeting on the Absorb Bioresorbable Vascular Scaffold System. *JACC Cardiovasc Interv* 2016; **9**: 1757-1764 [PMID: 27609249 DOI: 10.1016/j.jcin.2016.06.027]
- 69 **Zeng Y**, Tateishi H, Cavalcante R, Tenekecioglu E, Suwannasom P, Sotomi Y, Collet C, Nie S, Jonker H, Dijkstra J, Radu MD, Räber L, McClean DR, van Geuns RJ, Christiansen EH, Fahrni T, Koolen J, Onuma Y, Bruining N, Serruys PW. Serial Assessment of Tissue Precursors and Progression of Coronary Calcification Analyzed by Fusion of IVUS and OCT: 5-Year Follow-Up of Scaffolded and Nonscaffolded Arteries. *JACC Cardiovasc Imaging* 2017; **10**: 1151-1161 [PMID: 28330651 DOI: 10.1016/j.jcmg.2016.11.016]

P- Reviewer: Kin T, Ueda H **S- Editor:** Ji FF
L- Editor: Filipodia **E- Editor:** Wu YXJ



Takotsubo syndrome - different presentations for a single disease: A case report and review of literature

Alberto Fuensalida, Maurice Cortés, Luigi Gabrielli, Manuel Méndez, Alejandro Martínez, Gonzalo Martínez

Alberto Fuensalida, Maurice Cortés, Luigi Gabrielli, Manuel Méndez, Alejandro Martínez, Gonzalo Martínez, Division of Cardiovascular Diseases, Pontificia Universidad Católica de Chile, Santiago 833024, Metropolitana, Chile

ORCID number: Alberto Fuensalida (0000-0001-9936-2260); Maurice Cortés (0000-0002-3107-1982); Luigi Gabrielli (0000-0002-1551-7147); Manuel Méndez (0000-0003-4753-8943); Alejandro Martínez (0000-0002-6836-8990); Gonzalo Martínez (0000-0002-7120-855X).

Author contributions: Fuensalida A and Martinez G designed the report; Fuensalida A and Cortes M collected the clinical data; Gabrielli L performed the echocardiographies; Martinez A, Mendez M and G Martinez reviewed the coronary angiographies; Fuensalida A, Cortes M and Martinez G wrote the paper; Gabrielli L, Martinez A and Mendez M revised and commented the final manuscript.

Supported by a CONICYT research Grant (FONDECYT Iniciación 11170205) for Dr Gonzalo Martínez

Informed consent statement: All patients agreed to treatment and data collection by written consent at our institution.

Conflict-of-interest statement: The authors do not have any conflict of interest to report.

CARE Checklist (2013) statement: The authors have read the CARE Checklist (2013), and the manuscript was prepared and revised according to the CARE Checklist (2013).

Open-Access: This article is an open-access article which was selected by an in-house editor and fully peer-reviewed by external reviewers. It is distributed in accordance with the Creative Commons Attribution Non Commercial (CC BY-NC 4.0) license, which permits others to distribute, remix, adapt, build upon this work non-commercially, and license their derivative works on different terms, provided the original work is properly cited and the use is non-commercial. See: <http://creativecommons.org/licenses/by-nc/4.0/>

Manuscript source: Unsolicited manuscript

Correspondence to: Gonzalo Martínez, MD, MPhil, Assistant

Professor, Division of Cardiovascular Diseases, Pontificia Universidad Católica de Chile, Marcoleta 367, 2nd floor, Santiago 833024, Metropolitana, Chile. gmartinezr@med.puc.cl
Telephone: +56-223-543114

Received: June 5, 2018

Peer-review started: June 5, 2018

First decision: June 14, 2018

Revised: July 25, 2018

Accepted: July 22, 2018

Article in press: August 31, 2018

Published online: October 26, 2018

Abstract

We report three cases of Takotsubo syndrome (TS) with atypical myocardial involvement. All three cases were triggered by physical or mental stress, resulting in transient myocardial compromise. However, the clinical presentation, localization and extent of myocardial damage varied in each case, ranging from low-risk acute chest pain to cardiogenic shock with low ejection fraction and dynamic obstruction of the left ventricular outflow tract. These cases outline the range of possible presentations of this rare entity and illustrate atypical forms of TS.

Key words: Coronary angiography; Acute coronary syndrome; Stress cardiomyopathy; Takotsubo syndrome

© The Author(s) 2018. Published by Baishideng Publishing Group Inc. All rights reserved.

Core tip: Although less frequent, atypical presentations of Takotsubo syndrome - different from the classical apical ballooning - need prompt recognition by physicians. In addition to being a diagnostic challenge, this malady can present with severe complications, such as cardiogenic shock, arrhythmias and others. Herein, we show the presentation and management of atypical cases, with emphasis on their clinical recognition.

Fuensalida A, Cortés M, Gabrielli L, Méndez M, Martínez A, Martínez G. Takotsubo syndrome - different presentations for a single disease: A case report and review of literature. *World J Cardiol* 2018; 10(10): 187-190 Available from: URL: <http://www.wjgnet.com/1949-8462/full/v10/i10/187.htm> DOI: <http://dx.doi.org/10.4330/wjc.v10.i10.187>

INTRODUCTION

Takotsubo syndrome (TS) was described almost 3 decades ago as an entity mainly affecting older women (post menopause), triggered by emotional stress, with ST-segment elevation on the electrocardiogram and with a characteristic pattern of apical ballooning of the left ventricle^[1-3]. However, it is currently recognized that TS may have a more heterogeneous presentation, affecting also men, with different electrocardiographic alterations and diverse patterns of myocardial compromise^[4,5]. These atypical TS cases may comprise up to 18% of cases^[4,5].

We now describe three cases of atypical TS that presented at our institution and were managed by the authors between May 2014 and September 2016.

CASE REPORTS

Case 1

A 57-year-old man presented with irregular wide-complex tachyarrhythmia at 180 beats *per* minute during anaesthetic induction for elective pituitary macroadenoma surgery. He received intravenous (IV) propranolol and adenosine, after which he reverted to sinus rhythm. However, severe hemodynamic compromise ensued, requiring support with IV norepinephrine and pseudoephedrine. The electrocardiogram showed ST-segment depression from leads V1 to V5 and a transesophageal echocardiogram demonstrated diffuse left ventricular (LV) hypokinesis, with a left ventricular ejection fraction (LVEF) of 35%. Urgent coronary angiography showed absence of obstructive coronary artery disease in the epicardial arteries, whereas a LV angiogram confirmed an extensive area of akinesis involving the basal and middle segments of the anterior and inferior walls, with concomitant hyperkinesis of the apical segments (Figure 1A and 1B). An LVEF of 20% was estimated. Initial management included hemodynamic support with IV noradrenaline and dobutamine along with mechanical ventilation. Very rapid clinical improvement was evident and the patient was extubated 24 h after the event. High-sensitivity troponin peaked at 950 pg/mL. An echocardiogram performed 48 h later showed improvement in LVEF to 60%. Two months later, on beta-blockers, the macroadenoma was resected with no adverse events.

Case 2

A 53-year-old woman with Parkinson's disease arrived to the emergency department complaining of rest

angina after suffering severe emotional stress while she was attending a trial in a police court, 4 h earlier. Electrocardiography showed sinus rhythm with antero-lateral ST-segment depression. Coronary angiography showed no obstructive disease in the epicardial coronary arteries and LV angiography revealed akinesis in the midventricular segments, with LVEF 60% (Figure 1C and D). High-sensitivity troponin peaked at 108 pg/mL. Trans-thoracic echocardiography at 24 h showed a normal size left ventricle with minimal infero-lateral hypokinesis and preserve global function. Three months later, echocardiography showed complete recovery of the infero-lateral defect.

Case 3

A 70-year old female, with a prior history of hypertension and type-2 diabetes, presented to the emergency room with a 3-d history of intermittent oppressive chest pain, associated with dyspnoea and cough. On admission, she was tachycardic and hypotensive. The electrocardiogram showed sinus rhythm with ST-segment elevation in leads V1 to V4. Urgent coronary angiography revealed absence of obstructive coronary epicardial lesions and the left ventriculogram showed akinesis of the apex and anterior and inferior apical segments, associated with basal segment hypercontractility and severe mitral regurgitation (Figure 1D and F). The intraventricular pressure pullback showed a gradient at the level of the left ventricle outflow tract of 47 mmHg. She was urgently managed with intensive volume replacement with IV saline, resulting in a prompt recovery. Echocardiogram showed akinesis of the anterior and apical walls, with a LVEF of 45%. Peak high-sensitivity troponin was 240 pg/mL. Due to intense back pain and the presence of meningeal signs on physical examination, a magnetic resonance imaging of the spine was performed revealing spinal subarachnoid haemorrhage with a thrombosed aneurysm of the right posterior spinal artery at the T1-T2 level. She had uneventful neurological and cardiological recovery, and was discharged on beta-blockers, statins and acetylsalicylic acid. Follow-up echocardiogram at 1 mo showed complete recovery of the ventricular motion defect and a LVEF of 65%.

DISCUSSION

This case series highlights the heterogeneous clinical presentation of TS (Table 1). The affected myocardial segments were different in each case: (1) basal (or so called inverse TS); (2) midventricular and (3) apical with LV outflow tract obstruction and mitral regurgitation due to systolic anterior motion, secondary to hypercontractility of the basal segments. However, all three have in common the presence of a trigger factor (physical or emotional stress), dissociation between the magnitude of the myocardial damage extension and biomarker elevation, the absence of epicardial coronary disease on angiography and the complete or almost

Table 1 Overview of clinical presentation of the 3 cases

| | Sex | Age | Trigger | Clinical presentation | ECG abnormalities | Type of motility defect | LVEF | Peak hsTroponin | Follow- up | Recurrence |
|--------|--------|-----|--------------------------------|---|--|---|------|-----------------|------------|------------|
| Case 1 | Male | 57 | Surgery / Anesthetic induction | Ventricular arrhythmia and cardiogenic shock | ST depression leads V1 to V5 QTc: 500 msec | Basal | 35% | 950 pg/mL | 15 mo | No |
| Case 2 | Female | 53 | Emotional stress | Acute myocardial infarction without ST elevation | ST depression leads V4 to V6, DI and aVL QTc: 490 msec | Midventricular | 60% | 108 pg/mL | 38 mo | No |
| Case 3 | Female | 70 | Spinal aneurysm rupture | Acute myocardial infarction with ST elevation and shock | 2 mm ST elevation leads V1 to V4 QTc: 510 msec | Apical ballooning, LV outflow tract obstruction | 45% | 240 pg/mL | 16 mo | No |

ECG: Electrocardiography; hsTroponin: high-sensitivity troponin; LVEF: Left ventricular ejection fraction.

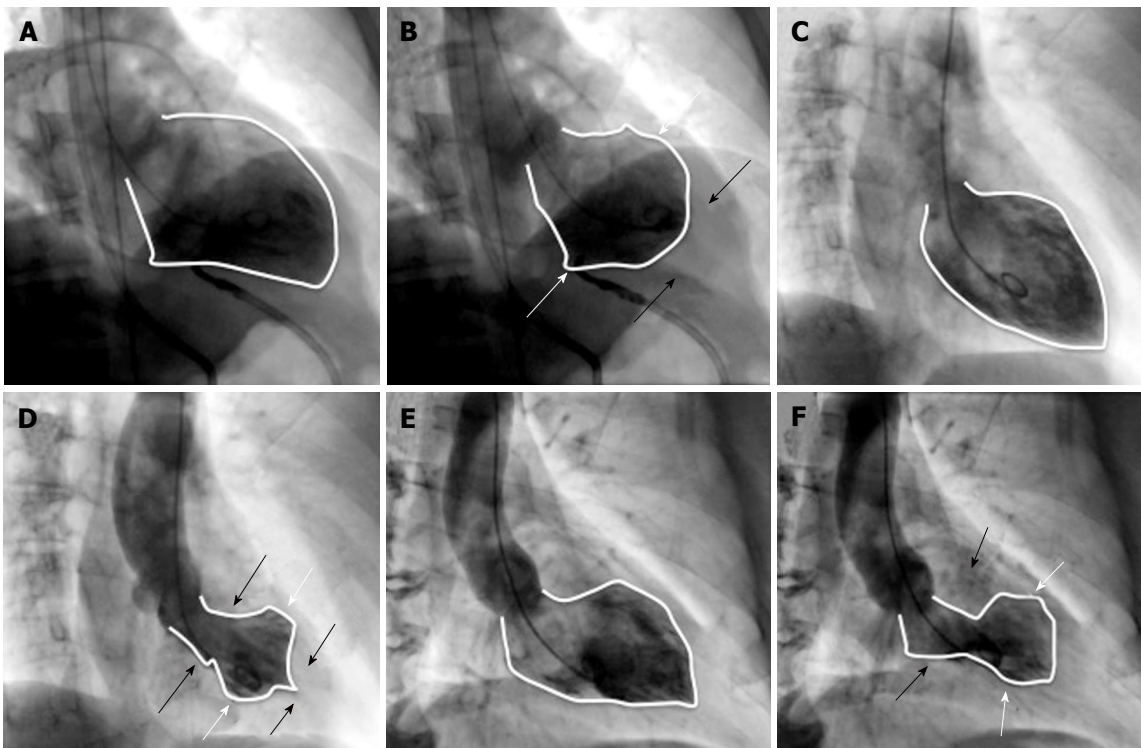


Figure 1 Ventriculography of the 3 cases. A and B are the ventriculography of case 1. A: LV at end diastole; B: LV at end systole with motion defect (white arrows show inferior and anterior basal hypokinesis; black arrows show hypercontractility of apical segments); LVEF: 20%. C and D are the ventriculography of case 2. C: LV at end diastole; D: LV at end systole with motion defect (white arrows show inferior and anterior midventricular hypokinesis; black arrows show hypercontractility of inferior and anterior basal and apical segments); LVEF: 60%. E and F are the ventriculography of case 3; E: LV at end diastole; F: LV at end systole with apical ballooning (white arrows show apical inferior and anterior hypokinesis; black arrows show inferior and anterior basal segments hypercontractility); LVEF: 45%, with severe mitral regurgitation. LV: Left ventricle; LVEF: Left ventricular ejection fraction.

complete recovery of the defect during follow-up.

The mechanisms resulting in TS are not yet fully understood, but the currently most accepted theories are transient myocardial dysfunction secondary to an exaggerated release of catecholamines, coronary vasospasm and transient microvascular dysfunction^[3,6].

The management of acute heart failure is the mainstay of treatment, and in some patients it is necessary to provide support with vasoactive drugs and/or ventricular assistance to achieve hemodynamic stability^[6,7]. Once the acute episode has been

resolved, a favourable long-term prognosis is generally expected^[3], although recent reports have challenged this notion^[8]. Some series suggest that this entity can have an estimated annual rate of 9.9% major events and 5.6% mortality^[5], in association with a recurrence risk of 5%-10%^[6]. The magnitude of ventricular dysfunction is the main prognostic marker^[4], although factors influencing late prognosis have not yet been clearly defined.

It has been reported that atypical TS has a better prognosis than the common form, which theoretically

could be explained by the lesser amount of affected myocardium and better ventricular function^[4], although information regarding such cases is scarce. Finally, we believe that clinicians caring for patients with myocardial infarction should be familiar with these less common presentations of TS, which should be considered in patients with acute coronary syndromes without obstructive coronary disease and with cardiac enzyme elevations lower than expected in relation to the degree of apparent myocardial damage, particularly when triggered by obvious emotional or physical stress.

ARTICLE HIGHLIGHTS

Case characteristics

Patients presenting as acute coronary syndrome with left ventricular (LV) dysfunction, shock or LV outflow tract obstruction, and in whom no stenosis were found in angiography and full recovery of LV abnormality was achieved.

Clinical diagnosis

Acute Coronary Syndrome, cardiogenic shock.

Differential diagnosis

Acute coronary syndrome due to plaque rupture, spontaneous coronary artery dissection.

Laboratory diagnosis

Elevated highsensitive troponin, electrocardiogram with different abnormalities such as ST depression and elevation, as well as ventricular arrhythmias.

Imaging diagnosis

Coronary angiography with no coronary arteries stenosis. LV dysfunction with distinctive wall motion abnormalities not correlated to specific arterial segments. LV function recovery in follow-up echocardiogram.

Treatment

Beta blockers, volume replacement.

Related reports

Several reports of atypical cases with wall motion abnormalities different from apical ballooning. Retrospective study, InterTAK Registry, shows incidence about 10% to 18% of atypical cases.

Term explanation

Takotsubo syndrome (TS) is a cardiomyopathy that simulate acute coronary syndrome, but no coronary abnormalities are present in angiography. Wall motion abnormality typically presents as apical ballooning, however, in some cases (as presented in this report) different LV segments might be affected.

Experiences and lessons

Myocardial compromise in TS is not limited to the classical apical involvement and clinical presentations can range from life-threatening hemodynamic

compromise to low-risk chest pain. A normal coronary angiogram and discordant LV involvement are key diagnostic features. Prompt recognition of complications and subsequent treatment allow for a favourable prognosis.

REFERENCES

- 1 Sato H, Tateishi H, Uchida T. Takotsubo-type cardiomyopathy due to multi-vessel spasm. In: Kodama K, Haze K, Hon M, editors. Clinical aspect of myocardial injury: from ischemia to heart failure. Tokyo: Kagakuhyouronsya; 1990: 56–64
- 2 Prasad A, Lerman A, Rihal CS. Apical ballooning syndrome (Tako-Tsubo or stress cardiomyopathy): a mimic of acute myocardial infarction. *Am Heart J* 2008; **155**: 408–417 [PMID: 18294473 DOI: 10.1016/j.ahj.2007.11.008]
- 3 Núñez Gil IJ, Andrés M, Almendro Delia M, Sionis A, Martín A, Bastante T, Córdoba Soriano JG, Linares Vicente JA, González Sucarrats S, Sánchez-Grande Flecha A; RETAKO investigators. Characterization of Tako-tsubo Cardiomyopathy in Spain: Results from the RETAKO National Registry. *Rev Esp Cardiol (Engl Ed)* 2015; **68**: 505–512 [PMID: 25544669 DOI: 10.1016/j.rec.2014.07.026]
- 4 Ghadri JR, Cammann VL, Napp LC, Jurisic S, Diekmann J, Bataiosu DR, Seifert B, Jaguszewski M, Sarcon A, Neumann CA, Geyer V, Prasad A, Bax JJ, Ruschitzka F, Lüscher TF, Templin C; International Takotsubo (InterTAK) Registry. Differences in the Clinical Profile and Outcomes of Typical and Atypical Takotsubo Syndrome: Data From the International Takotsubo Registry. *JAMA Cardiol* 2016; **1**: 335–340 [PMID: 27438117 DOI: 10.1001/jamacardio.2016.0225]
- 5 Templin C, Ghadri JR, Diekmann J, Napp LC, Bataiosu DR, Jaguszewski M, Cammann VL, Sarcon A, Geyer V, Neumann CA, Seifert B, Hellermann J, Schwyzer M, Eisenhardt K, Jenewein J, Franke J, Katus HA, Burgdorf C, Schunkert H, Moeller C, Thiele H, Bauersachs J, Tschöpe C, Schultheiss HP, Laney CA, Rajan L, Michels G, Pfister R, Ukena C, Böhm M, Erbel R, Cuneo A, Kuck KH, Jacobshagen C, Hasenfuss G, Karakas M, Koenig W, Rottbauer W, Said SM, Braun-Dullaues RC, Cuculi F, Banning A, Fischer TA, Vasankari T, Airaksinen KE, Fijalkowski M, Rynkiewicz A, Pawlak M, Opolski G, Dworakowski R, McCarthy P, Kaiser C, Osswald S, Galiuto L, Crea F, Dichtl W, Franz WM, Empen K, Felix SB, Delmas C, Lairez O, Erne P, Bax JJ, Ford I, Ruschitzka F, Prasad A, Lüscher TF. Clinical Features and Outcomes of Takotsubo (Stress) Cardiomyopathy. *N Engl J Med* 2015; **373**: 929–938 [PMID: 26332547 DOI: 10.1056/NEJMoa1406761]
- 6 Bybee KA, Prasad A. Stress-related cardiomyopathy syndromes. *Circulation* 2008; **118**: 397–409 [PMID: 18645066 DOI: 10.1161/CIRCULATIONAHA.106.677625]
- 7 De Backer O, Debonnaire P, Gevaert S, Missault L, Gheeraert P, Muyldermans L. Prevalence, associated factors and management implications of left ventricular outflow tract obstruction in takotsubo cardiomyopathy: a two-year, two-center experience. *BMC Cardiovasc Disord* 2014; **14**: 147 [PMID: 25339604 DOI: 10.1186/1471-2261-14-147]
- 8 Scally C, Rudd A, Mezincescu A, Wilson H, Srivanasan J, Horgan G, Broadhurst P, Newby DE, Henning A, Dawson DK. Persistent Long-Term Structural, Functional, and Metabolic Changes After Stress-Induced (Takotsubo) Cardiomyopathy. *Circulation* 2018; **137**: 1039–1048 [PMID: 29128863 DOI: 10.1161/CIRCULATIONAHA.117.031841]

P- Reviewer: Korosoglou G, Bagur R, Nurzynska D S- Editor: Dou Y

L- Editor: Filipodia E- Editor: Wu YXJ





Published by **Baishideng Publishing Group Inc**
7901 Stoneridge Drive, Suite 501, Pleasanton, CA 94588, USA
Telephone: +1-925-223-8242
Fax: +1-925-223-8243
E-mail: bpgoffice@wjgnet.com
Help Desk: <http://www.f6publishing.com/helpdesk>
<http://www.wjgnet.com>

